# The protease adaptor YjbH is involved in the nitrosative stress response in *Listeria monocytogenes* and requires its thioredoxin active motif for function

Brittany R. Ruhland

A dissertation
submitted in partial fulfillment of the
requirements for the degree of

Doctor of Philosophy

University of Washington
2020

Reading Committee:
Michelle Reniere, Chair
Matthew Parsek
Nina Salama

Program Authorized to Offer Degree:
Department of Microbiology

University of Washington

## Abstract

The protease adaptor YjbH is involved in the nitrosative stress response in *Listeria monocytogenes* and requires its thioredoxin active motif for function

Brittany R. Ruhland

Chair of the Supervisory Committee:
Michelle Reniere
Department of Microbiology

Tight regulation of virulence proteins is essential for the facultative intracellular pathogen *Listeria monocytogenes* to successfully infect host cells. The gene encoding the annotated thioredoxin YjbH was identified in two forward genetic screens as required for virulence factor production. However, the function of YjbH in *L. monocytogenes* has not been investigated. This dissertation provides evidence that *L. monocytogenes* YjbH is a protease adaptor for the redox-responsive transcriptional regulator SpxA1, and is involved in the nitrosative stress response. Whole-cell proteomics demonstrated that YjbH alters the abundance of at least 8 proteins in addition to SpxA1, and we showed that YjbH physically interacted with all 9 in bacterial two-hybrid assays. Thioredoxin proteins canonically require active motif cysteines for function, but other YjbH homologues do not. We demonstrated that cysteine residues of the YjbH thioredoxin domain active motif are essential for *L. monocytogenes* sensitivity to nitrosative stress, cell-to-cell spread in a tissue culture model of infection, and several protein-protein interactions. Together, these results demonstrated that the function of YjbH in *L. monocytogenes* requires its thioredoxin active motif and that YjbH has a role in the post-translational regulation of several proteins, including SpxA1.

# Table of Contents

# Acknowledgements

I would like to thank all current and previous members of the Reniere Lab for their support in the generation of this dissertation during my years of research, months of writing, and weeks of quarantine during the COVID-19 pandemic. Thank you to my thesis committee, who provided sound guidance and thoughtful feedback during my exams and departmental presentations, and my reading committee, who took on a lot of extra reading during quarantine. The administrative team in the UW Microbiology Department was also of great help during the last five years, especially Amy Gundlach and Andrea Pardo.

I thank all the labs in the UW Microbiology Department for their help and generosity with reagents, lab equipment, and protocol advice over the years. In particular I would like to thank the laboratory of Josh Woodward, for years of great feedback and collaboration during our joint lab meetings, happy hours, and coffee breaks.

The laboratory of Joseph Mougous (UW Microbiology) very generously helped me with whole-cell proteomics preparation for data presented in Chapter 3. Proteomics services in this dissertation (Chapters 2 and 3) were performed by the Northwestern Proteomics Core Facility, generously supported by NCI CCSG P30 CA060553 awarded to the Robert H. Lurie Comprehensive Cancer Center and the National Resource for Translational and Developmental Proteomics, supported by P41 GM108569.

Research in the Reniere Lab was funded by the National Institutes of Health [RO1 AI132356]. My own research in the Reniere Lab was funded by the National Institute of General Medical Sciences [PHS NRSA T32GM007270].

# List of tables and figures

## Chapter 1



## Chapter 2



## Chapter 3



## Chapter 4



## Chapter 6

# Chapter 1: Background

## Introduction to *Listeria monocytogenes*

*Listeria monocytogenes* is a Gram-positive saprophtye that is ubiquitous in the environment. Once ingested by a host, *L. monocytogenes* is an intracellular pathogen capable of causing the disease listeriosis in humans. Ingestion of *L. monocytogenes* typically occurs via contaminated food items like deli meats, soft cheeses, and produce[1,2]. *L. monocytogenes* is one of the most common etiologic agents of hospitalization due to foodborne pathogens, and in recent years there have been listeriosis outbreaks traced back to fruits, dairy products, and individually wrapped hard-boiled eggs[3]. Its high tolerance to heat, cold, salt, and acidity mean that foods contaminated during the production process will remain contaminated in the transit from producer to consumer, and indeed, this bacterium can continue replicating at refrigerator temperatures, rendering it especially dangerous in the food industry[1]. *L. monocytogenes* is capable of infecting a wide range of hosts, from frogs to livestock to humans.

Healthy humans who ingest food contaminated with *L. monocytogenes* are not typically at serious risk from listeriosis, but immunocompromised populations (the elderly, pregnant people, and young children) can experience severe disease outcomes[4]. This foodborne pathogen is capable of crossing the intestinal barrier to cause gastroenteritis, crossing the blood-brain barrier to cause meningitis[5], and crossing the placental barrier to cause pre-term birth and abortions[6,7]. In the case of at-risk populations, the mortality rates of listeriosis can reach frightening heights (approximately 70% for bacteremia and septicemia, 20% for central nervous system infections, and 10-20% for neonatal listeriosis)[8].

Exquisite protein regulation is required for *L. monocytogenes* to navigate the transition from saprophyte to cytosolic pathogen. To survive this transition, it must properly respond to myriad oxidative and nitrosative stressors in a number of microenvironments[9]. After the host ingests *L. monocytogenes* from contaminated food or soil, the pathogen is either engulfed by phagocytic cells or taken up via receptor-mediated endocytosis by non-phagocytic cells[10] (Fig. 1). *L. monocytogenes* is able to survive the highly oxidative phagosome, which may contain peroxides, nitric oxide, and a lowered pH[11]. Escape into the reducing cytosol is mediated by the action of the pore-forming toxin listeriolysin O (LLO)[12]. Once in the cytosol, the bacterium begins replicating and recruits host actin via its surface protein ActA, which enables cell-to-cell spread with actin-based motility[13,14]. Each stage of this intracellular lifecycle requires tight regulation of virulence proteins. When the intracellular lifecycle is properly regulated, it leads to a successful infection.

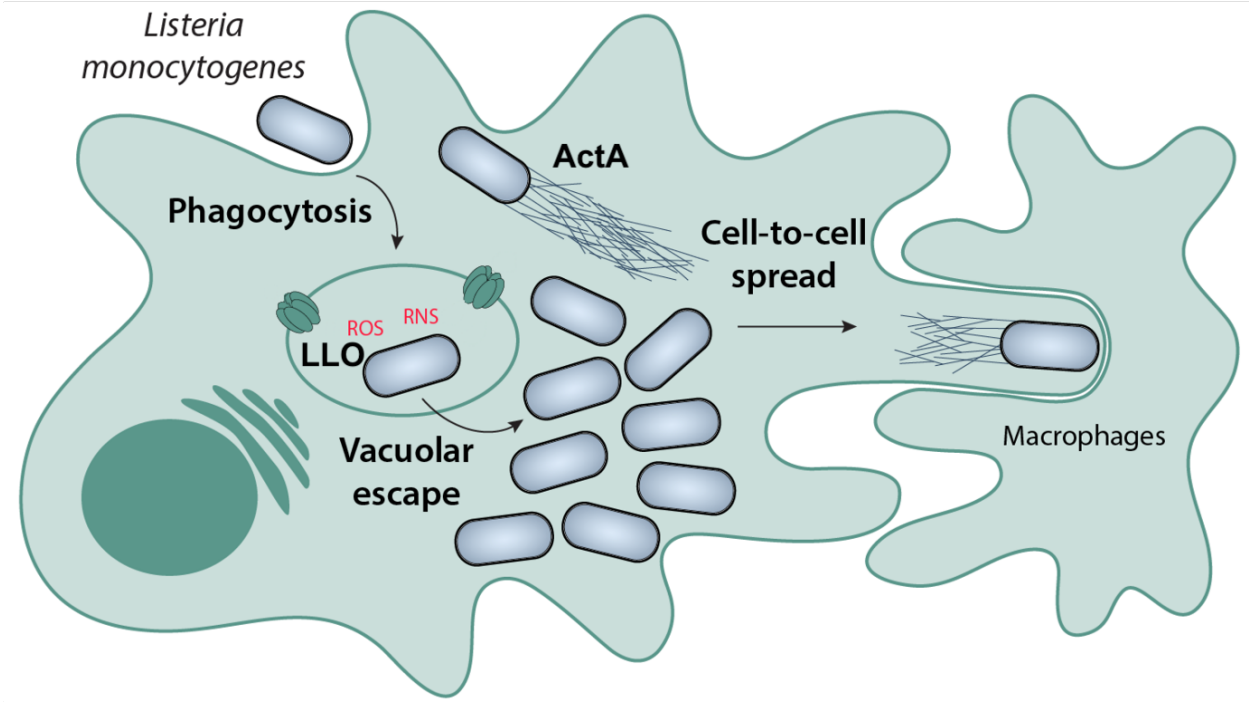


**Figure 1**. Schematic depicting the intracellular lifecycle of *L. monocytogenes*. After phagocytosis or receptor-mediated entry, *L. monocytogenes* is enclosed in the highly oxidative phagosome or endosome, where they encounter reactive oxygen and nitrogen species (abbreviated ROS and RNS). The bacterium escapes the phagosome via the action of LLO and reaches the reducing cytosol, where bacterial replication begins and the dramatic upregulation of the virulence factor ActA takes place. ActA facilitates the polar polymerization of host actin and thus cell-to-cell spread.

## Regulation of major *L. monocytogenes* virulence factors

PrfA is known as the 'master virulence regulator' in *L. monocytogenes*, as it directly activates all nine virulence genes and indirectly regulates over 140 additional genes[15,16]. PrfA is absolutely essential for virulence and a Δ*prfA* mutant is attenuated over four-logs in a murine infection model[17]. Conversely, constitutive PrfA activation results in significantly decreased extracellular growth[18], highlighting the requirement for appropriately localized PrfA activation specifically in the intracellular compartment. To that end, PrfA is regulated transcriptionally by multiple promoter regions[19,20], post-transcriptionally by a temperature-sensitive riboswitch and a 5' untranslated region (UTR)[21,22], and post-translationally by an allosteric ligand that modulates the activation state of PrfA[23].

PrfA is a member of the cAMP receptor protein family, which is characterized by allosteric activation by a small molecule cofactor. It was recently determined that the abundant low-molecular-weight thiol glutathione is the allosteric activator of PrfA[17]. Reduced glutathione binds PrfA in an intraprotein tunnel region previously predicted to be the site of 'activator'

binding[24,25]. Upon binding to reduced glutathione, PrfA undergoes a slight conformational shift that promotes DNA binding and transcriptional activation. PrfA activation is further regulated by the redox state of the environment via its four cysteine residues: all eight thiols of the PrfA homodimer must be in the reduced state for PrfA to bind DNA[17]. Together, these findings suggest a model in which PrfA is reduced upon *L. monocytogenes* entering the host cytosol, enabling it to bind DNA. Bacterial- or host-derived glutathione then binds and activates PrfA, promoting transcription of virulence genes (Fig. 2).

Importantly, PrfA activation is also closely connected to the metabolic changes that occur as *L. monocytogenes* shifts from a saprophytic to parasitic lifestyle. The most apparent example of this is the hexose phosphate transporter, directly regulated by PrfA, which enables uptake of glucose-6-phosphate from the host cytosol[26]. PrfA activity is high when grown in the presence of carbohydrates abundant in the mammalian cytosol, such as glycerol or glucose-6-phosphate. In contrast, PrfA activity is repressed in the presence of carbon sources commonly found outside the host environment, such as plant-derived cellobiose[10]. Therefore, as *L. monocytogenes* switches to a virulent state, its metabolic reprogramming is redox-regulated via PrfA activity.

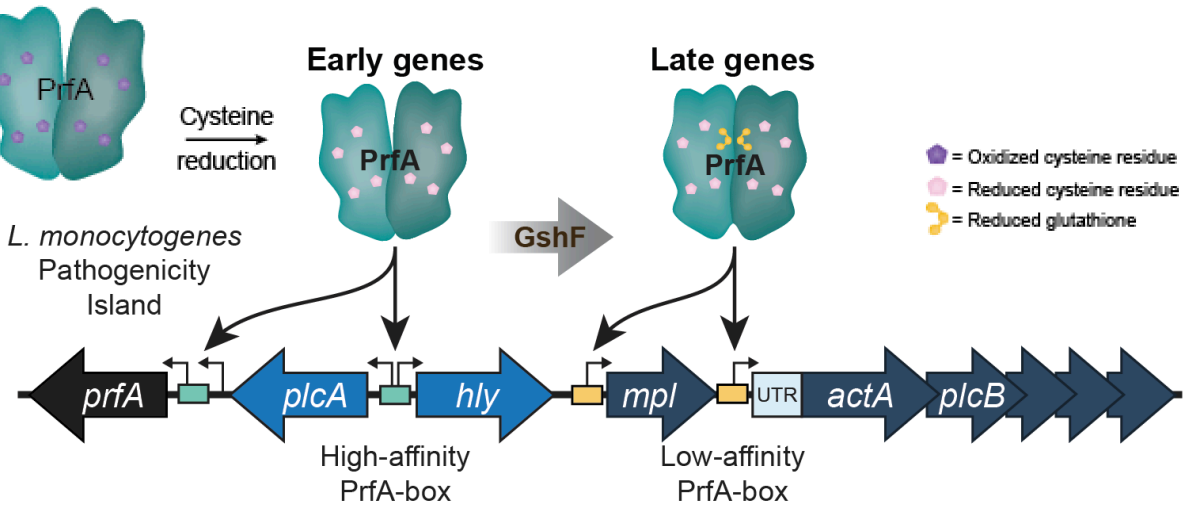


**Figure 2**. PrfA is a homodimer that binds to a 14-bp palindromic repeat referred to as a 'PrfA box'. Reduction of the protein thiols allows PrfA to bind to high-affinity PrfA boxes containing perfect palindromic sequences. During infection, allosteric binding of glutathione to PrfA induces the active conformation that promotes transcription of all PrfA boxes. High-affinity PrfA-boxes are teal and low-affinity PrfA-boxes are yellow.

Proper regulation of PrfA results in the direct transcriptional upregulation of a suite of "early" virulence genes designated by their high-affinity PrfA boxes, including the *hly*-encoded LLO[27] (Fig. 2). LLO is a member of the cholesterol-dependent cytolysin protein family, the pore-forming activity of which allows *L. monocytogenes* to escape the phagosome[28]. Like other cholesterol-dependent cytolysins, LLO is secreted as monomeric components that insert themselves into a lipid membrane to form oligomeric pores[29]. This protein is essential for virulence in a murine model of infection[30]. Although its transcriptional activation by PrfA has been well-characterized, the full mechanism of LLO regulation remains incompletely understood.

It is critical to a successful infection that LLO concentrations are "just right": neither too little nor too much. Too little LLO results in the bacterium becoming trapped in the phagosome, leading to an inability to spread cell to cell and an unsuccessful infection[31]. The 5' UTR of the hly transcript is essential for sufficient production of LLO protein during infection[31]. *L. monocytogenes* must also avoid the potentially cytotoxic effects of over-active LLO on the host cell, which is prevented by elements of LLO structure, function, and post-translational regulation that combine to dampen its pore-forming activity[30,32]. First, the LLO protein has a low optimal pH suited to the phagosomal microenvironment[33]. Second, an important structural element with control over LLO activity is the N-terminal PEST-like sequence, which is rich in proline (P), glutamate (E), serine (S), and threonine (T) residues. Without this PEST-like sequence in LLO, *L. monocytogenes* is significantly more toxic to host cells and is attenuated in a mouse model compared to wild type[34]. It has also been shown that synonymous mutations within the PEST-like sequence increase both the translation of LLO and toxicity to the host cell[35,36]. These factors combine to alter LLO activity, but despite years of work on this topic, the exact mechanism of post-transcriptional LLO regulation remains to be elucidated.

The major virulence determinant, encoded by *actA*, is controlled by a low-affinity PrfA box that activates transcription only when *L. monocytogenes* reaches the host cytosol. At this point, *actA* is upregulated over 200-fold and is transited to the cell surface, where it is enriched at one pole[37]. Thus, the polymerization of host actin filaments results in actin-based motility that propels bacteria forward and allows them to form membrane protrusions that resolve into secondary spreading vacuoles in neighboring host cells[14]. ActA protein production is therefore critically important to a successful infection, demonstrated by Δ*actA* mutants that are severely attenuated in a murine model of infection[13,38].

Precise regulation of ActA is achieved at several different levels. First, transcriptional regulation is mediated directly by PrfA, which recognizes and binds a low-affinity PrfA box

upstream of *actA* once *L. monocytogenes* reaches the host cytosol during infection[27]. Reduced PrfA can bind low-affinity PrfA boxes in the absence of glutathione, but PrfA binding to high-affinity PrfA-boxes requires the conformational change caused by the allosteric activator glutathione[17]. Two separate promoters with the aforementioned low-affinity PrfA boxes drive transcription of *actA*: *actA1p* is the proximal promoter located just upstream of the *actA* 5' UTR, and *actA2p* is a read-through promoter which transcribes *actA* in an operon with the upstream gene *mpl*, which encodes a metalloprotease[39]. Both promoters are required to produce wild-type levels of ActA protein[40], and the 149-nucleotide actA 5' UTR is essential for ActA protein production[22]. It has been suggested that the three-dimensional structure of the actA UTR, rather than the sequence itself, is important for post-transcriptional regulation[22]. Currently, it is unknown whether the predicted structural elements in the actA UTR might bind a protein or protein complex, recognize an RNA molecule, or otherwise act as a riboswitch.

## Oxidative and nitrosative stress in bacteria

Bacteria are constantly experiencing abrupt changes in their environment that require immediate adaptation. These perturbations and the ability to respond to them are often life or death situations, such as conditions of nutrient depletion or exposure to deadly reactive oxygen species (ROS). ROS, including hydrogen peroxide, superoxide, and hydroxyl radicals, are generated endogenously during aerobic respiration and exogenously by the host respiratory burst during infection[9]. In addition, ROS are generated in the environment by chemical and photochemical processes, as well as by plants and bacteria that excrete redox-cycling compounds to kill competitors[41,42].

The severity of potential defects caused by altered redox homeostasis explains why bacteria have evolved myriad mechanisms to sense and detoxify ROS, as well as repair oxidatively damaged DNA, proteins, and lipids. The ability of pathogenic bacteria to inhabit the host environment is then, in part, determined by bacterial defenses against ROS and other redox stressors found in the host. Changes at the transcriptional level can be enacted by transcriptional regulators, such as regulators that respond to oxidative stress[43]. Adaptation via protein regulation is rapid and can include post-translational modifications to alter activity, regulated changes in protein solubility, and protease-dependent degradation[44–46].

Organic hydroperoxides (OHPs) are strong oxidizers that easily generate free radicals. When bacteria encounter OHPs, peroxiredoxins in the OsmC/OhrA family detoxify the dangerous compounds to prevent damage to cellular macromolecules. OhrA peroxiredoxins are commonly regulated by redox-responsive transcriptional repressors of the MarR-family named

OhrR. In the model bacterium *Bacillus subtilis*, OhrR regulates OhrA, which shares 63% similarity to *L. monocytogenes* OhrA[47]. *B. subtilis* OhrR is a functional dimer that senses OHPs via S-thiolation at a conserved cysteine residue[48]. S-thiolated OhrR dissociates from DNA, resulting in derepression of *ohrA* transcription and relief from OHP stress (Fig. 3A). *L. monocytogenes ohrA* is encoded in an operon with a transcriptional regulator that has 68% amino acid similarity to *B. subtilis* OhrR[40].

Infected macrophages produce abundant phagosomal OHPs, requiring intracellular pathogens to detoxify them. For example, *Mycobacterium smegmatis ohrA* is derepressed in this environment, suggesting that OhrR is oxidized during infection[49]. Further, the *L. monocytogenes* Δ*ohrA* mutant exhibits a growth defect in macrophages that is likely due to host-derived OHP toxicity. In addition to its role in detoxifying OHPs, *ohrA* was identified as being required for proper regulation of virulence factors during *L. monocytogenes* infection[40]. These findings demonstrate that OhrA is important for OHP detoxification in *L. monocytogenes*, and that redox regulation is tied to virulence gene regulation.

Hydrogen peroxide is generated endogenously from incomplete reduction of oxygen during aerobic respiration, and produced exogenously by the mammalian host to kill invading pathogens[9]. Peroxides exert their toxicity through the oxidation of iron-sulfur clusters and cysteine residues[50]. Consequently, bacteria possess mechanisms to directly sense peroxides and up-regulate genes required for their detoxification. The primary peroxide-sensing transcriptional repressor in Firmicutes is PerR, which normally binds DNA and represses transcription of target genes (Fig. 3B). The irreversible oxidation of two PerR histidine residues upon peroxide exposure leads to its degradation, and derepression of its regulon[51,52]. Genes repressed by *L. monocytogenes* PerR include the iron homeostasis regulator (*fur*), catalase (*kat*), heme biosynthesis machinery (*hemA*), an iron efflux pump (*fvrA*), the iron storage protein (*fri*), thioredoxin reductase (*trxB*), and a predicted peroxiredoxin (*lmo1604*)[53].

It is clear from the PerR regulon that the response to peroxide stress is intimately intertwined with metal homeostasis. Indeed, PerR has two metal-binding sites upon which PerR activity depends: the first is a structural Zn(II)-binding site and the second binds Fe(II) or Mn(II) and serves a regulatory function[54]. Mn(II)-bound PerR represses *fur* and *perR* itself, while Fe(II)-bound PerR represses peroxide-detoxification genes[55]. Thus, the iron status of the cell directly regulates PerR activity[56]. During peroxide stress, iron-catalyzed oxidation of PerR histidine residues results in dissociation of the regulatory metal ions and derepression of the PerR regulon. The regulation of Fur and iron homeostasis is therefore critical to redox homeostasis. Although not expanded upon here, the importance of Fur cannot be overlooked.

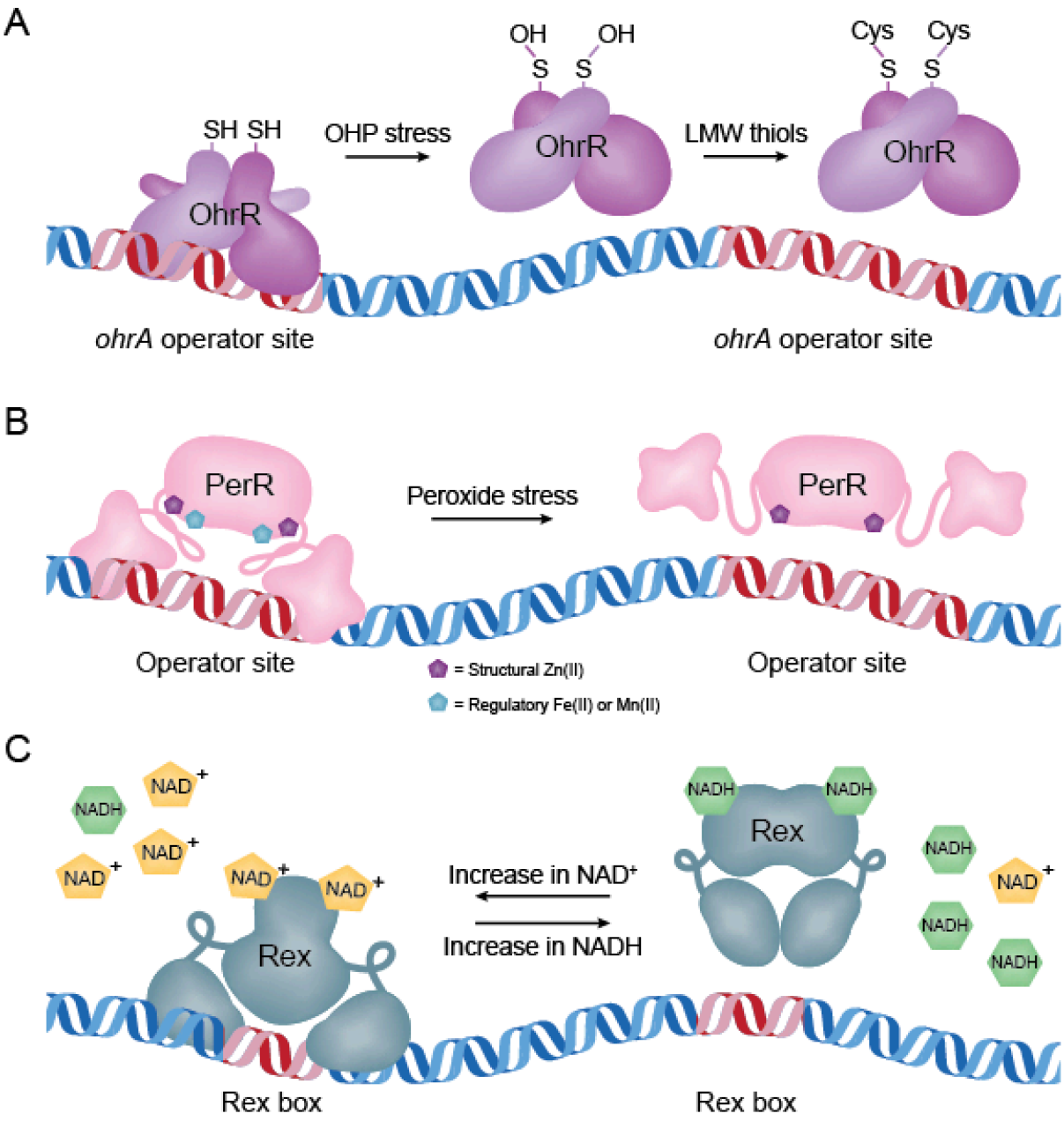


**Figure 3**. Schematic depicting the functions of OhrR, PerR, and Rex. Red DNA represents specific DNA-binding sequences recognized by each transcriptional repressor. **(A)** Dimerized, reduced OhrR binds to specific DNA sequences and represses downstream genes. OHP stress oxidizes a cysteine residue on each monomer to sulfenic acid (-OH). This can then be S-thiolated by the low-molecular-weight thiols cysteine or glutathione, resulting in nonfunctional protein and derepression of *ohrA*. **(B)** In the absence of stress and in the presence of sufficient metals, PerR binds to DNA and represses expression of target genes. Peroxide induces oxidation of Fe(II)-bound PerR, altering the conformation such that it releases from the DNA and the PerR regulon is derepressed. Oxidized PerR is then targeted for degradation. Dysregulation of the PerR regulon also occurs in conditions of excess Zn(II) or Mn(II). **(C)** When $NAD^+$ concentrations are sufficient, Rex represses target genes by binding a specific DNA sequence, referred to as a 'Rex box'. However, as NADH increases, it competes with $NAD^+$ for binding to Rex and NADH-bound protein does not bind DNA, thereby relieving repression of the Rex regulon.

*L. monocytogenes* strains lacking *perR* form small colonies on a rich medium and exhibit increased sensitivity to peroxide stress, suggesting important roles for PerR in both routine detoxification of endogenously produced peroxides as well as exogenous ROS stress[53]. These growth defects are due in part to iron starvation that results from derepression of the PerR regulon; specifically, increased Fur expression and repression of iron-acquisition genes[56]. The Δ*perR* strain was also attenuated 100-fold in a murine model of infection[53]. Together, these phenotypes demonstrate the importance of peroxide-sensing to *L. monocytogenes* survival and pathogenesis.

Nicotinamide adenine dinucleotide (NAD) exists in the oxidized ($NAD^+$) or reduced (NADH) state and is a coenzyme critical for cellular redox reactions. The ratio of $NAD^+$ to NADH is a measure of the redox state of the cell and must be carefully regulated to maintain homeostasis. To monitor this balance, many low G+C Gram-positive bacteria encode the transcriptional repressor Rex (Fig. 3C), which directly binds $NAD^+$ to regulate carbohydrate and energy metabolism[57]. Although Rex has not yet been studied in *L. monocytogenes*, the protein (encoded by *lmo2072*) is highly similar to its homologues in *B. subtilis* and *Staphylococcus aureus*, sharing 65% and 52% amino acid identity, respectively. In these bacteria, Rex binds a specific DNA consensus sequence to repress target genes when the NADH:$NAD^+$ ratio is low[57,58]. In contrast, NADH-bound Rex is unable to bind DNA, thus relieving repression of its regulon when NADH is more abundant. For example, high $NAD^+$ levels in *B. subtilis* result in Rex repression of *ndh* (encoding NADH dehydrogenase), which decreases NADH oxidation to restore homeostasis[58]. In addition to NADH dehydrogenase, the Rex regulon typically includes genes encoding lactate dehydrogenase, pyruvate formate lyase, respiratory nitrate reductase, and cytochrome oxidases[59]. A bioinformatics approach to understanding Rex function in 119 bacterial genomes found considerable variability in Rex-dependent genes, likely corresponding to the different niches of individual species[57]. Therefore, while we can make predictions about Rex function in *L. monocytogenes*, its regulon and role during infection remain to be experimentally determined.

## Spx-family proteins

To sense and adapt to redox stress many Firmicutes, including *L. monocytogenes*, encode one or more copies of an arsenate reductase (ArsC) family protein, named Spx in the model organism *B. subtilis*[60]. Spx is a global regulator that activates and represses transcription in response to oxidative stress via direct interaction with the α-subunit of RNA polymerase (RNAP)[60–63]. Oxidative stress is sensed through the conserved CxxC motif that is reduced under

normal growth conditions. Importantly, oxidative stress results in disulfide stress, in which cysteine residues are oxidized. This results in overoxidation or erroneous intra- and intermolecular disulfide bridges that induce conformational changes in thiol-containing proteins[64]. However, proteins with redox switches can exhibit differential functions during disulfide stress. For example, the oxidized cysteine residues of the Spx CxxC motif form an intramolecular disulfide bond that stabilizes the Spx-RNAP-DNA interaction and allows for Spx-mediated activation of transcription[61]. In *B. subtilis,* over 100 genes are activated in an Spx-dependent manner, including those important for thiol homeostasis, such as: thioredoxin, thioredoxin reductase, and bacillithiol biosynthesis[62,65,66]. In addition to maintaining redox homeostasis, Spx homologues regulate organosulfur metabolism[67], cell wall homeostasis[68,69], competence[70], and biofilm formation[71]. Spx also has "anti-sigma factor" activity, as it represses over 170 genes, including biosynthetic machinery for amino acids, vitamins, and nucleic acids[62]. Spx-family proteins have been demonstrated to be important for virulence of *Enterococcus faecalis*[72], *Streptococcus mutans*[73,74], and *S. sanguinis*[75].

*L. monocytogenes* encodes two Spx paralogues named SpxA1 and SpxA2 that share 56% amino acid similarity. While SpxA1 is essential for *L. monocytogenes* aerobic growth and pathogenesis, a Δ*spxA2* mutant exhibits only slightly impaired growth *in vitro* and is fully virulent in mice[76]. Strikingly, a strain lacking *spxA1* can only be generated anaerobically and is killed upon exposure to oxygen[76]. However, there exists a knockdown strain *P-spxA1::Tn* that transcribes 10-fold less *spxA1* than wild type *L. monocytogenes* and is able to grow aerobically[40]. $Spx_{Bs}$ functionally complements the *L. monocytogenes* Δ*spxA1* mutant, demonstrating that the physical interaction with RNA polymerase is conserved between *L. monocytogenes* and *B. subtilis*[76]. In spite of this trans-complementation, the severe defects of the Δ*spxA1* mutant indicates that the *L. monocytogenes* SpxA1 regulon must be distinct from that of $Spx_{Bs}$, which is not required for growth. The abundance and activity of Spx homologues are tightly regulated to control the disulfide stress response and the myriad other effects of the large Spx regulon[77]. The activity of the protease adaptor YjbH, described in the following section, represents an important part of this regulation at the post-translational level.

## Introduction to YjbH

Over a decade ago, a forward genetic screen of *L. monocytogenes* for hypohemolytic mutants identified the annotated thioredoxin gene *yjbH* ($yjbH_{Lm}$) as required for LLO secretion and virulence[78]. $yjbH_{Lm}$ was again identified in a later screen that aimed to discover bacterial genes involved in *actA* regulation. This screen utilized a “suicide strain” of *L. monocytogenes*

that expresses Cre recombinase from the *actA* promoter[40]. Cre expression is therefore only activated in the cytosol of host cells. Once expressed, the recombinase removes several essential genes and the origin of replication, which were all engineered to have flanking *loxP* sites. A transposon library was generated in this suicide strain and subsequently used to infect macrophages. To survive the infection, a mutant must have disrupted *actA* regulation. This screen found *yjbH* to be required for ActA production in *L. monocytogenes*, likely via post-transcriptional regulation of the actA 5' UTR[40]. Despite the importance of $YjbH_{Lm}$ to virulence, its function in *L. monocytogenes* has not been explored.

YjbH is a cytosolic protein with a predicted N-terminal thioredoxin domain and is conserved among *Firmicutes*[78–80]. While there is an operon that encodes *yjbEFGH* in *Escherichia coli*[81], the *E. coli yjbH* does not have any significant similarity to $yjbH_{Lm}$ or $yjbH_{Bs}$ by BLAST. It is striking to compare the genomic context of *yjbH* in *L. monocytogenes EGD-e, B. subtilis* 168*,* and *S. aureus NCTC* 8325[82–84] (Fig. 4). While there are many homologous coding regions downstream of *yjbH* among the three species, the region upstream of *yjbH* is only conserved between *B. subtilis* and *S. aureus*. This region is particularly interesting because of the proximity to *yjbH* of the ArsC-family redox-responsive transcriptional regulator *spx*. In *L. monocytogenes*, the *spx* homologue *spxA1* is encoded far away from *yjbH* at the locus *lmo2191.* Much of what is known about YjbH comes from studies on *B. subtilis*, in which it is a protease adaptor for Spx[85].

*B. subtilis* YjbH ($YjbH_{Bs}$) maintains low *B. subtilis* Spx ($Spx_{Bs}$) concentrations during steady state by binding to $Spx_{Bs}$ and enhancing its ClpXP-mediated degradation[85–87] (Fig. 5). During disulfide stress, $YjbH_{Bs}$ aggregation prevents the enhancement of $Spx_{Bs}$ degradation and therefore results in increased $Spx_{Bs}$ concentrations[88]. Spx-family proteins are important transcriptional regulators of hundreds of genes and operons[65]. Due to the far-reaching effects of the Spx regulon, the phenotypes of $\Delta yjbH_{Bs}$ have all been attributed to the increase in Spx abundance in that strain. These mutant phenotypes include increased resistance to disulfide stress, a significant growth defect, reduced sporulation, and a decrease in competency[85]. An additional study found $\Delta yjbH_{Bs}$ to have decreased resistance to nitrosative stress[80]. In the published literature to date, no Spx-independent functions of $YjbH_{Bs}$ have been explored.

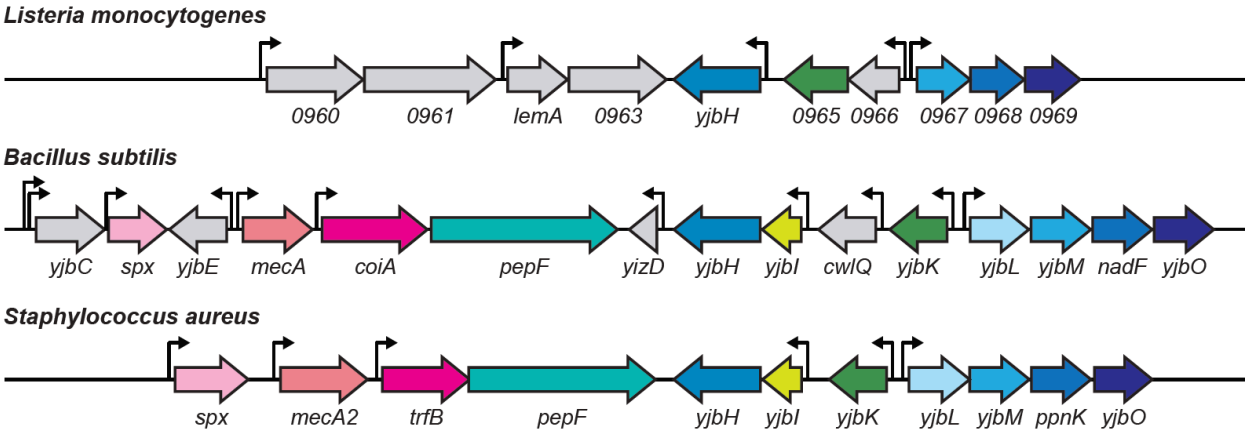


**Figure 4**. Genomic *yjbH* loci alignment. Comparison of genomic context in *Listeria monocytogenes EGD-e, Bacillus subtilis 168*, and *Staphylococcus aureus NCTC* 8325. Predicted transcription start sites are marked with thin black arrows. Genes of identical colors encode proteins that are highly similar at the amino acid level (>27% identical), as determined by BLAST. Genes colored gray have no homologues in the pictured loci.

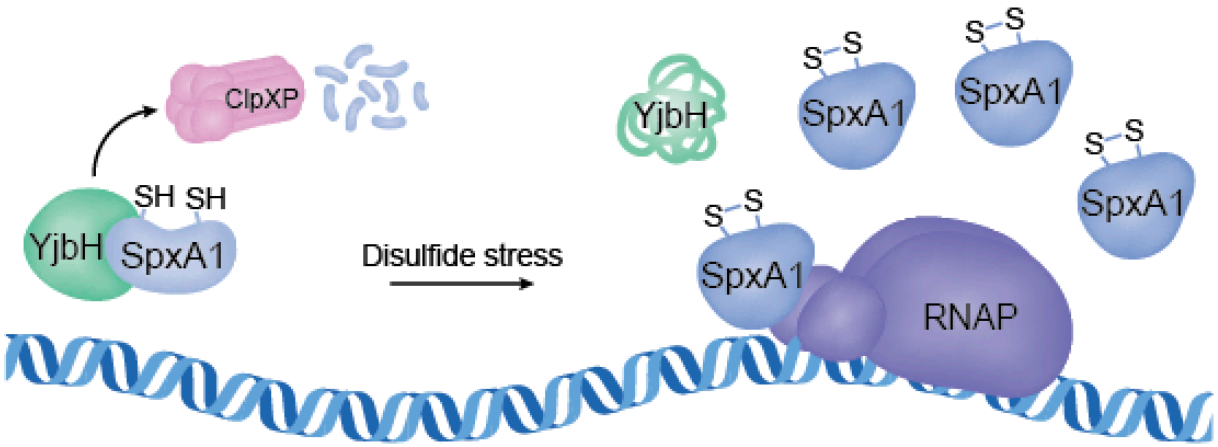


**Figure 5**. YjbH is a protease adaptor for Spx-family proteins. In the absence of stress, Spx abundance is kept low by ClpXP-mediated degradation, which requires the protease adaptor protein YjbH. Disulfide stress induces YjbH aggregation, resulting in increased Spx abundance. Spx does not possess DNA-binding activity on its own, but activate or repress target genes through its interaction with the αCTD of RNA polymerase.

It has been an area of interest in the field to understand how YjbH$_{Bs}$ itself is regulated. Three post-translational mechanisms of regulation have been discovered. First, an unbiased yeast two-hybrid screen in *B. subtilis* identified the small inhibitor protein YirB that competes with Spx$_{Bs}$ to bind YjbH$_{Bs}$[89]. When bound, YirB prevents YjbH$_{Bs}$ from mediating the degradation of Spx$_{Bs}$. Second, YjbH$_{Bs}$ is relatively unstable and prone to aggregation[88]. Aggregated YjbH$_{Bs}$ cannot enhance Spx$_{Bs}$ degradation. YjbH$_{Bs}$ has been found to form aggregates during disulfide stress, heat, and ethanol, although the oxidative stressors peroxide and paraquat did not induce YjbH$_{Bs}$ aggregation[88]. And third, the YjbH$_{Bs}$ protein sequence contains a histidine- and cysteine-rich area at the N-terminus. It has been proposed that this region coordinates at least one zinc (II) atom that is released upon oxidation, potentially altering YjbH$_{Bs}$ activity[86]. However, this metal-binding region is not well-conserved among other YjbH homologues.

Work on *S. aureus* YjbH (YjbH$_{Sa}$), which is highly similar to YjbH$_{Bs}$, has also focused on the important relationship between YjbH$_{Sa}$ and Spx$_{Sa}$. Like the homologous system in *B. subtilis*, YjbH$_{Sa}$ is a protease adaptor for Spx$_{Sa}$[90,91]. Unlike *B. subtilis*, *S. aureus* is a clinically important human pathogen. YjbH$_{Sa}$ has been of interest in understanding virulence mechanisms in *S. aureus*. The *S. aureus* $\Delta$*yjbH$_{Sa}$* mutant results in mild $\beta$-lactam antibiotic resistance, increased peptidoglycan cross-linking, and increased resistance to disulfide stress[79]. More virulence-focused studies have characterized a decrease in staphyloxanthin pigment production and protease activity in a *yjbH$_{Sa}$* mutant, and increased colonization ability in a mouse model of infection[92–94]. These $\Delta$*yjbH$_{Sa}$* phenotypes have likewise been attributed to the myriad genes that Spx$_{Sa}$ regulates.

YjbH$_{Lm}$ has not yet been studied to understand whether the central relationship between YjbH and Spx is conserved in *L. monocytogenes*. YjbH$_{Lm}$ is known to be important in the control of LLO activity and/or abundance, and in a murine model of infection[40,78], but basic questions remain to be answered in this system. For example: Does YjbH$_{Lm}$ physically interact with SpxA1? Are there other important interactions involving YjbH$_{Lm}$? Is the predicted YjbH thioredoxin domain important for function in *L. monocytogenes*?

## The YjbH thioredoxin domain

Thioredoxins help maintain redox homeostasis in the cell[95,96]. Their oxidoreductase activity allows them to reduce erroneously oxidized disulfide bridges in or between their substrates, and thioredoxins are then reduced by a corresponding thioredoxin reductase. The canonical mechanism of reduction by a thioredoxin requires a CxxC active motif[95,96]. One thioredoxin CxxC cysteine will attack a disulfide bridge on its oxidized substrate, forming a

transient intermolecular disulfide bridge (Fig. 6). The second thioredoxin CxxC cysteine, termed the resolving cysteine, will attack the transient disulfide bond, resulting in an oxidized thioredoxin and a reduced substrate. Without either of these two cysteines, thioredoxin chemistry is impossible. Some groups have taken advantage of this thioredoxin chemistry to design so-called "trapping mutants" whose mutated cysteine-x-x-serine (CxxS) motifs cause the thioredoxin to become trapped in a disulfide bond with its substrate protein due to the absence of a resolving cysteine[97]. This technique has proven useful in identifying the substrates of predicted thioredoxin proteins.

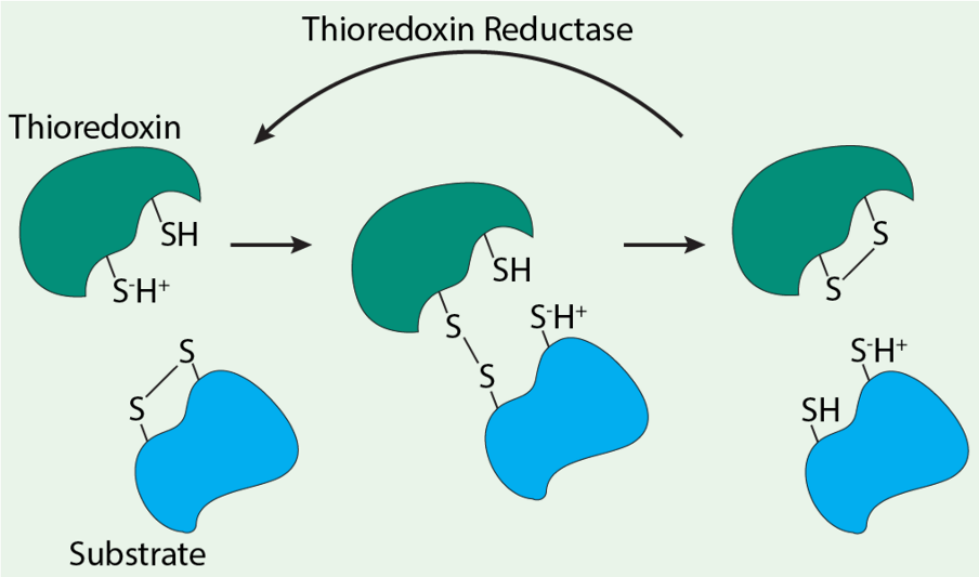


**Figure 6**. Schematic depicting canonical thioredoxin activity. Thioredoxin proteins play an important role in maintaining redox homeostasis within a cell. The CxxC motifs are indicated for both thioredoxin and substrate proteins.

Although all YjbH homologues have a predicted thioredoxin domain, and many have the canonical CxxC thioredoxin active motif, thioredoxin activity has not been tested in any species. Both YjbH$_{Lm}$ and YjbH$_{Bs}$ have a CxxC motif in the thioredoxin domain, and YjbH$_{Sa}$ has SxxC and CxC motifs[90] (Fig. 7). Cysteine residues are not required for YjbH$_{Bs}$ to mediate the degradation of Spx, or to properly aggregate in *B. subtilis*[90]. There is some disagreement in the literature concerning the necessity of cysteine residues in YjbH$_{Sa}$. One study found that replacing all four cysteine residues with glycines in YjbH$_{Sa}$ resulted in an inability to respond to disulfide stress like the wild type protein[79]. A later study instead mutated the cysteine residues to alanines and found that cysteines are, in fact, dispensable to the function of YjbH$_{Sa}$ as a protease adaptor for

$Spx_{Sa}$[90]. The argument supporting the latter study holds that glycine residues are less stable in an α-helix, where the YjbH CxxC motif is located[98], and that could in turn result in altered protein activity[90]. To date, there has been no rigorous evidence that cysteine residues are required for YjbH function in any species. The CxxC cysteines and the two cysteines located outside of the CxxC motif in $YjbH_{Lm}$ have never been tested for their contribution to $YjbH_{Lm}$ function or involvement in the potential $YjbH_{Lm}$-SpxA1 interaction.


**Figure 7**. YjbH amino acid sequence alignment for *Listeria monocytogenes EGD-e, Bacillus subtilis 168*, and *Staphylococcus aureus NCTC* 8325. Fully conserved residues (gray bars), strongly similar residues (blue bars), and weakly similar residues (yellow bars) are indicated. Cysteine residues are in red. Alignment was generated with Clustal Omega Multiple Sequence Alignment.

## YjbH and Spx interaction and structure

An important part of the $YjbH_{Bs}$ model involves the $YjbH_{Bs}$-induced conformational change of $Spx_{Bs}$ such that $Spx_{Bs}$ can be recognized and degraded by the protease ClpXP[87]. ClpXP is a AAA+ protease, comprising six ATPase ClpX subunits and 14 proteolytic ClpP subunits. There are several different kinds of protease adaptors for AAA+ proteases. Some, like MecA, bind the protease unfoldase subunit (ClpC) and allow it to properly oligomerize and become activated[99]. Other protease adaptors alter their substrate proteins via a phosphorylation event or conformational change that results in activating the protease to recognize the altered substrate[100]. Scaffolding protease adaptors will simultaneously bind to the substrate and protease, which increases the relative concentration of the substrate and thus results in increased proteolysis[46]. YjbH binding to Spx changes the conformation of Spx such that a C-terminal degron is exposed that can be easily recognized by ClpXP[101]. In this way, YjbH primes Spx for degradation but does not bind ClpX on its own.

Studies investigating physical interactions or crystal structures involving YjbH homologues are summarized in Table 1. None of these studies have focused on $YjbH_{Lm}$ or $YjbH_{Sa}$. Although work in this field has largely centered on $YjbH_{Bs}$, $YjbH_{Bs}$ is so aggregation-prone that other YjbH homologues with greater stability often are used for interaction-based or structural experiments, notably from *Geobacillus thermodenitrificans* and *G. kaustophilus*[87,98]. $YjbH_{Gt}$ has been shown to interact with $Spx_{Bs}$ via affinity column. The interaction between $YjbH_{Bs}$ and $Spx_{Bs}$ has been demonstrated by yeast two-hybrid assay and immunoprecipitation[86,89], the latter of which required $YjbH_{Bs}$ to be purified from inclusion bodies and re-folded due to its propensity for aggregation.

Recently, the co-crystal structure of the thermostable $YjbH_{Gk}$ with $Spx_{Bs}$ was solved[98] (Fig. 8). $YjbH_{Gk}$ is a multi-domain protein containing a thioredoxin domain with an alpha-helical insertion and a C-terminal winged-helix domain connected by a linker region. Elements of the thioredoxin domain and the alpha-helical insertion are at the interface of the $YjbH_{Gk}$-$Spx_{Bs}$ heterodimer[98]. As shown in Figure 8, the protein-protein interface is relatively large but does not seem to directly include the two cysteine residues in the CxxC motif. The co-crystal structure was solved both with $YjbH_{Gk}$ in the reduced (PDB: 6GHB) and oxidized (PDB: 6GHO) form with respect to its CxxC motif, demonstrating that the YjbH-Spx interaction is independent of the YjbH oxidation state, at least for these two homologues.

**Table 1.** All tested interactions and structural work involving YjbH homologues.

| | **Affinity Column or Immunoprecipitation** | **Two-Hybrid System** | **Structural Studies** |
|---|---|---|---|
| ***L. monocytogenes*** | No | No | No |
| ***B. subtilis*** | Column: $YjbH_{Gt}$ + $Spx_{Bs}$[87]<br>IP: $YjbH_{Bs}$ + $Spx_{Bs}$[89] | Yeast two-hybrid:<br>$YjbH_{Bs}$ + $Spx_{Bs}$[86] | Co-crystal:<br>$YjbH_{Gk}$ + $Spx_{Bs}$[98]<br>Crosslinking MS:<br>$YjbH_{Gk}$ + $Spx_{Bs}$[102] |
| ***S. aureus*** | No | No | No |

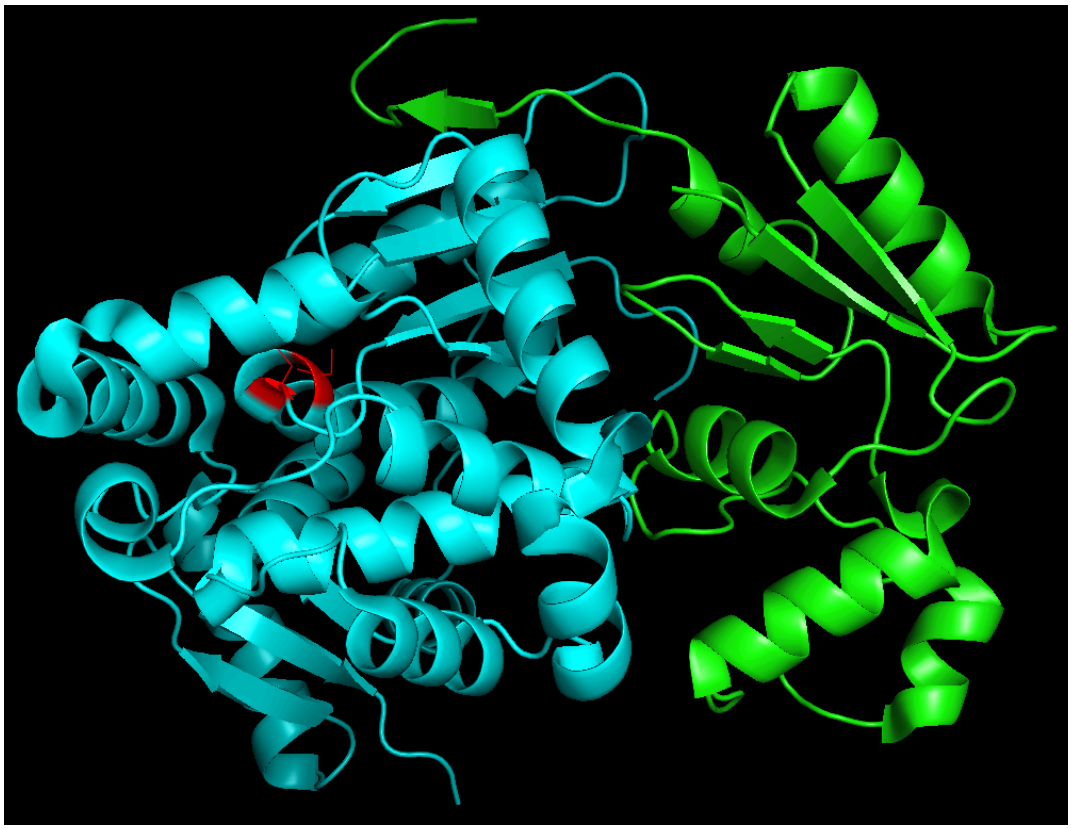

**Figure 8**. Co-crystal structure of YjbH$_{Gk}$ and Spx$_{Bs}$ heterodimer. The interface of YjbH$_{Gk}$ (left, blue) and Spx$_{Bs}$ (right, green) covers a relatively large amount of area and includes part of the YjbH thioredoxin domain. The CxxC motif cysteines are colored red. Image was generated in PyMOL from the PDB structure 6GHO.

# Chapter 2: Using co-immunoprecipitation to study YjbH interactions

## Introduction

The physical interaction between YjbH and Spx is central to YjbH function in *B. subtilis*[86]. $YjbH_{Lm}$ shares 39% amino acid identity with $YjbH_{Bs}$, so we questioned whether the YjbH-Spx interaction was conserved in *L. monocytogenes*. We began by searching for interacting partners using the native $YjbH_{Lm}$ protein in co-immunoprecipitation (co-IP) experiments, as the native protein will help us to understand the nuances of YjbH function specific to *L. monocytogenes*. We next attempted to purify recombinant $YjbH_{Lm}$ from *E. coli* for use as co-IP bait in *L. monocytogenes* lysate. As detailed in the following sections, we discovered several fundamental difficulties with these experiments that could not be resolved by our changes to methodology. Foremost among these inhibiting parameters were the extremely low abundance of both $YjbH_{Lm}$ and SpxA1, and the tendency of $YjbH_{Lm}$ to aggregate when purified.

## Results

### Co-immunoprecipitations with tagged $YjbH^{C27S}$

To interrogate whether $YjbH_{Lm}$ binds SpxA1 by co-IP, we overexpressed the $YjbH^{C27S}$ mutant in the $\Delta yjbH_{Lm}$ *clpX::Tn* background, which is deficient for the ClpXP protease. The $YjbH^{C27S}$ allele harbors an SxxC motif (C27S) instead of the wild type CxxC motif and is referred to as a "trapping mutant". Trapping mutants like this have been successfully used by other groups to identify the substrate proteins of thioredoxin-like proteins[97]. The mutated SxxC motif is expected to result in substrate proteins that are "trapped" with the thioredoxin via an intermolecular disulfide bridge[97] (Fig. 6). To successfully purify $YjbH^{C27S}$, the protein must be sufficiently abundant. In *B. subtilis*, the abundance of soluble $YjbH_{Bs}$ is affected by stressors such as ethanol, diamide, and heat[88]. However, natively expressed $YjbH_{Lm}$ was undetectable in all conditions tested, including elevated temperature and treatment with sublethal concentrations of ethanol, diamide, SNP, or hydrogen peroxide (Fig. 9). For this reason, the co-IP was performed in a *clpX*-null background. The *clpX::Tn* mutation may increase our chance of success by preventing $YjbH_{Lm}$ degradation. However, it is worth noting that while the *clpX::Tn* mutation prevents protein degradation, we are unsure of the full implications of looking for $YjbH_{Lm}$ interacting partners in a mutant background.

The co-IP was performed by culturing the aforementioned strain to mid-log phase, lysing by sonication, and using $Ni^{2+}$ resin to separate the StrepII- and 6X-His-tagged $YjbH^{C27S}$ protein. To control for non-specific binding to the resin, wild type *L. monocytogenes* was used in simultaneous and identical co-IPs. The first problem was that much of the tagged $YjbH^{C27S}$ bait remained in the insoluble fraction of the lysate. Second, many rounds of optimization were required to detect $YjbH^{C27S}$ in the elution fraction of the co-IP by immunoblotting. Parameters that were optimized included: changing the $OD_{600}$ at which cultures were harvested; including or omitting the crosslinking agent paraformaldehyde; varying the number and length of rounds of sonication while lysing; varying the volume of packed $Ni^{2+}$ resin to separate $YjbH^{C27S}$; lengthening the incubation period for lysate mixed with $Ni^{2+}$ resin; and including an additional anti-StrepII purification step with eluate from $Ni^{2+}$ resin. The final methods can be found in Chapter 6. In co-IPs that eluted detectable levels of $YjbH^{C27S}$ by immunoblotting, no $YjbH^{C27S}$-specific bands could be detected by SDS-PAGE and silver staining analysis when compared to the wild type control (data not shown). In particular, we did not observe any enrichment in bands around 15 kD, the size of SpxA1. Given the extremely low native abundance of $YjbH_{Lm}$ (Fig. 9), and the low abundance of SpxA1, it is not surprising that we were unable to detect bait-specific bands in a co-IP directly from *L. monocytogenes*. We sought to overcome this problem by increasing the concentration of bait protein, as described in the following section.

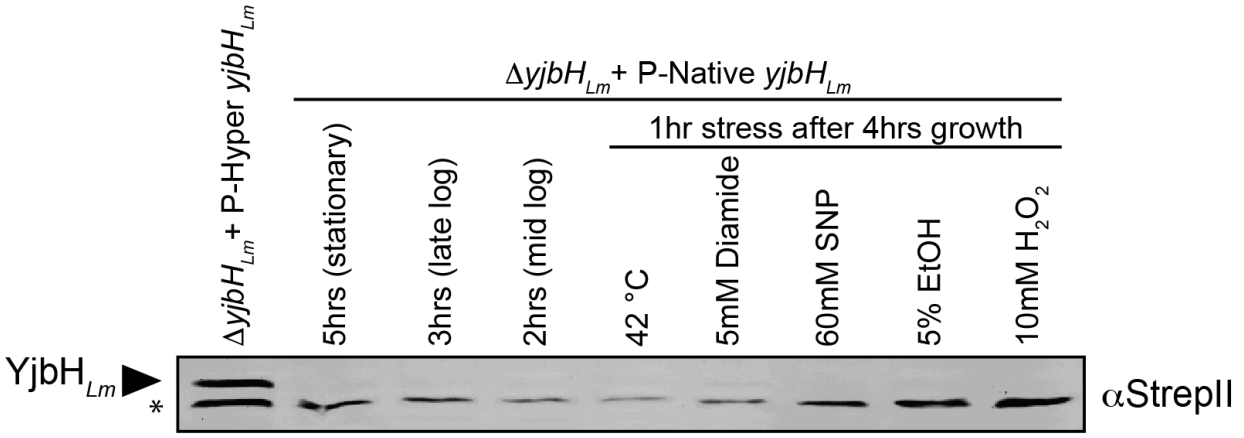


**Figure 9**. Natively expressed $YjbH_{Lm}$ is undetectable by immunoblot. YjbH was detectable when overexpressed from the P-Hyper promoter in the Δ*yjbH*$_{Lm}$ background, shown here at early stationary phase (five hours of growth after subculture). However, $YjbH_{Lm}$ was undetectable when expressed from its native promoter in any growth phase tested and after treatment with heat, diamide, SNP, EtOH, or $H_2O_2$ stress. Cultures were exposed to the stated stressors for 30 minutes (not shown) or one hour in separate trials, with no effect seen on YjbH. This image is representative of three independent experiments. * denotes nonspecific band, which indicates approximately equal loading.

## Recombinant YjbH$_{Lm}$ protein expression

To address the problem of low-abundance bait, we purified recombinant YjbH$_{Lm}$ from *E. coli* and combined that bait protein with *L. monocytogenes* lysate. This would increase the amount of available YjbH$_{Lm}$ for immunoprecipitation. To produce purified wild type YjbH$_{Lm}$ bait protein, we expressed 6X-His-tagged YjbH$_{Lm}$ as a fusion protein with the 43-kD maltose binding protein (MBP) in *E. coli* BL21(DE3) to enhance solubility because of the known instability of YjbH$_{Bs}$[88]. The expression construct was engineered to have a TEV protease site between the two ORFs to obtain purified YjbH$_{Lm}$ by digestion after expression.

The *E. coli* strain carrying the MBP-YjbH$_{Lm}$ expression plasmid was induced during mid-log phase growth to express the recombinant protein. See Chapter 6 for detailed methods. Briefly, induced cultures were lysed by sonication and recombinant protein was collected with $Ni^{2+}$ resin. All pellet, lysate, flowthrough, wash, and elution fractions were analyzed by SDS-PAGE and Coomassie staining (Fig. 10). This purification was successful, as there was a band corresponding to MBP-YjbH$_{Lm}$ in all three elutions with very few non-specific bands in those elutions. The stained gel in Figure 10 shows a relatively large amount of MBP-YjbH$_{Lm}$ separating from the resin with the imidazole-containing washes, but a sufficient amount of relatively pure MBP-YjbH$_{Lm}$ was present in the elutions. Future iterations of this purification could increase the yield, but decrease the purity, of elutions by washing with a higher concentration of imidazole.

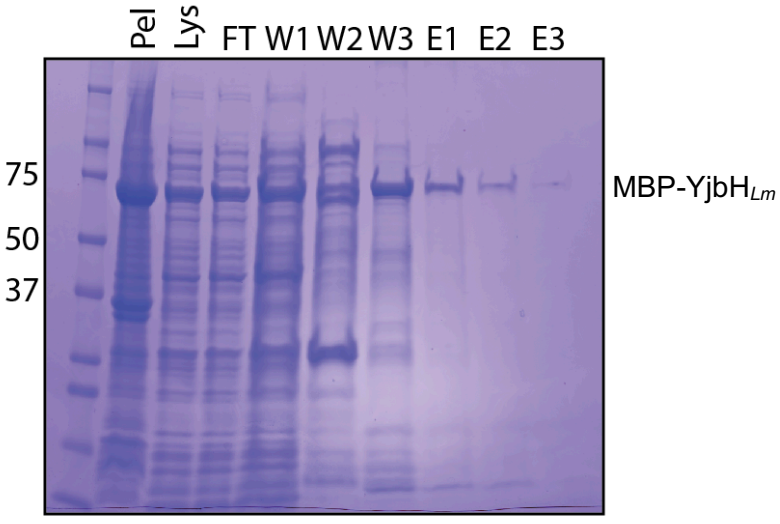


**Figure 10**. Representative Coomassie-stained gel of MBP-YjbH$_{Lm}$ protein purification. Lane 1 is a molecular weight marker with kD sizes denoted on the left side. Samples of the pellet and lysate represent the insoluble and soluble fractions, respectively. Three washes with increasing concentrations of imidazole were performed. Three elutions with imidazole were performed. MBP-YjbH$_{Lm}$ size is noted on the right side.

The three MBP-YjbH$_{Lm}$ elutions were combined before dialysis and concentration, then digested with TEV protease to remove MBP. However, all attempts at TEV digestion resulted in the insolubility of YjbH$_{Lm}$. While this prevented us from purifying YjbH$_{Lm}$ alone, it aligned with what is currently known about the instability of YjbH homologues. YjbH$_{Bs}$ is known to be prone to aggregation and tricky to purify[86,88]. Because YjbH$_{Lm}$ alone was insoluble, full-length MBP-YjbH$_{Lm}$ protein was instead used as bait in these co-IP experiments. To control for the presence of the fusion protein MBP, purified 6X-His-tagged MBP cleaved from MBP-YjbH$_{Lm}$ by TEV protease was used as bait in identical co-IP experiments. The MBP bait would serve to demonstrate non-specific binding to the MBP moiety of MBP-YjbH$_{Lm}$. Soluble MBP-YjbH$_{Lm}$ and MBP were each dialyzed and concentrated with a 50-kD-cutoff filter to approximately 0.3 mg/mL, then checked for purity by SDS-PAGE and Coomassie-staining (data not shown).

### MBP-YjbH$_{Lm}$ complements Δ*yjbH$_{Lm}$* in a plaque assay

Before using MBP and MBP-YjbH$_{Lm}$ as bait in co-IPs, we needed to verify that MBP-YjbH$_{Lm}$ could complement a Δ*yjbH$_{Lm}$* mutant. This would indicate that the normal interactions and functions of YjbH were taking place. To test this, we expressed pPL2.*mbp.yjbH$_{Lm}$* from the predicted native *yjbH$_{Lm}$* promoter at an ectopic locus in the Δ*yjbH$_{Lm}$* background[82]. The Δ*yjbH$_{Lm}$* strain has a significant defect in a plaque assay compared to wild type[40], leading us to question whether MBP-YjbH$_{Lm}$ could complement that defect. Murine fibroblasts were infected and cell-to-cell spread was measured three days post-infection[103]. We found that MBP-YjbH$_{Lm}$ rescued the Δ*yjbH$_{Lm}$* defect (Fig. 11A). This indicated MBP-YjbH$_{Lm}$ retains at least partial function and interaction partners. However, the complementation was not fully back to wild type levels. This partial complementation could suggest that certain interactions are not physically possible when YjbH$_{Lm}$ is expressed as a fusion with MBP.

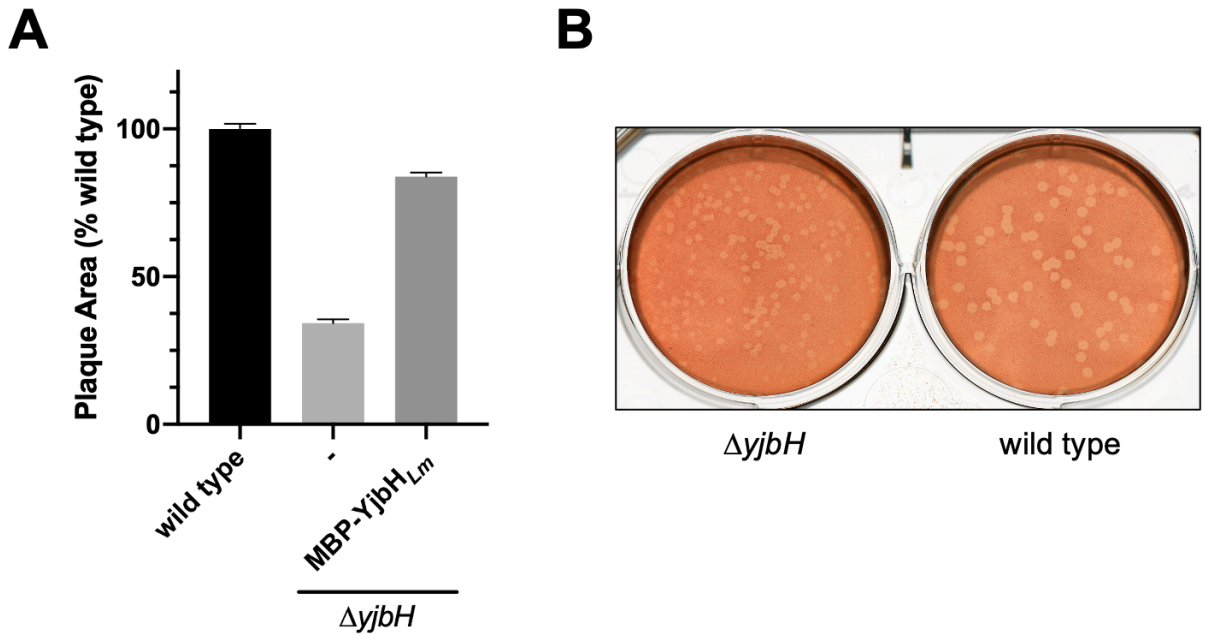


**Figure 11**. MBP-YjbH$_{Lm}$ rescues Δ*yjbH*$_{Lm}$ in a plaque assay**. (A)** Graphed data represent three biological replicates of plaque area in murine L2 cells, normalized to wild type *L. monocytogenes*. **(B)** One representative image of L2 plaques formed by Δ*yjbH*$_{Lm}$ and wild type.

## Co-immunoprecipitations with MBP-YjbH$_{Lm}$ and MBP bait

To identify the proteins YjbH$_{Lm}$ is able to bind in *L. monocytogenes*, we performed co-IPs using 6X-His-MBP-YjbH$_{Lm}$ protein as bait in biological triplicate. We used 6X-His-MBP as control bait. Each bait protein was combined with Δ*yjbH*$_{Lm}$ lysate and incubated with magnetic HisPur Ni-NTA resin for 30 minutes. Full methods can be found in Chapter 6. The bait proteins, lysate, flowthrough, wash, and elution fractions of the MBP and MBP-YjbH$_{Lm}$ co-IPs were analyzed by SDS-PAGE and silver staining (Fig. 12). MBP is purer than MBP-YjbH$_{Lm}$, demonstrated by the nonspecific bands present in the MBP-YjbH$_{Lm}$ bait sample in Figure 12. Two imidazole-containing washes (50 mM and 100 mM) removed loosely- and non-specifically bound proteins from the Ni-NTA resin, and an elution buffer containing 1 M imidazole separated proteins that bound the resin specifically. Promisingly, there appeared to be at least one elution band specific to MBP-YjbH$_{Lm}$ (Fig. 12, asterisk). We used mass spectrometry to compare the proteins eluted with MBP bait and MBP-YjbH$_{Lm}$ bait (Fig. 12, "E" lanes). Because the detected peptides were mapped to the *L. monocytogenes* genome, we reasoned that the relatively impure MBP-YjbH$_{Lm}$ protein would not significantly hinder the results, since the contaminating proteins were of *E. coli* origin.

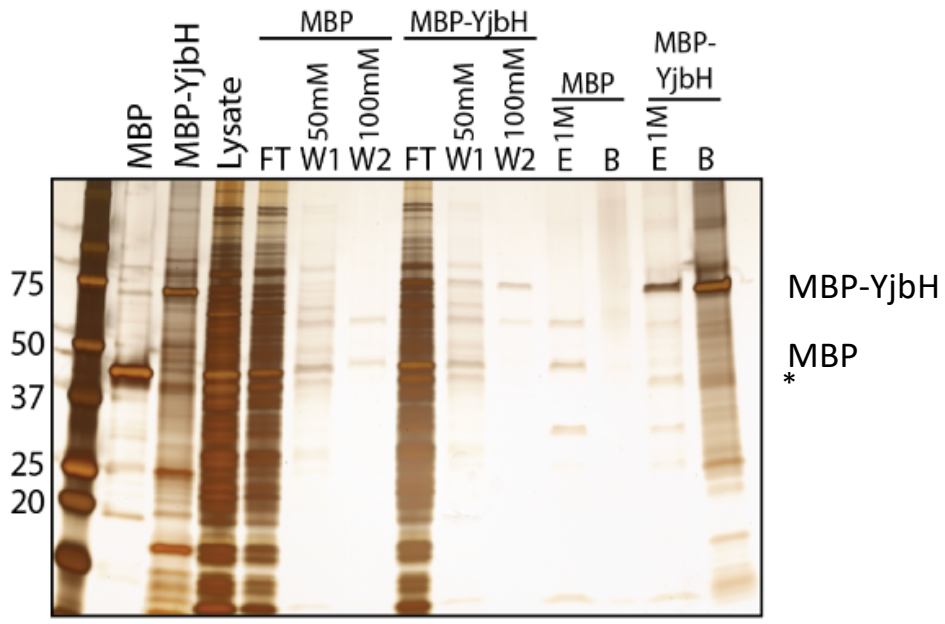


**Figure 12**. SDS-PAGE and silver stain analysis of MBP-YjbH$_{Lm}$ co-IP. Lane 1 is a molecular weight marker with kD sizes denoted on the left side. Lanes 2-3 are purified protein samples. All other fractions are labeled, with the concentration of imidazole noted for the washes and elutions (50 mM, 100 mM, 1 M). Lanes labeled "B" are resin boiled in loading dye after elutions were taken. Sizes of the bait proteins are denoted on the right side. This silver stain represents one out of three biological replicates of the co-IPs. * indicates a band specific to MBP-YjbH.

Table 2 displays the spectral peptide counts of proteins that were pulled down by MBP-YjbH$_{Lm}$, with proteins that were unique to MBP-YjbH$_{Lm}$ samples highlighted in gray. As a proof of concept, YjbH$_{Lm}$ was the most highly abundant protein in these samples. We observed that ClpX, the ATP-binding subunit of the ClpXP protease that degrades Spx in *B. subtilis*[85,86], was included in our list of MBP-YjbH$_{Lm}$ binding partners. However, YjbH$_{Bs}$ has not been found to interact with ClpX by pull-downs or yeast two-hybrid[86,89], and is instead thought to mediate Spx$_{Bs}$ degradation by lowering the conformational entropy of Spx$_{Bs}$[98]. Therefore, we did not follow up with ClpX as a protein of interest.

We followed up on two of the MBP-YjbH$_{Lm}$-specific hits from this co-IP, *lmo2638* and *mntA*. Both of these proteins were only detected in one out of three biological samples, which was true for all proteins that immunoprecipitated with MBP-YjbH$_{Lm}$ bait (Table 2). The only proteins that immunoprecipitated with MBP-YjbH$_{Lm}$ and were not included in Table 2 were four ribosomal proteins that were deemed not biologically significant. To probe for an interaction between MBP-YjbH$_{Lm}$ and Lmo2638, we generated the strain Δ*yjbH*$_{Lm}$ pPL2.P-Hyper.*lmo2638.FLAG* that overexpressed FLAG-tagged *lmo2638*. We combined each bait protein (MBP or MBP-YjbH$_{Lm}$) with lysate from Δ*yjbH*$_{Lm}$ pPL2.P-Hyper.*lmo2638.FLAG* and used

amylose resin to bind to the MBP moiety. A sample of each co-IP fraction was analyzed by SDS-PAGE and immunoblotting (Fig. 13). In this immunoblot, an anti-StrepII antibody was used to detect MBP-YjbH$_{Lm}$, and an anti-FLAG antibody was used to detect Lmo2638. These immunoblots indicate that MBP-YjbH$_{Lm}$ was present in the elution fraction, but Lmo2638 was not. The co-IP was repeated in the same way, and we were still unable to observe an interaction between Lmo2638 and MBP-YjbH$_{Lm}$.

Next, we sought to verify the interaction between MBP-YjbH$_{Lm}$ and another top hit from the mass spectrometry data, the manganese-binding lipoprotein MntA. To do this, we generated a strain of Δ*yjbH*$_{Lm}$ that over-expressed a 6X-His-tagged *mntA* construct and we performed a co-IP as before. We were unable to detect an interaction between MBP-YjbH$_{Lm}$ and MntA in these studies (data not shown).

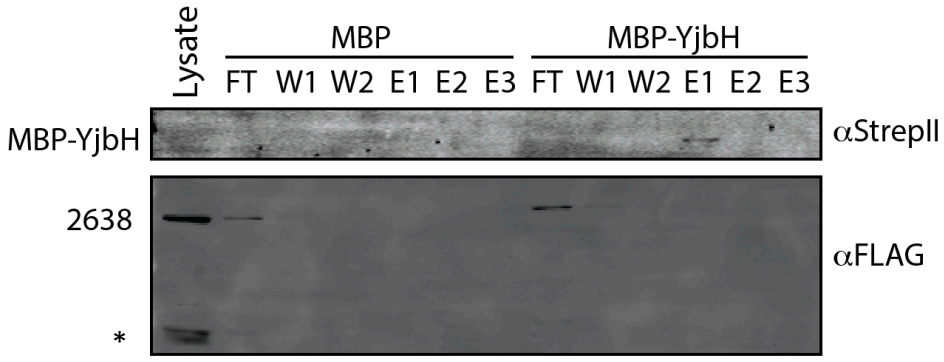


**Figure 13**. Lmo2638 does not interact with MBP-YjbH$_{Lm}$. Flowthrough, wash, and elution fractions are from a co-IP using MBP or MBP-YjbH$_{Lm}$ as bait and Δ*yjbH*$_{Lm}$ pPL2.P-Hyper.*lmo2638.FLAG* as lysate, flowed over amylose resin. This immunoblot is representative of two biological replicates. The anti-strepII antibody detects MBP-YjbH$_{Lm}$ and the anti-FLAG antibody detects Lmo2638. * denotes a non-specific band. Approximate band locations are indicated by the labels along the left side.

**Table 2**. Co-immunoprecipitation identifies proteins that specifically bind MBP-YjbH$_{Lm}$.

| Gene Locus[#] | Predicted Function | Protein | Spectral Peptide Counts (Biological Triplicate) | | |
|---|---|---|---|---|---|
| *lmo0964* | Protease adaptor and predicted thioredoxin protein | YjbH | 82 | 49 | 51 |
| *lmo1268* | Clp protease ATP-binding subunit | ClpX | 5 | 0 | 0 |
| *lmo1847* | Manganese-binding lipoprotein | MntA | 4 | 0 | 0 |
| *lmo2637* | Predicted lipoprotein | PplA | 3 | 0 | 0 |
| *lmo2638* | NADH dehydrogenase (in operon with *lmo2637*) | - | 2 | 0 | 0 |

[#]Genes listed here were only detected in MBP-YjbH$_{Lm}$ samples, not MBP samples.

## Conclusions

Understanding the native interactions of YjbH is central to understanding its cellular function. YjbH$_{Bs}$ is inherently aggregation-prone and therefore tricky to express and purify. This has led groups who study YjbH$_{Bs}$ to purify the protein from inclusion bodies or otherwise use a more stable homologue of YjbH from *G. thermodenitrificans* or *G. kaustophilus*. It was our goal to use the native YjbH$_{Lm}$ protein to identify interacting partners, as this will help us to understand the nuances of YjbH function specific to *L. monocytogenes*. However, we found that we could not detect YjbH$_{Lm}$-interacting proteins by SDS-PAGE and silver stain analysis after performing a co-IP directly from *L. monocytogenes*. It is possible that analyzing these co-IP elution fractions by mass spectrometry could have revealed interacting partners, like SpxA1, which may not have been visible by eye on a silver-stained gel. We surmised that a low concentration of bait protein could be hindering our attempts at co-IPs, leading us to instead purify recombinant MBP-YjbH$_{Lm}$ from *E. coli* to use as bait in *L. monocytogenes* lysate. The resulting elution fractions from this co-IP were analyzed by mass spectrometry.

Several major system limitations exist that prevented the initial success of these co-IP experiments. First, YjbH$_{Lm}$ is present at an extremely low abundance in *L. monocytogenes* and is unstable, such that over-expressing the protein results in the majority being insoluble and therefore challenging in a co-IP. Second, we were unable to successfully purify soluble YjbH$_{Lm}$ as bait without a large solubility fusion protein. We performed a co-IP with MBP-YjbH$_{Lm}$ as bait and analyzed the results with mass spectrometry, although our attempts to follow up on the top hits revealed that there was likely a high degree of non-specific binding.

While we cannot make any definitive conclusions about the interactions of YjbH$_{Lm}$ from these experiments, it could be very informative to return to these mass spectrometry data in the future as a supplement to the protein-protein interaction data presented in Chapter 3. For example, now that we have a bacterial two-hybrid assay set up for our system, we can use that technique to verify individual proteins of interest detected in this co-IP. In the bacterial two-hybrid experiments presented in Chapter 3, ClpX was not found to interact with YjbH$_{Lm}$. Therefore, we think it possible that the detection of ClpX in this immunoprecipitation is likely an artifact of using a fusion protein as bait. However, there may still be biologically significant proteins on this list and therefore it is a worthy endeavor to follow up with this list in future experiments.

We have shown here that, similar to what has been reported for YjbH$_{Bs}$, the YjbH$_{Lm}$ homologue is inherently unstable and prone to aggregation. Additionally, these experiments have shed light on the unique parameters of our system that differ from *B. subtilis* and *S.*

*aureus*. In the latter two species, YjbH is abundant enough during normal growth conditions that it can be easily detected by immunoblotting. Regulation of YjbH in *L. monocytogenes* appears to be different enough that $YjbH_{Lm}$ cannot be detected during normal growth unless *clpX* is disrupted, or $yjbH_{Lm}$ is over-expressed from a strong promoter. This knowledge has informed the experiments described in the following chapters and heightened our understanding of the basic characteristics of $YjbH_{Lm}$.

# Chapter 3: YjbH requires its thioredoxin active motif for the nitrosative stress response, cell-to-cell spread, and protein-protein interactions in *Listeria monocytogenes*

## Introduction

Despite its importance to virulence in *L. monocytogenes,* $YjbH_{Lm}$ and its function had not been investigated before this study. Here, we aimed to elucidate its role. *L. monocytogenes* encodes SpxA1, which is 83% identical in amino acid sequence to $Spx_{Bs}$. We showed that $YjbH_{Lm}$ interacted with SpxA1 and was involved in the nitrosative stress response. Additionally, whole-cell mass spectrometry revealed ten proteins with increased abundance in a $\Delta yjbH_{Lm}$ mutant. We found that $YjbH_{Lm}$ physically interacted with nine of these proteins. Interestingly, our work demonstrated that $YjbH_{Lm}$ uniquely requires its CxxC motif cysteine residues for function, unlike homologues in other species[104].

## Results

### *L. monocytogenes* YjbH

*L. monocytogenes* encodes a YjbH homologue that shares 39% and 30% amino acid identity with homologues from *B. subtilis* and *S. aureus*, respectively (Fig. 7). All three homologues have a predicted thioredoxin domain at the N-terminus and a C-terminal domain of unknown function. A notable difference at the amino acid level between homologues is the presence of cysteine residues. *B. subtilis* and *L. monocytogenes* YjbH share a thioredoxin active motif (CxxC), while $YjbH_{Sa}$ lacks this motif and instead has SxxC and CxC motifs.

The *B. subtilis* and *S. aureus yjbH* genomic loci are quite conserved with regards to *spx*, the protein product of which is a known interacting partner of YjbH[86,89]. *spx* is encoded near *yjbH* in both *B. subtilis* and *S. aureus* (Fig. 4). Interestingly, while there is synteny downstream of $yjbH_{Lm}$, the region upstream of the $yjbH_{Lm}$ locus is highly dissimilar to *B. subtilis* and *S. aureus*. Most notably, $yjbH_{Lm}$ (*lmo0964*) is not encoded near the *spx* homologue (*spxA1*, *lmo2191*) as it is in the other two species. These protein similarities and genomic differences led us to question if the function of YjbH is conserved in *L. monocytogenes*.

### *B. subtilis* YjbH functionally complements *L. monocytogenes* $\Delta yjbH$

$YjbH_{Bs}$ was first identified because the $\Delta yjbH_{Bs}$ mutant was more sensitive to the nitrosative stressor sodium nitroprusside (SNP)[80]. Therefore, we first examined the role of $YjbH_{Lm}$ in *L. monocytogenes* SNP resistance using a minimum inhibitory concentration (MIC) assay that tested growth in 20 mM increments of SNP from 0 to 120 mM. Contrary to what has

been shown in both *B. subtilis* and *S. aureus*[79,80], Δ*yjbH*$_{Lm}$ was significantly more resistant to SNP than wild type (Fig. 14A). To test the conservation of YjbH homologues across species, *yjbH*$_{Bs}$ was expressed from the predicted *yjbH*$_{Lm}$ native promoter at an ectopic locus in the *L. monocytogenes* Δ*yjbH* genome[82]. Expression of *yjbH*$_{Bs}$ complemented the Δ*yjbH*$_{Lm}$ mutant (Fig. 2A), suggesting that despite the species' disparate phenotypes, essential functions of YjbH are conserved.

We next tested whether YjbH$_{Bs}$ could functionally complement the Δ*yjbH*$_{Lm}$ mutant during infection using a plaque assay. Murine fibroblasts were infected and cell-to-cell spread was measured three days post-infection[103]. The Δ*yjbH*$_{Lm}$ mutant formed plaques approximately 60% smaller than those formed by wild type, indicating it is defective for cell-to-cell spread, as previously reported[40]. The Δ*yjbH*$_{Lm}$ strain expressing the *yjbH*$_{Bs}$ allele formed plaques approximately the size of wild type (Fig. 14B), demonstrating that YjbH$_{Bs}$ is functional in *L. monocytogenes* during infection of mammalian cells.

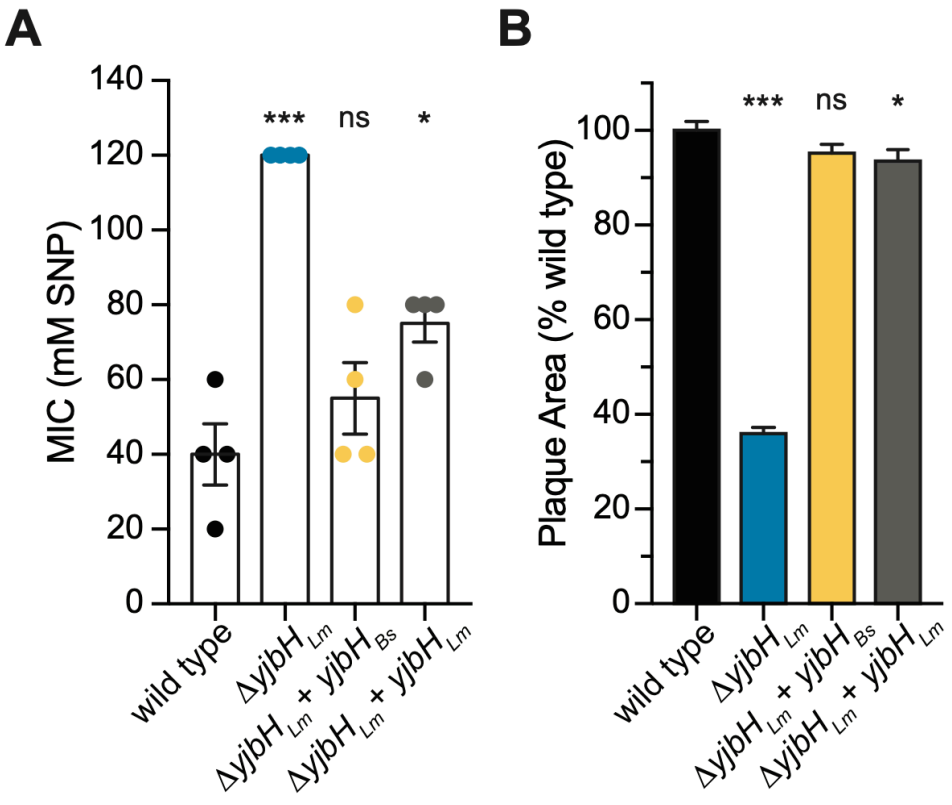


**Figure 14**. YjbH$_{Bs}$ functionally complements Δ*yjbH*$_{Lm}$ for SNP sensitivity and cell-to-cell spread. **(A)** Sensitivity to sodium nitroprusside (SNP) was measured by MIC in tryptic soy broth at 37 °C. Data represent three biological replicates graphed as means and standard error of the mean (SEM). **(B)** Plaque area in murine L2 cells, normalized to wild type *L. monocytogenes*. Data represent three biological replicates graphed as means and SEMs. In both panels, mutant strains are compared to wild type by Student's unpaired *t*-test (ns, $p > 0.05$; *, $p < 0.05$; ***, $p < 0.001$).

### *L. monocytogenes* YjbH and SpxA1 interact

In other *Firmicutes*, the physical interaction between YjbH and Spx is critical for the bacteria to maintain redox homeostasis[86,87,98]. Expression of *yjbH*$_{Bs}$ in the Δ*yjbH*$_{Lm}$ background restored its SNP sensitivity to wild type levels, leading us to hypothesize that the interaction with the *L. monocytogenes* Spx homologue (SpxA1) may also be conserved. As detailed in Chapter 2, we attempted to perform a co-IP to test for interactions between YjbH$_{Lm}$ and SpxA1. However, because both proteins are present in extremely low abundance in *L. monocytogenes* and YjbH proteins are prone to aggregation[87,88], we were unable to detect an interaction. Instead, we used the bacterial adenylate cyclase two-hybrid (BACTH) system, in which proteins of interest are heterologously expressed in *E. coli* BTH101 cells as fusion proteins with the *Bordetella pertussis* adenylate cyclase T18 and T25 domains[105,106]. BTH101 strains used in these assays harbor both T18 and T25 fusion protein plasmids and if the proteins of interest interact, cAMP is produced, leading to β-galactosidase production.

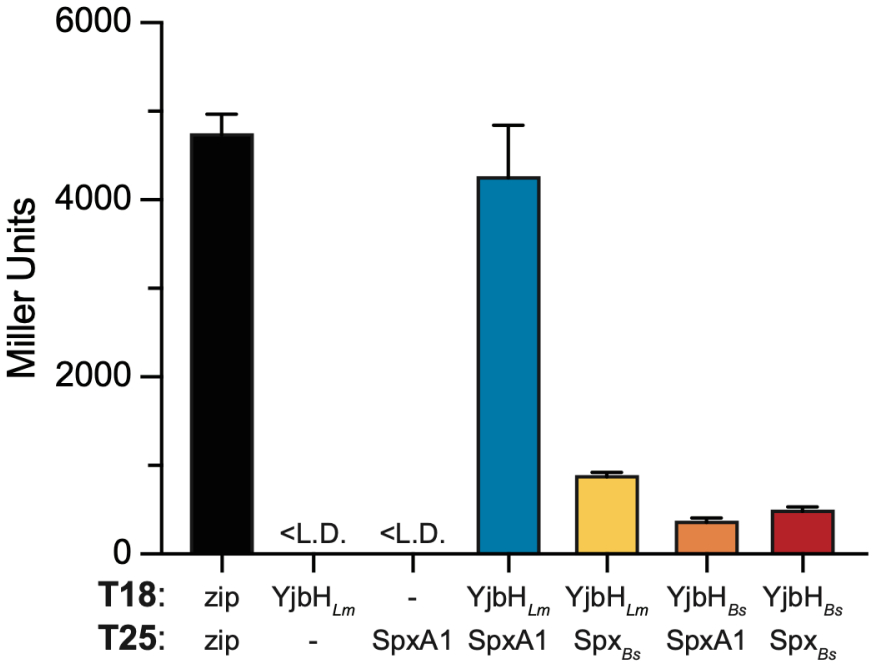


**Figure 15**. *L. monocytogenes* YjbH$_{Lm}$ and SpxA1 physically interact. Interaction was measured by BACTH assay of overnight cultures of LB broth. The positive control is T18 and T25 each fused to a leucine zipper region, and negative controls are YjbH$_{Lm}$-T18 with T25 alone and SpxA1-T25 with T18 alone. Data represent three biological replicates graphed as means and SEMs with the exception of the SpxA1-T25 with T18 negative control, which represents two biological replicates.

BTH101 cells harboring YjbH$_{Lm}$-T18 and SpxA1-T25 expression plasmids grown overnight in rich broth demonstrated that YjbH$_{Lm}$ and SpxA1 physically interact (Fig. 15). This interaction was specific, as no interaction was detected either between YjbH$_{Lm}$ and the T25 domain alone, or SpxA1 and the T18 domain alone. Because expressing the *yjbH*$_{Bs}$ allele functionally complemented the Δ*yjbH*$_{Lm}$ mutant, we next investigated interactions between the *L. monocytogenes* and *B. subtilis* proteins. We observed that YjbH$_{Lm}$ interacted with Spx$_{Bs}$, and that YjbH$_{Bs}$ interacted with SpxA1, confirming that this important physical interaction is conserved between *L. monocytogenes* and *B. subtilis* proteins (Fig. 15). We also observed an interaction between YjbH$_{Bs}$ and Spx$_{Bs}$, as previously reported[86,89].

**YjbH$_{Lm}$ and SpxA1 are involved in the nitrosative stress response and LLO regulation**

The only documented role for YjbH in *Firmicutes* is to modulate levels of Spx such that a strain lacking *yjbH* has increased Spx abundance[85,86,90]. The physical interaction between YjbH$_{Lm}$ and SpxA1 was conserved in *L. monocytogenes*, leading us to question if the phenotypes associated with the Δ*yjbH*$_{Lm}$ strain are SpxA1-dependent. The roles of *yjbH*$_{Lm}$ and *spxA1* were first examined in an SNP MIC assay. An *spxA1* knockdown strain (*P-spxA1::Tn*) that expresses 10-fold less *spxA1* transcript was used for these experiments, as a strain deleted for *spxA1* does not grow in the presence of oxygen[76]. The *spxA1* knockdown strain grows aerobically and is more sensitive to hydrogen peroxide and diamide[40], but has not yet been tested in the presence of SNP. While the Δ*yjbH*$_{Lm}$ mutant was 3-fold more resistant to SNP, *P-spxA1::Tn* was much more sensitive to SNP than wild type (Fig. 16A). If Δ*yjbH*$_{Lm}$ was more resistant to SNP due to increased SpxA1 abundance, as in other *Firmicutes*, then knocking down *spxA1* would restore Δ*yjbH*$_{Lm}$ sensitivity to wild type levels. Indeed, the MIC of the Δ*yjbH*$_{Lm}$ *P-spxA1::Tn* strain was similar to that of wild type (Fig. 16A). These data suggested that the increased resistance of Δ*yjbH*$_{Lm}$ to SNP was due to increased SpxA1 abundance.

In addition to its role in the nitrosative stress response, *yjbH*$_{Lm}$ is required for LLO production and/or secretion[40,78]. The virulence factor LLO is essential for *L. monocytogenes* to escape the phagosome during infection and is also expressed at low levels during growth in rich broth. We examined whether the Δ*yjbH*$_{Lm}$ defect in LLO secretion is SpxA1-dependent by analyzing immunoblots of secreted proteins in broth. As previously published[40] both the Δ*yjbH*$_{Lm}$ and *P-spxA1::Tn* mutants secreted less LLO than wild type *in vitro* (Fig. 16B). LLO secretion in the double mutant was not significantly different from the *spxA1* knock-down strain, suggesting that the LLO secretion defect of Δ*yjbH*$_{Lm}$ is not solely SpxA1-dependent (Fig. 16C). We hypothesized that the LLO defect in Δ*yjbH*$_{Lm}$ happens at the level of translation or secretion.

Indeed, hly transcript abundance was unchanged from wild type (1.1-fold change in Δ*yjbH*$_{Lm}$ compared to wild type, $p = 0.76$). The observation that the YjbH$_{Lm}$-dependent post-translational regulation of LLO may not entirely be explained by SpxA1 levels led us to speculate that YjbH$_{Lm}$ may interact with additional proteins in *L. monocytogenes*.

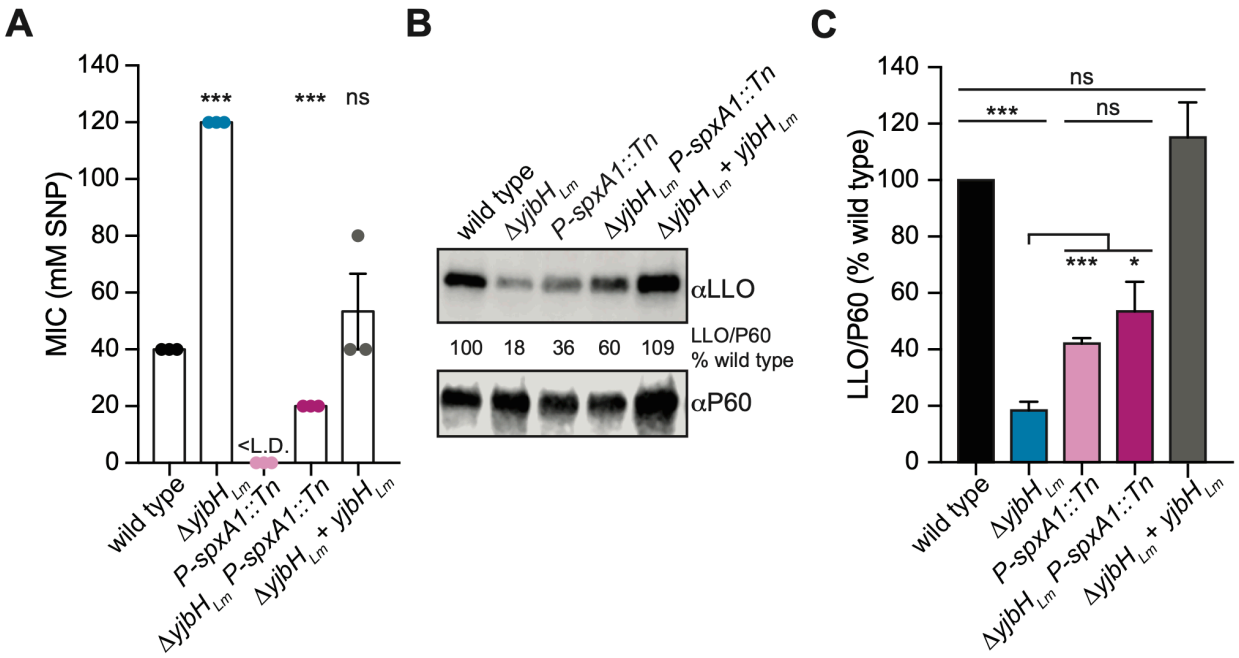


**Figure 16**. YjbH$_{Lm}$ and SpxA1 are involved in the nitrosative stress response and LLO regulation. **(A)** Sensitivity to SNP was measured by MIC in tryptic soy broth at 37 °C. *P-spxA1::Tn* transcribes 10-fold less *spxA1* than wild type and grows aerobically. Data represent three biological replicates graphed as means and SEMs. <L.D. indicates the MIC was below the limit of detection. All mutant strains are compared to wild type by Student's unpaired *t*-test (ns, $p > 0.05$; ***, $p < 0.001$). **(B)** One representative immunoblot of LLO secretion measured in cultures grown in BHI broth at 37 °C. The protein P60 was used as a loading control. Immunoblots were analyzed by calculating the ratio of LLO/P60 as a percent of wild type. **(C)** Quantification of three biological replicates of LLO secretion shown in **B**, graphed as means and SEMs. All statistical analyses are Student's unpaired *t*-tests (ns, $p > 0.05$; *, $p < 0.05$; ***, $p < 0.001$).

## Whole-cell proteomic profiling of *L. monocytogenes* Δ*yjbH*

Given the known role of YjbH$_{Bs}$ as a protease adaptor, we sought to determine whether YjbH$_{Lm}$ is involved in the regulation of proteins other than SpxA1 in *L. monocytogenes*. YjbH$_{Lm}$ abundance was first investigated in various growth conditions to identify ideal parameters for this analysis. As described in Chapter 2, native YjbH$_{Lm}$ was undetectable in all conditions tested, including elevated temperature and treatment with sublethal concentrations of ethanol, diamide, SNP, or hydrogen peroxide (Fig. 9). Therefore, early stationary phase was selected for proteomic analysis due to the pronounced LLO phenotype exhibited by the Δ*yjbH*$_{Lm}$ strain in rich broth at this time point (Fig. 16B and 16C), indicating that YjbH$_{Lm}$ is likely functional in this

growth condition. Whole-cell proteomic profiling was used as an unbiased approach to identify proteins with altered abundance in Δ*yjbH*$_{Lm}$. Cultures were prepared in biological triplicate and proteins were analyzed by LC-MS/MS. The fold change of average peptide spectral counts was calculated between wild type and Δ*yjbH*$_{Lm}$ samples, and analyzed with Student's *t*-test.

We focused on the nine proteins significantly more abundant in Δ*yjbH*$_{Lm}$ than wild type (Table 3). SpxA1 was also more abundant in Δ*yjbH*$_{Lm}$, although this change was not statistically significant due to its complete absence in wild type samples and the variability of peptide counts between Δ*yjbH*$_{Lm}$ replicates. These data demonstrated for the first time that SpxA1$_{Lm}$ is more abundant in the absence of *yjbH*$_{Lm}$, supporting the hypothesis that YjbH$_{Lm}$ functions similarly to YjbH$_{Bs}$ with respect to regulating SpxA1 abundance[85,86]. To assess whether the observed changes in protein concentration were the result of transcriptional or post-transcriptional regulation, quantitative RT-PCR was performed comparing gene expression in wild type and Δ*yjbH*$_{Lm}$ cultures (Fig. 17A). Five transcripts (*lmo1258, lmo1387, lmo1636, lmo1782, lmo2390*) were significantly more abundant in Δ*yjbH*$_{Lm}$ than wild type, suggesting that increased protein concentration may result from transcriptional regulation. It is possible these five genes are also post-transcriptionally regulated to result in increased protein levels. Five genes (*spxA1, lmo0218, lmo0256, lmo0597, lmo1647*) were expressed at or below wild type levels in Δ*yjbH*$_{Lm}$, indicating the increases in protein abundance observed by mass spectrometry were not due to transcriptional regulation. These results suggested that YjbH$_{Lm}$ is involved in the post-transcriptional or post-translational regulation of multiple proteins in *L. monocytogenes*.

## YjbH interacts with multiple *L. monocytogenes* proteins

Bacterial adenylate cyclase two-hybrid (BACTH) assays were next used to test the hypothesis that YjbH$_{Lm}$ function in *L. monocytogenes* involves direct interaction with proteins in addition to SpxA1. BTH101 strains were generated that each harbored a plasmid expressing YjbH$_{Lm}$-T18 in addition to a plasmid expressing a T25 fusion with each of the proteins listed in Table 3. We were unable to express *lmo0597* in *E. coli*, and therefore could not test for an interaction with YjbH$_{Lm}$. Interestingly, BACTH assays revealed a physical interaction between YjbH$_{Lm}$ and each of the eight proteins identified by mass spectrometry as more abundant in the Δ*yjbH*$_{Lm}$ strain (Fig. 17B). Some chaperone proteins are known to interact with the ATPase and substrate-binding subunit of the protease as well as with the protein substrate[107]. ClpC and ClpX ATPase subunits have both been implicated in Spx$_{Bs}$ degradation in *B. subtilis*, though YjbH$_{Bs}$-mediated Spx$_{Bs}$ degradation is specific to ClpXP[86,108]. However, we were unable to detect an interaction between YjbH$_{Lm}$ and ClpC or ClpX by BACTH (Fig. 17B). Together, these results

indicated that YjbH$_{Lm}$ is able to physically interact with at least nine *L. monocytogenes* proteins, including SpxA1.

**Table 3**. Whole-cell proteomics revealed proteins more abundant in Δ*yjbH*$_{Lm}$ than wild type.

| Gene Locus | Predicted Function | Protein | Wild Type [a] | Δ*yjbH*$_{Lm}$[a] | *p*-value |
|---|---|---|---|---|---|
| *lmo0218* | Polyribonucleotide nucleotidyltransferase domain | - | 1.53 | 3.68 | 0.006 |
| *lmo0256* | S-adenosylmethionine-dependent methyltransferase activity | - | 1.22 | 3.00 | 0.045 |
| *lmo0597* | Crp/Fnr-family transcriptional regulator | - | 0.31 | 2.24 | 0.006 |
| *lmo1258* | Putative lipase | - | n.d. | 2.82 | 0.028 |
| *lmo1387* | Pyrroline-5-carboxylate reductase | - | 0.61 | 2.68 | 0.045 |
| *lmo1636* | ABC transporter ATP-binding protein | - | 2.14 | 4.47 | 0.011 |
| *lmo1647* | 1-acylglycerol-3-phosphate O-acyltransferase | - | 0.61 | 2.56 | 0.007 |
| *lmo1782* | 3'-exo-deoxyribonuclease | - | 1.23 | 3.93 | 0.009 |
| *lmo2191* | Transcriptional regulator | SpxA1 | n.d. | 2.76 | 0.214 |
| *lmo2390* | Ferredoxin-NADP reductase 2 | - | 2.45 | 5.94 | 0.005 |

[a] average spectral peptide counts from three independent samples are listed. n.d. indicates no peptides were detected. Genes included in this Table were at least 2-fold more abundant in Δ*yjbH*$_{Lm}$ than wild type and statistically significant, with the exception of SpxA1, which was not statistically significant.

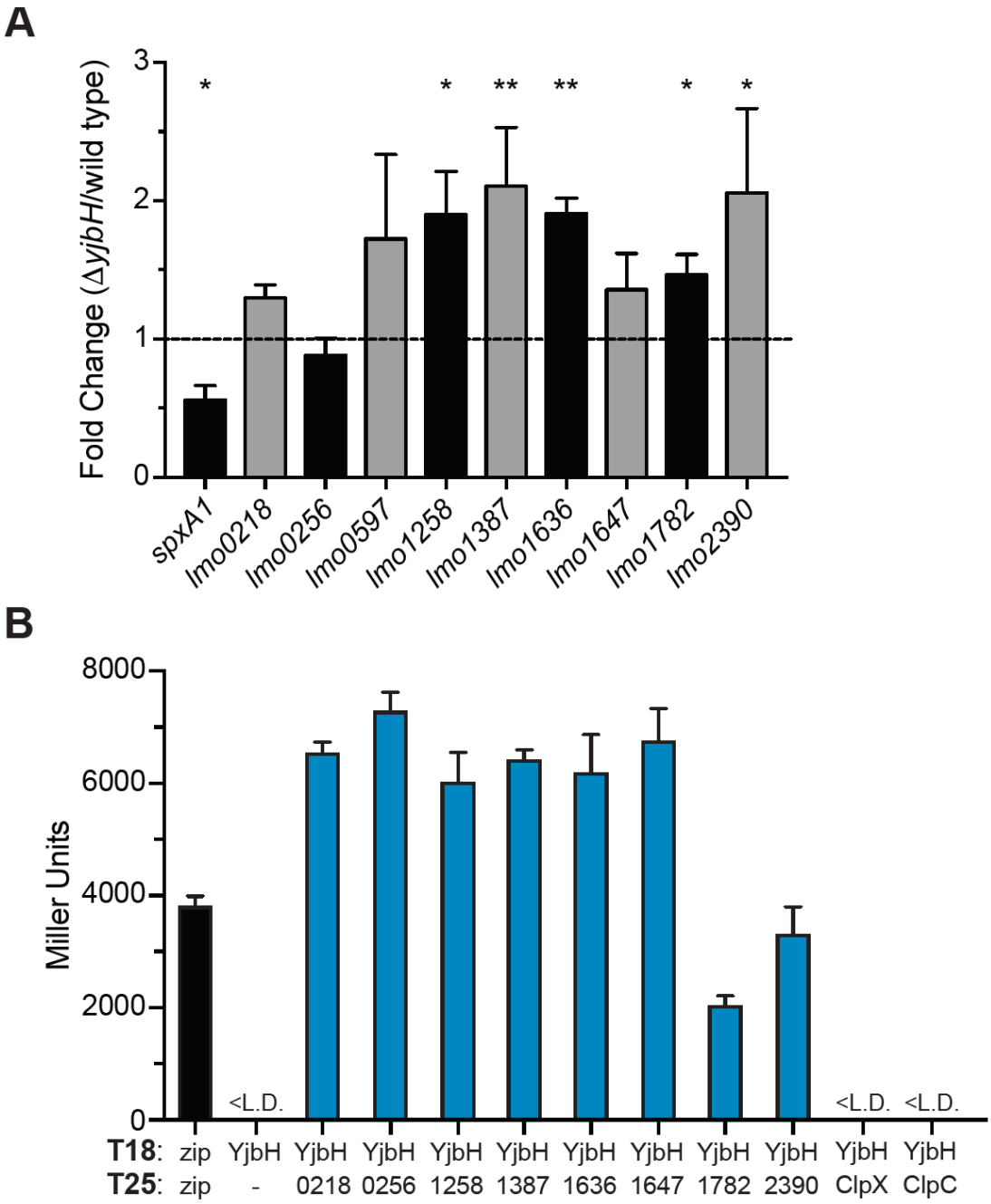


**Figure 17**. YjbH$_{Lm}$ interacts with multiple *L. monocytogenes* proteins. **(A)** Gene expression was measured in wild type and Δ*yjbH*$_{Lm}$ by qRT-PCR and are graphed as the fold change in Δ*yjbH*$_{Lm}$ compared to wild type. Student's unpaired *t*-test was used to compare transcript fold change between Δ*yjbH*$_{Lm}$ and wild type (ns, $p > 0.05$; *, $p < 0.05$; **, $p < 0.01$). **(B)** Interactions with YjbH$_{Lm}$ were measured by BACTH assay of overnight cultures of LB broth. T25 fusion proteins are labeled with their *lmo* locus number or protein name. Data represent three biological replicates graphed as means and SEMs. <L.D. indicates Miller Units below the limit of detection.

**YjbH cysteine residues influence function and protein-protein interactions**

Although all YjbH homologues have a thioredoxin-like domain, and many have a CxxC catalytic motif (Fig. 7), it remains unknown whether thioredoxin activity is important for YjbH function in *L. monocytogenes*. Canonical thioredoxin activity involves a transient intermolecular disulfide bond between the thioredoxin CxxC motif and substrate proteins. To test the role of the four cysteine residues of YjbH$_{Lm}$, Δ*yjbH*$_{Lm}$ strains were engineered to express *yjbH*$_{Lm}$ encoding cysteine-to-alanine point mutations from the predicted *yjbH*$_{Lm}$ native promoter (Table 5, Chapter 6). These strains include each of the four cysteines mutated individually (YjbH$^{C27A}$, YjbH$^{C30A}$, YjbH$^{C63A}$, YjbH$^{C89A}$), as well as a mutated CxxC motif (YjbH$^{C27/30A}$), both cysteines outside the CxxC motif mutated (YjbH$^{C63/89A}$), and all four cysteine residues mutated (YjbH$^{\Delta cys}$). The mutant YjbH$_{Lm}$ proteins were as abundant as wild type YjbH$_{Lm}$ when over-expressed (Fig. 18), indicating that the cysteine-to-alanine substitutions did not affect overall protein stability.

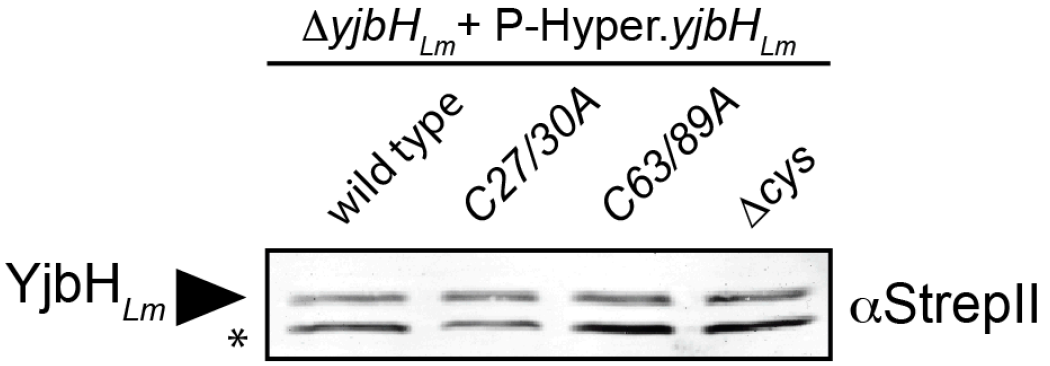


**Figure 18**. YjbH cysteine mutants are equally as stable as wild type YjbH. YjbH, YjbH$^{C27/30A}$, YjbH$^{C63/89A}$, and YjbH$^{\Delta cys}$ are all overexpressed in a Δ*yjbH*$_{Lm}$ background. This is a representative image of three independent experiments. All single cysteine mutants phenocopied their corresponding double mutant in plaque assays, SNP sensitivity, and LLO secretion, and therefore only the double mutants and the quadruple mutant were tested for stability here. * denotes nonspecific band, which indicates approximately equal loading.

To investigate the role of the cysteine residues in YjbH$_{Lm}$ function, the aforementioned mutants were tested for cell-to-cell spread by plaque assay, nitrosative stress resistance via SNP MIC assay, and LLO secretion by immunoblot. The data revealed that YjbH$^{C63A}$, YjbH$^{C89A}$, and YjbH$^{C63/89A}$ fully complemented the Δ*yjbH*$_{Lm}$ mutant for cell-to-cell spread (Fig. 19A, dark purple bars), SNP resistance (Fig. 19B), and LLO secretion (Fig. 19C and 19D). However, all strains with mutations in the CxxC motif failed to fully rescue the Δ*yjbH*$_{Lm}$ phenotypes (Fig. 19A-

D, lavender bars). These data suggested that the CxxC motif is required for YjbH$_{Lm}$ function in the context of the known phenotypes, while the other two cysteine residues are dispensable.

We next used BACTH assays to assess whether the YjbH$_{Lm}$ cysteine residues are required for protein-protein interactions. YjbH$^{C63/89A}$ retained interactions with all tested proteins except SpxA1 and Lmo0218 (Fig. 19E). The protein with altered CxxC motif (YjbH$^{C27/30A}$) interacted only with Lmo1258 and Lmo1387 (Fig. 19E). Together, these results demonstrated that YjbH$_{Lm}$ cysteine residues are required for its physical interaction with some proteins.

As described previously, the CxxC motifs of thioredoxin domains are known to form transient intermolecular disulfide bonds with substrate proteins. Of those tested here, only the following proteins contain cysteine residues: SpxA1, Lmo0256, Lmo1258, Lmo1387, Lmo1782, and Lmo2390 (Fig. 6E, underlined). If intermolecular disulfide bonds involving the CxxC motif were essential for YjbH$_{Lm}$ to interact with any of the cysteine-containing proteins, we would expect the interacting proteins to bind wild type YjbH$_{Lm}$ protein but not the YjbH$^{C27/30A}$ mutant. The observation that YjbH$^{C27/30A}$ could still bind two proteins suggested that YjbH$_{Lm}$ can interact with proteins at a site other than the CxxC motif. These results demonstrated that not all YjbH$_{Lm}$ protein interactions require intermolecular disulfide bond formation, as is typical for thioredoxins. However, we can't rule out a role for disulfide bonds in all interactions.

**Figure 19**. (Following page) Cysteine residues contribute to YjbH$_{Lm}$ function. **(A)** Plaque area in murine L2 cells, normalized to wild type *L. monocytogenes*. Data represent three biological replicates graphed as means and SEMs. **(B)** Sensitivity to SNP was measured by MIC in tryptic soy broth at 37 °C. Data represent three biological replicates graphed as means and SEMs. **(C)** One representative immunoblot of LLO secretion, measured as in Figure 4C. **(D)** Graphed data represent three biological replicates of LLO secretion shown in **C**, graphed as means and SEMs. **(E)** Interactions with YjbH$^{C27/30A}$ (lavender bars) and YjbH$^{C63/89A}$ (dark purple bars) were by BACTH assay as in Figure 5B. Gene names that are underlined encode proteins with at least one cysteine residue. <L.D. indicates Miller Units below the limit of detection. Data represent three biological replicates graphed as means and SEMs. In panels **A, B,** and **D**, Student's *t*-test was used to compare lavender bars to Δ*yjbH*$_{Lm}$, and dark purple bars to wild type (ns, $p > 0.05$; *, $p < 0.05$; **, $p < 0.01$; ***, $p < 0.001$).

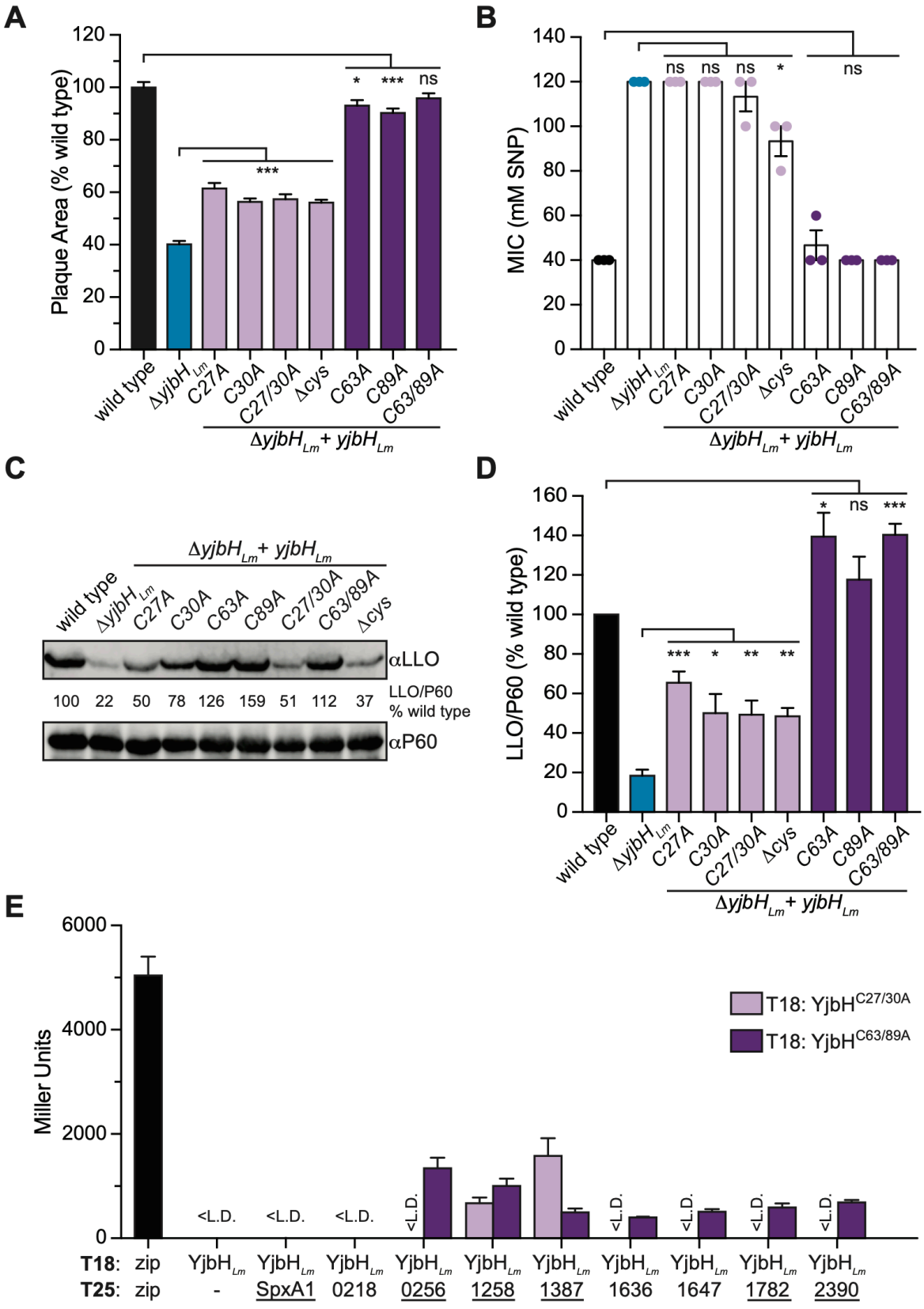
A
Plaque Area (% wild type)
wild type
ΔyjbH Lm
C27A
C30A
C27/30A
Δcys
C63A
C89A
C63/89A
ΔyjbH Lm + yjbH Lm
B
MIC (mM SNP)
C
αLLO
LLO/P60
% wild type
100 22 50 78 126 159 51 112 37
αP60
D
LLO/P60 (% wild type)
E
Miller Units
T18: YjbH C27/30A
T18: YjbH C63/89A
<L.D.
T18: zip YjbH Lm YjbH Lm YjbH Lm YjbH Lm YjbH Lm YjbH Lm YjbH Lm YjbH Lm YjbH Lm YjbH Lm
T25: zip - SpxA1 0218 0256 1258 1387 1636 1647 1782 2390

## Conclusions

In this study, we investigated the role of the annotated thioredoxin YjbH$_{Lm}$ in *L. monocytogenes*. Strains lacking *yjbH$_{Lm}$* do not have a growth defect intracellularly or in rich broth, but exhibit defects in cell-to-cell spread, the production of ActA and LLO, and are attenuated in a mouse model of infection[40]. Our results demonstrated that YjbH$_{Lm}$ physically interacts with the redox-responsive transcriptional regulator SpxA1, and that Δ*yjbH$_{Lm}$* is more resistant to nitrosative stress than wild type in an SpxA1-dependent manner. This study also presented data that suggest a possible SpxA1-independent role for YjbH$_{Lm}$ in LLO secretion. Whole-cell proteomics provided a more holistic picture of the scope of YjbH$_{Lm}$ function, revealing several proteins whose abundance was YjbH$_{Lm}$-dependent. Further, eight proteins that were more abundant in Δ*yjbH$_{Lm}$* physically interacted with YjbH$_{Lm}$ in BACTH assays. The interactions of YjbH$_{Lm}$ with SpxA1 and six other proteins were disrupted in the absence of an intact YjbH$_{Lm}$ CxxC motif. Results from this study demonstrated that YjbH$_{Lm}$ requires its thioredoxin active motif for SNP sensitivity, cell-to-cell spread, and LLO secretion, and that YjbH$_{Lm}$ plays a role in the post-translational regulation of several proteins.

In *B. subtilis*, YjbH$_{Bs}$ physically interacts with Spx$_{Bs}$ to accelerate degradation of Spx$_{Bs}$ by the ClpXP protease[86]. The results presented here suggest that YjbH$_{Lm}$ functions similarly as a protease adaptor for SpxA1. First, BACTH assays demonstrated a physical interaction between YjbH$_{Lm}$ and SpxA1. YjbH$_{Lm}$ did not interact with the protease substrate-binding subunits ClpC or ClpX, although this was consistent with YjbH$_{Bs}$, which does not physically interact with ClpX[87]. These data are more rigorous than the co-immunoprecipitation data presented in Chapter 2 that suggested an MBP-YjbH$_{Lm}$-ClpX interaction. We predict that, as in *B. subtilis*, YjbH$_{Lm}$ acts as an adaptor by lowering the conformational entropy of SpxA1, thereby increasing the efficiency of SpxA1 binding to ClpX[98]. This is the most likely hypothesis, given that SpxA1 shares 83% amino acid identity with Spx$_{Bs}$ and expressing *spx$_{Bs}$* functionally complements the Δ*spxA1* mutant[76]. The second piece of evidence that YjbH$_{Lm}$ is a protease adaptor for SpxA1 comes from whole-cell proteomics, which revealed increased SpxA1 protein in the Δ*yjbH$_{Lm}$* strain. Although protein levels were increased, spxA1 transcript abundance was decreased in *yjbH$_{Lm}$*, indicating YjbH$_{Lm}$-dependent post-transcriptional regulation. Finally, the Δ*yjbH$_{Lm}$* strain with increased SpxA1 abundance had a corresponding increase in SNP resistance, demonstrating that the response to nitrosative stress in *L. monocytogenes* is SpxA1-dependent. Taken together, these results support a model in which YjbH$_{Lm}$ is a protease adaptor that regulates SpxA1 protein abundance.

It is interesting to note that the Δ*yjbH$_{Lm}$* mutant was more resistant to nitrosative stress while the *B. subtilis* and *S. aureus* Δ*yjbH* mutants are more sensitive[80,92]. However, expressing

the YjbH$_{Bs}$ protein in Δ*yjbH*$_{Lm}$ fully restored its sensitivity to SNP. While these results may seem counterintuitive at first, we propose that the nitrosative stress phenotypes of bacteria lacking *yjbH* are dependent on factors regulated by Spx. We demonstrated that both YjbH$_{Lm}$ and YjbH$_{Bs}$ interact with SpxA1 and will therefore similarly affect expression of SpxA1-dependent proteins. Defining the SpxA1 regulon is the next step to more completely define the differences between the organisms with respect to the differing YjbH-dependent responses to nitrosative stress.

Regulation of LLO production, secretion, and activity is complex and incompletely understood in *L. monocytogenes*[30,109]. YjbH$_{Lm}$ was found to play a role in LLO regulation over a decade ago, yet the mechanism behind this phenotype remains to be elucidated. We demonstrated here that the Δ*yjbH*$_{Lm}$ defect in LLO secretion is likely partially SpxA1-independent. The Δ*yjbH*$_{Lm}$ strain, which has more SpxA1 than wild type, is severely deficient in LLO secretion. Conversely, the *spxA1* knock-down strain is also deficient in LLO. Together, these data revealed that LLO production is partially regulated in an SpxA1-dependent manner. Although SpxA1 is a transcriptional regulator and *hly* transcript is unchanged, this regulation could be through post-transcriptional effects of the SpxA1 regulon. However, the fact that deleting *yjbH*$_{Lm}$ in the *spxA1* knock-down strain did not rescue the LLO secretion defect suggests that part of this phenotype may be YjbH$_{Lm}$-dependent and SpxA1-independent. No other studies on YjbH homologues have shown evidence of Spx-independent functions of YjbH.

To elucidate YjbH$_{Lm}$ function in an unbiased manner, we performed whole-cell proteomics on Δ*yjbH*$_{Lm}$. In this study, we focused on proteins that were more abundant in the absence of *yjbH*$_{Lm}$, due to the known role of YjbH$_{Bs}$ as a protease adaptor. With the exception of SpxA1, we concentrated on proteins whose increased abundance was statistically significant. It is possible that more proteins on this list are biologically significant, but fall outside the bounds of statistical significance. There was also an extensive list of proteins significantly less abundant in Δ*yjbH*$_{Lm}$ than wild type (Table 4). While the study of these proteins was outside the scope of this work, future work will investigate how YjbH$_{Lm}$ is capable of increasing the concentration of proteins like LLO when its only known role is that of a protease adaptor. Even more intriguing is the fact that YjbH$_{Lm}$ regulates two transcription factors: SpxA1 and Lmo0597. The regulons of SpxA1 and Lmo0597 have not been reported and thus it is unknown how altering levels of SpxA1 and Lmo0597 may contribute to Δ*yjbH*$_{Lm}$ phenotypes. Of the five genes significantly increased in expression in Δ*yjbH*$_{Lm}$, only one has a homologue in *B. subtilis* that is regulated by Spx$_{Bs.}$ The putative 3'-exo-deoxyribonuclease *lmo1782* is 69% identical to *exoA* and upregulated by Spx$_{Bs}$ during diamide stress[65]. Ongoing experiments are aimed at deciphering the downstream effects of YjbH-dependent regulation of SpxA1 and Lmo0597.

**Table 4**. Whole-cell proteomics revealed proteins less abundant in Δ*yjbH*$_{Lm}$ than wild type.

| Gene Locus | Predicted Function | Protein | Wild Type[a] | Δ*yjbH*$_{Lm}$[a] | *p*-value |
|---|---|---|---|---|---|
| *lmo2102* | Converts glutamine to glutamate and ammonia | PdxT | 16.0 | n.d. | 0.001 |
| *lmo0202* | Listeriolysin O | LLO | 15.0 | 0.4 | 0.001 |
| *lmo0399* | PTS fructose transporter subunit IIB | - | 11.0 | 1.0 | <.001 |
| *lmo2006* | Acetolactate synthase | AlsS | 22.0 | 2.7 | 0.004 |
| *lmo0355* | Fumarate reductase subunit A; succinate dehydrogenase activity | - | 11.0 | 1.7 | 0.001 |
| *lmo1530* | Queuine tRNA-ribosyltransferase | Tgt | 6.0 | 0.8 | 0.013 |
| *lmo0415* | Peptidoglycan deacetylase | PdgA | 19.0 | 4.0 | 0.004 |
| *lmo0401* | Alpha-mannosidase | - | 5.0 | n.d. | <.001 |
| *lmo0536* | 6-phospho-beta-glucosidase | - | 4.0 | n.d. | 0.025 |
| *lmo2101* | Pyridoxal 5'-phosphate synthase subunit | PdxS | 145.0 | 33.9 | 0.001 |
| *lmo0398* | PTS sugar transport subunit IIA | - | 4.0 | n.d. | <.001 |
| *lmo2079* | Hypothetical lipoprotein | - | 4.0 | 0.4 | 0.011 |
| *lmo2569* | Peptide ABC transporter substrate-binding protein | - | 4.0 | 0.4 | 0.005 |
| *lmo1737* | Oxidoreductase | - | 4.0 | 0.4 | 0.016 |
| *lmo0181* | Sugar ABC transporter substrate-binding protein | - | 20.0 | 5.3 | 0.002 |
| *lmo2487* | Hypothetical protein | - | 11.0 | 3.4 | 0.009 |
| *lmo2767* | Hypothetical protein | - | 3.0 | n.d. | 0.007 |
| *lmo0786* | FMN-dependent NADH-azoreductase 2 | AzoR2 | 6.0 | 1.6 | 0.044 |
| *lmo1676* | Menaquinone-specific isochorismate synthase | MenF | 14.0 | 5.2 | 0.038 |
| *lmo2802* | rRNA small subunit methyltransferase G | RsmG | 3.0 | 0.3 | 0.017 |
| *lmo0487* | Putative hydrolase | - | 3.0 | n.d. | 0.006 |
| *lmo0814* | Nitronate monooxygenase | - | 3.0 | n.d. | 0.039 |
| *lmo1592* | Probable tRNA sulfurtransferase | ThiL | 4.0 | 1.0 | 0.025 |
| *lmo1604* | 2-cysteine peroxiredoxin | - | 7.0 | 2.3 | 0.031 |
| *lmo1221* | Phenylalanine-tRNA ligase alpha subunit | PheS | 6.0 | 2.4 | 0.012 |
| *lmo0689* | Chemotaxis and phosphorelay signal transduction | CheV | 2.0 | n.d. | 0.001 |

| | | | | | |
|---|---|---|---|---|---|
| *lmo1936* | Glycerol-3-phosphate dehydrogenase | GpsA | 15.0 | 6.1 | 0.018 |
| *lmo0856* | UDP-N-acetylmuramoyl-tripeptide-D-alanyl-D-alanine ligase | MurF | 5.0 | 1.9 | 0.023 |
| *lmo2779* | Ribosome-binding ATPase | YchF | 10.0 | 4.4 | 0.005 |
| *lmo1454* | RNA polymerase sigma factor | SigA | 7.0 | 3.1 | 0.032 |
| *lmo1401* | Hypothetical protein | - | 7.0 | 3.3 | 0.023 |
| *lmo1902* | 3-methyl-2-oxobutanoate hydroxymethyltransferase | PanB | 5.0 | 2.2 | 0.032 |
| *lmo1937* | GTPase | Der | 9.0 | 3.9 | 0.024 |
| *lmo1892* | Penicillin-binding protein 2A; glycosyltransferase | PbpA | 2.0 | 0.3 | 0.015 |
| *lmo2125* | Maltodextrin-binding protein | - | 23.0 | 11.0 | <.001 |
| *lmo1710* | Flavodoxin-like domain | - | 8.0 | 3.8 | 0.044 |
| *lmo2556* | Fructose-bisphosphate aldolase activity | FbaA | 64.0 | 31.5 | 0.003 |

[a]Average spectral peptide counts from three independent samples are listed. n.d. indicates no peptides were detected. Genes included in this Table were at least 2-fold less abundant in $\Delta yjbH_{Lm}$ than wild type and statistically significant.

Protease adaptor activity is dependent on direct interactions between the adaptor and substrate proteins. In BACTH assays with *L. monocytogenes* proteins, we found that YjbH$_{Lm}$ interacted with eight out of ten tested proteins in addition to SpxA1. This was intriguing, as the only characterized YjbH$_{Bs}$ interacting partners are Spx$_{Bs}$ and the small inhibitor protein YirB, which is not conserved among *Firmicutes* and is not present in *L. monocytogenes*. An unbiased yeast two-hybrid screen of a *B. subtilis* genomic fusion library detected seven additional proteins that interacted with YjbH$_{Bs}$[89]. Thus, while there is precedent for YjbH$_{Bs}$ to bind proteins other than Spx$_{Bs}$, it is not known if any of these uncharacterized binding partners contribute to YjbH$_{Bs}$ function. In *L. monocytogenes*, whole-cell proteomics showed that SpxA1 and the eight uncharacterized interacting partners were more abundant in Δ*yjbH*$_{Lm}$, raising the possibility that YjbH$_{Lm}$ post-translationally regulates other proteins in addition to SpxA1. From their predicted functions, it was not obvious what these interacting partners have in common or what roles they may play in the cell. However, the ability of YjbH$_{Lm}$ to interact with such a wide variety of proteins will inform future work to explain the myriad phenotypes exhibited by *L. monocytogenes* Δ*yjbH*$_{Lm}$.

YjbH homologues share a conserved thioredoxin domain at the N-terminus. A CxxC motif is required for catalytic activity in thioredoxin-family proteins, but YjbH$_{Bs}$ and YjbH$_{Sa}$ do not require CxxC motif cysteines for function[88,90]. We demonstrated here that the cysteine residues of the YjbH$_{Lm}$ CxxC motif were required to fully complement a Δ*yjbH*$_{Lm}$ mutant for SNP sensitivity, LLO secretion, and cell-to-cell spread. However, the YjbH$_{Lm}$ protein with a mutated CxxC motif still retained partial functionality, perhaps through protein-protein interactions at a site other than the CxxC motif. For example, two out of nine proteins (Lmo1258 and Lmo1387) were still able to interact with YjbH$^{C27/30A}$, which lacks a functional CxxC motif. The two cysteine residues located outside the CxxC motif were required for interacting with SpxA1 and Lmo0218, although C63 and C89 were dispensable for YjbH function during cell-to-cell spread and SNP stress. In *B. subtilis*, the YjbH$_{Bs}$ cysteine residues are not required for enhancing Spx$_{Bs}$ degradation or for auto-aggregation[88,90]. Cysteines are also dispensable to YjbH$_{Sa}$ function in virulence and Spx$_{Sa}$ degradation[90,92]. YjbH$_{Sa}$ does not encode a CxxC motif, but instead has an SxxC motif that aligns with the *L. monocytogenes* and *B. subtilis* N-terminal CxxC motif, and a CxC motif at position 114-116[90,92]. The lack of conservation of the CxxC motif across all YjbH homologues, and the apparent lack of conserved cysteine essentiality, suggests either that thioredoxin activity is not necessary for function or that CxxC motifs have disparate functions between species. These experiments have shed light on another parameter that impeded our efforts to identify the interacting partners of YjbH$_{Lm}$ in an unbiased way, as described in Chapter

2. We now know that the CxxC motif is important for a subset of protein-protein interactions, and a CxxC mutant protein does not fully complement Δ*yjbH*$_{Lm}$. Therefore, our attempts to detect interactions with YjbH$^{C27S}$ bait were more biased than we originally thought and trapping mutants will not be used in future co-IP experiments.

This is the first work to characterize YjbH$_{Lm}$, and will serve as a foundation for future studies aimed at uncovering the full scope of its role. YjbH$_{Sa}$ trans-complements Δ*yjbH*$_{Bs}$[90], and we have shown here that YjbH$_{Bs}$ complements the *L. monocytogenes* mutant. Together with our findings that Δ*yjbH*$_{Lm}$ results in increased SpxA1 abundance, which indicates that YjbH$_{Lm}$ is post-translationally regulating SpxA1, this demonstrates conserved function between *Firmicutes*. However, YjbH$_{Lm}$ has unique characteristics that set it apart from other homologues. For example: YjbH$_{Lm}$ is present in very low abundance in every growth condition examined, the LLO secretion defect is at least partially SpxA1-independent, it has a role in the post-transcriptional regulation of at least nine proteins, and YjbH$_{Lm}$ requires the CxxC motif cysteines for function. The basic characterization presented here is thus both broadly applicable to other *Firmicute* species and a step forward in understanding the uniquely complex role of YjbH$_{Lm}$ in *L. monocytogenes*.

# Chapter 4: Bluhland production during the SNP response

## Introduction

We have demonstrated that YjbH$_{Lm}$ is important for the nitrosative stress response in *L. monocytogenes*. Δ*yjbH*$_{Lm}$ is more resistant to the nitric oxide donor sodium nitroprusside (SNP) than wild type, and that phenotype is SpxA1-dependent[104]. However, the mechanism behind the increased SNP resistance is unclear. While SNP is often used as a nitric oxide donor, its chemical structure also allows for the donation of cyanide groups. Cyanide prevents cellular respiration and is therefore toxic to cells. It is currently not known whether resistance to cyanide is important or relevant in the *L. monocytogenes* SNP phenotype.

Additionally, we made a surprising observation in the SNP MIC assays presented in Chapter 3. The MIC assay entails subculturing bacteria in rich media supplemented with increasing concentrations of SNP (full details on methodology in Chapter 6). We found that after approximately 24 hours of growth in those conditions, the media turned a dark blue color in wells containing heavy bacterial growth. Here, we used a combination of approaches to begin narrowing down the identity of the blue substance, referred to as “bluhland”.

## Results

### *L. monocytogenes* produces bluhland in SNP MIC assays

As described in Chapter 3, we examined the role of YjbH$_{Lm}$ in *L. monocytogenes* SNP resistance using an MIC assay that tested growth in a 96-well plate in tryptic soy broth (TSB) supplemented with 20 mM increments of SNP from 0 to 120 mM. Δ*yjbH*$_{Lm}$ was significantly more resistant to SNP than wild type after 24 hours of growth at 37 °C (Fig. 14). These assays were performed in biological triplicate. At the same timepoint, we observed an accumulation of dark blue color (bluhland) in the SNP-treated wells containing heavy bacterial growth of both wild type and Δ*yjbH*$_{Lm}$ (Fig. 20A). The lowest tested concentration of SNP was 4 mM, in which robust bacterial growth and SNP was observed.

We also tested wild type and Δ*yjbH*$_{Lm}$ in another chemical sensitivity assay, disk diffusions, in biological triplicate. In this assay, filter paper disks saturated with 2 M SNP were placed onto Tryptic Soy Agar plates seeded with wild type or Δ*yjbH*$_{Lm}$ and incubated for 24 hours at 37 °C. The resulting zone of growth inhibition surrounding the disk is proportional to the SNP sensitivity of the strain. After 24 hours of growth, similar to SNP MIC assays, these disk diffusion assays demonstrated that Δ*yjbH*$_{Lm}$ is indeed more resistant to SNP than wild type. No bluhland was observed on either agar plate, revealing that specific conditions, perhaps relating

to bacterial density or oxygen availability, are required for visible bluhland production (data not shown).

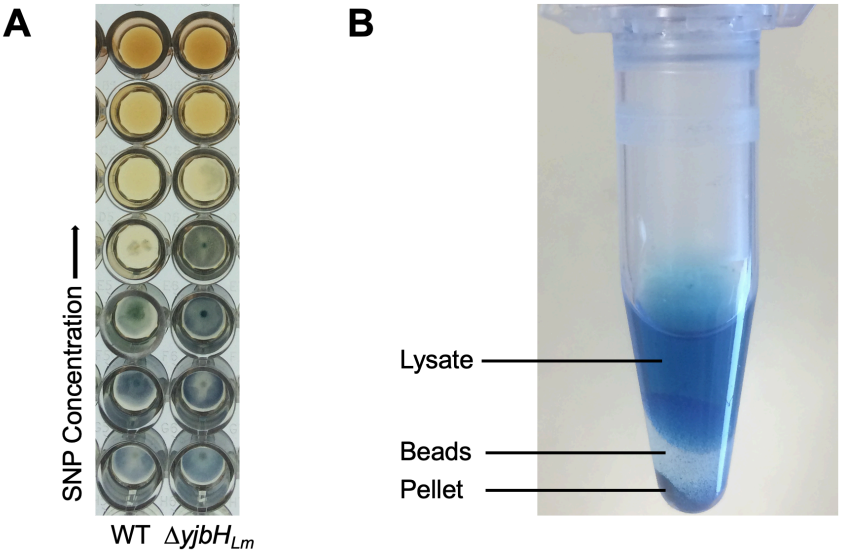


**Figure 20**. *L. monocytogenes* growth in SNP-treated media produces bluhland. **(A)** SNP MIC assay after 24 hours of growth. Bluhland is localized to wells containing heavy bacterial growth. **(B)** Photograph of Eppendorf tube containing bacterial growth from an SNP MIC assay that was lysed and centrifuged. As indicated in the figure, the tube contains blue lysate, a layer of white zirconium beads, and a blue pellet.

## Bluhland is likely a protein, not a small molecule

To begin characterizing bluhland, we investigated its solubility by centrifuging a sample collected from both wild type and $\Delta yjbH_{Lm}$ bluhland-containing SNP MIC wells. If bluhland was present in the resulting supernatant it could indicate that bluhland was a soluble protein or small molecule. However, after centrifuging, we only observed bluhland in the pellet. This suggested that bluhland was either part of an insoluble aggregate, or otherwise localized to the bacteria. To clarify these two possibilities, we collected the blue pellet and lysed the bacteria by bead-beating in the presence of 0.1% NP-40. We reasoned that if bluhland was a soluble protein or small molecule inside the bacteria, centrifuging the lysed bacteria would result in blue lysate. After centrifugation, we indeed observed blue lysate and a blue pellet (Fig. 20B). The blue pellet could indicate partial lysis, or that a fraction of the bluhland was trapped in protein aggregates or other insoluble material. The presence of bluhland in the lysate suggests that it is a soluble species produced inside the bacteria, or closely associated with the cell surface.

To determine if bluhland was likely a small molecule or a protein, we utilized a 3-kD-cutoff filter. If bluhland was a protein, we would expect its size to prevent passage through the

3-kD filter. Conversely, a small molecule would pass through the filter. When we separated the bluhland-containing lysate with a 3-kD-cutoff filter, bluhland was too large to be filtered. A size greater than 3 kD indicates that bluhland is likely a protein or bound to a protein.

### MIC assays with a nitric oxide donor and a cyanide donor

SNP is able to donate cyanide groups as well as nitric oxide, although it is unclear whether cyanide detoxification is relevant to the *L. monocytogenes* SNP response. For this reason, we sought to determine whether bluhland production was due to the presence of nitric oxide or that of cyanide. To do this, we first tested wild type and Δ*yjbH*$_{Lm}$ in an MIC assay with the nitric oxide donor diethylamine NONOate (DEA NONOate). The MIC assay was set up in a 96-well plate with TSB supplemented with the aforementioned concentrations of SNP, alongside TSB supplemented with DEA NONOate in increments of 5 mM from 0 to 40 mM, and performed in biological duplicate. After 24 hours of growth at 37 °C, bluhland was observed as before in SNP-treated wells containing heavy bacterial growth. The range of DEA NONOate concentrations was appropriate to determine the wild type MIC, which was between 30 and 35 mM, but too low to determine the MIC for Δ*yjbH*$_{Lm}$, which was able to grow in 40 mM DEA NONOate (data not shown). However, no bluhland was observed in any DEA NONOate-treated wells after 24 hours. The second replicate was incubated for an additional 24 hours stationary at room temperature, after which there was still no accumulation of bluhland in any DEA NONOate-treated wells. This suggests that the presence of nitric oxide alone is not sufficient to drive the production of bluhland.

To determine if bluhland production was due to the effects of cyanide from SNP, we tested wild type and Δ*yjbH*$_{Lm}$ against the cyanide donor KCN in an MIC assay. This assay was performed in the same way as described for SNP and DEA NONOate, using TSB supplemented with serial two-fold dilutions of KCN from 0 mM to 100 mM. After several attempts to use KCN in an MIC assay, visible bacterial growth was observed in the range of concentrations containing the MIC, but growth was poor and varied between replicates. Some replicates had too little bacterial growth to determine MICs, some replicates revealed an equal KCN MIC between wild type and Δ*yjbH*$_{Lm}$, and other replicates showed a two-fold increase in KCN resistance in Δ*yjbH*$_{Lm}$ compared to wild type (data not shown).

The KCN MIC assays described above were performed in five biological replicates, in which the following parameters were modified: dissolving the KCN in TSB instead of water; using freshly made TSB; incubating the plate in a static incubator instead of a shaking plate reader; and increasing the inoculum of each well from $2 \times 10^4$ to $1 \times 10^5$ bacteria. Despite these

modifications, as stated above, conditions were not identified that resulted in consistent, robust bacterial growth. It is possible that smaller increments of KCN could yield greater bacterial growth. While no bluhland was observed in these KCN MIC assays, bluhland accumulation in the presence of SNP correlates with the amount of bacterial growth. Therefore, we cannot know if KCN treatment results in bluhland production until this assay is optimized for bacterial growth. Currently we cannot make conclusions about the effect of cyanide on bluhland production.

## Conclusions

The SNP stress response in *L. monocytogenes* is incompletely understood. Although commonly used as a nitric oxide donor, SNP is also able to donate toxic cyanide groups. It is unknown whether the increased resistance of Δ*yjbH*$_{Lm}$ to SNP compared to wild type is due to nitric oxide or cyanide. Here, we observed that a blue species (bluhland) was produced during *L. monocytogenes* growth in SNP-containing media. In this initial characterization of bluhland, we have determined that it is likely a soluble protein produced by *L. monocytogenes*. Proteins that appear colored to the naked eye often coordinate a metal ion like iron, cobalt, or copper, so it is possible that this blue protein is a metalloprotein.

We interrogated the cause of the SNP response in *L. monocytogenes* by testing the bacteria in the presence of a nitric oxide donor and a cyanide donor. MIC assays with DEA NONOate demonstrated that this nitric oxide donor does not induce bluhland production. These MIC assays must be performed more rigorously in a higher concentration range of DEA NONOate to make conclusions about the exact MICs of Δ*yjbH*$_{Lm}$ to compare to wild type. The two replicates presented here suggest that Δ*yjbH*$_{Lm}$ is modestly more resistant to a nitric oxide donor than wild type, but the highest DEA NONOate concentration used was too low to determine an exact MIC for Δ*yjbH*$_{Lm}$. Therefore, it is unclear whether the entire magnitude of increased SNP resistance in Δ*yjbH*$_{Lm}$ can be attributed to nitric oxide. We next tested *L. monocytogenes* in the presence of the cyanide donor KCN in an MIC assay. Despite several biological replicates, bacterial growth was too poor and too varied between experiments to draw conclusions. No bluhland was observed in the presence of KCN, but in SNP MIC assays, bluhland presence is positively correlated with bacterial growth. The future studies outlined here will be helpful in gaining a deeper understanding of the SNP response, and investigating the identity of bluhland.

In the environment, where *L. monocytogenes* is ubiquitous as a saprophyte, bacteria may encounter cyanide that is derived from the secondary metabolites of plants[110]. A common method of cyanide detoxification involves a rhodanese protein, which is a sulfurtransferase

enzyme that converts cyanide to the less-toxic thiocyanate. *L. monocytogenes* encodes a putative sulfurtransferase, *lmo1384*, and a gene with 33% identity to *lmo1384*, *lmo0609*. Neither of the proteins encoded by these genes were detected in the whole-cell proteomics data presented in Chapter 3, either in wild type or Δ*yjbH*$_{Lm}$. An unbiased method of determining which genes are changed in abundance in response to SNP would be to perform whole-cell proteomics in the presence of a sub-lethal concentration of SNP, conditions in which bluhland is produced. Testing the mutant strains Δ*lmo1384,* Δ*lmo0609*, and Δ*lmo1384* Δ*lmo0609* in SNP MIC assays will be a more direct way to investigate their possible roles in the SNP response. If the gene products of *lmo1384* and/or *lmo0609* results in the production of bluhland, we would predict an absence of blue in some or all of these proposed SNP MIC assays.

Thiocyanate, the product of cyanide detoxification by a sulfurtransferase, turns blue in the presence of cobalt (II) and red in the presence of iron (II). If the *L. monocytogenes* SNP response is due at least in part to cyanide, and if the bluhland protein exhibits sulfurtransferase activity, the addition of iron chloride or a similar iron-containing chemical to a solution of bluhland could indicate the presence or absence of thiocyanate. This has not been tested, but would be a straightforward method of examining whether detectable cyanide detoxification is taking place during SNP treatment. Importantly, thiocyanate is a small molecule, less than 3 kD in size, and therefore cannot be the colored species detected in our samples. However, ascertaining whether thiocyanate is produced will allow us to better understand the *L. monocytogenes* SNP response.

As theorized above, it is possible that both the expression of the bluhland protein and the increased SNP resistance exhibited by Δ*yjbH*$_{Lm}$ are caused by the presence of cyanide derived from SNP. However, bluhland production occurs both in wild type and Δ*yjbH*$_{Lm}$ during exposure to sub-lethal concentrations of SNP. An alternative hypothesis is that bluhland, which appears to correlate with the amount of bacterial growth regardless of *L. monocytogenes* genetic background, is simply upregulated in the presence of cyanide and is wholly separate from YjbH$_{Lm}$-dependent activity. In this untested speculation, we might suppose that the increased resistance of Δ*yjbH*$_{Lm}$ results from nitric oxide. If the MICs of wild type and Δ*yjbH*$_{Lm}$ in the presence of the cyanide donor KCN were equal, it would support this theory. It is difficult to conclude anything with certainty from the KCN MIC assays, given the poor bacterial growth and high variability between replicates.

Finally, it is possible that production of bluhland is a specific response to the presence of both cyanide and nitric oxide groups, and thus would only be detected when *L. monocytogenes* is tested in the presence of SNP, not KCN or DEA NONOate alone. Further assay optimization

will be required for future studies. Quantitative PCR to measure transcript levels of *lmo1384* and *lmo0609* should be performed in wild type and $\Delta yjbH_{Lm}$ cultured in the presence and absence of KCN and SNP to ascertain whether these two genes are upregulated during cyanide exposure, and whether $YjbH_{Lm}$ is involved in that regulation.

# Chapter 5: Future directions

## Introduction

The work presented in this dissertation is the first characterization of the protease adaptor YjbH in *L. monocytogenes*. While some similarities and conservation of function exists between YjbH$_{Lm}$ and its homologues in *B. subtilis* and *S. aureus*, it is also clear that this is a unique protein whose nuances have only begun to be understood. In the course of this work we have demonstrated that YjbH$_{Lm}$ is involved in the nitrosative stress response in an SpxA1-dependent manner; that YjbH$_{Lm}$ and SpxA1 physically interact, and that YjbH$_{Lm}$ can interact with multiple other proteins in *L. monocytogenes*; and finally, that the YjbH$_{Lm}$ thioredoxin active motif is required for SNP sensitivity, cell-to-cell spread, and LLO secretion. These findings are a foundation for future study of this system.

## Why is LLO less abundant in a Δ*yjbH*$_{Lm}$ mutant?

One of the outstanding questions in the field is how YjbH$_{Lm}$ regulates LLO, the cytolysin that navigates vacuolar escape during *L. monocytogenes* infection. YjbH$_{Lm}$ was first implicated in LLO regulation as part of a screen that detected hypohemolytic mutants[78]. Our whole-cell proteomics data presented in Chapter 3 likewise demonstrate that LLO is less abundant in Δ*yjbH*$_{Lm}$ compared to wild type. While the exact mechanism of LLO regulation by YjbH$_{Lm}$ is unknown, *hly* transcription is activated by the master virulence transcriptional regulator PrfA[27]. We have shown that *hly* transcription is unchanged between Δ*yjbH*$_{Lm}$ and wild type (see Chapter 3), but it remains possible that YjbH$_{Lm}$ acts either on the hly transcript or the LLO protein to regulate LLO abundance.

LLO protein production is dependent upon the hly 5' UTR, which comprises either 122 or 133 nucleotides depending on which of the two *hly* promoters drives transcription[31]. An electromobility shift assay (EMSA) would reveal if YjbH$_{Lm}$ directly binds the transcript. Of course, a false negative is possible with this experiment if YjbH$_{Lm}$ only binds the LLO 5' UTR in a complex with other proteins. An additional potential problem is the difficulty of purifying YjbH$_{Lm}$ without a large fusion protein for solubility (see Chapter 2). MBP-YjbH$_{Lm}$ protein could certainly be used in an EMSA with the LLO 5' UTR, but there is a chance the fusion protein could preclude YjbH$_{Lm}$ binding to the UTR and result in a false negative.

We can examine whether LLO and YjbH$_{Lm}$ are close enough to physically interact in *L. monocytogenes* by using a proximity labeling assay, discussed in the section, "A new method to detect protein-protein interactions". In unpublished data, we heterologously expressed YjbH$_{Lm}$

and LLO in a BACTH assay and were able to detect an interaction between the two proteins. However, the biological significance of these data is unknown. LLO is a secreted protein, but it is uncertain how much, if any, folded LLO is present in the cytosol. In contrast, YjbH proteins are cytosolic and encode no known secretion signal. As such, expressing these two proteins heterologously to test for an interaction is not the ideal experiment, because it cannot tell us whether LLO and YjbH$_{Lm}$ exist in the same subcellular compartment in *L. monocytogenes*.

## What is the role of YjbH$_{Lm}$ in ActA post-transcriptional regulation?

We first began characterizing YjbH$_{Lm}$ because it was found to play a role in ActA post-transcriptional regulation[40]. There are many similarities between the roles of YjbH$_{Lm}$ in up-regulating ActA compared to LLO: first, transcription of *actA* is unchanged in Δ*yjbH$_{Lm}$* compared to wild type, so YjbH$_{Lm}$ must either act at the transcript or protein level. ActA is secreted like LLO, and therefore a direct protein-protein interaction with the cytosolic YjbH$_{Lm}$ is technically possible but not likely given the current body of literature on ActA. Finally, the actA transcript includes a 149-nucleotide 5' UTR that is essential for protein production, similar to the size and role of the LLO 5' UTR, and has a predicted stem-loop structure that suggests a potential for protein binding[22]. ActA protein is not detectable during broth growth unless it is overexpressed. There is a combination of bacterial and host cues to which ActA regulation is responsive, resulting in the precise upregulation of ActA once *L. monocytogenes* reaches the cytosol during infection[10,17]. Because of these factors, ActA regulation by YjbH$_{Lm}$ will likely need to be studied in a tissue culture model of infection.

Given the similarities described above, many of the previously proposed approaches to studying YjbH$_{Lm}$ regulation of LLO could be applied to understanding ActA regulation. An EMSA can test whether YjbH$_{Lm}$ directly binds the actA transcript to regulate translation, although EMSAs are limited by their inherent bias. As an alternative method, labeled actA 5' UTR RNA could be used as a probe to detect UTR-binding proteins. This method is less biased, but presents a new problem. Due to the extremely precise nature of ActA regulation, the ideal source of *L. monocytogenes* lysate for this experiment is from bacteria grown in host cell cytosol. This would ensure that the *L. monocytogenes* proteomic profile is that of the intracellular lifecycle, when actA transcript is naturally present in the bacteria, and not the very different profile of broth growth[10]. It may be technically possible to probe for UTR-binding proteins in this way, but it would certainly be extremely difficult because of the low yield of bacteria from a dish of infected macrophages. Another desirable, but equally limiting, option is

to grow the bacteria in *Xenopus spp.* cell-free egg extract, in which ActA is upregulated [unpublished data].

Performing whole-cell proteomics that compares Δ*yjbH*$_{Lm}$ and wild type during infection could also be very informative. This experiment faces the same issues stated above, but we have shown that whole-cell proteomics yields biologically significant results when performed in broth, as we detected increased SpxA1 in Δ*yjbH*$_{Lm}$. There is reason to believe that this method could identify an indirect method of ActA upregulation by YjbH$_{Lm}$. If YjbH$_{Lm}$ itself does not bind the actA transcript or protein, it likely regulates the responsible protein or proteins, and that can be revealed through proteomics.

## A new method to detect protein-protein interactions

Throughout this dissertation, we have used several methods to understand what protein-protein interactions are important for YjbH$_{Lm}$ in *L. monocytogenes*. Our attempts at a co-IP were greatly hindered by the low natural abundance of YjbH$_{Lm}$ and its interaction partner, SpxA1, and also by the inherent instability of YjbH$_{Lm}$. This technique required YjbH$_{Lm}$ to be expressed and purified as a fusion protein with the 43 kD tag MBP, which could lead both to false positives and false negatives in our mass spectrometry data. Indeed, we were unable to verify any of our top hits from that list (Table 2), and SpxA1 was absent from these data, likely due to its own extremely low abundance. However, in spite of these challenges, future co-IP experiments can still yield important information. With what we know now about the importance of the CxxC motif to YjbH$_{Lm}$ function and the low abundance of SpxA1 as measured by mass spectrometry, we can modify our original co-IP. This experiment utilized a strain of *L. monocytogenes* that overexpressed the trapping mutant YjbH$^{C27S}$ as bait in the Δ*yjbH*$_{Lm}$ *clpX::Tn* background, and analyzed the results by silver-staining the resulting co-IP fractions. Future co-IP experiments should overexpress the wild type YjbH$_{Lm}$ protein in a Δ*yjbH*$_{Lm}$ background. Using the optimized protocol, if the bait protein can be detected in elution fractions, mass spectrometry should be used to analyze the elutions and identify interacting partners directly from *L. monocytogenes*.

We successfully demonstrated the interaction of YjbH$_{Lm}$ and SpxA1 by BACTH, in addition to showing that YjbH$_{Lm}$ has the potential to interact with multiple other *L. monocytogenes* proteins. Although biased, we believe this was the best method available to us at the time, given the previously stated system limitations we faced. However, BACTH is not typically the sole method used to rigorously demonstrate a protein-protein interaction because it requires heterologous expression, and expressing the proteins of interest as fusions with 18-kD and 25-kD proteins. For this reason, false negatives can be a problem with BACTH assays. This

assay also cannot provide insight into interactions that involve more than two proteins. In our system, we first attempted a co-IP because it is an unbiased method to detect YjbH$_{Lm}$ interactors in a specific growth condition in *L. monocytogenes*. BACTH has given us critical insight into the ability of YjbH$_{Lm}$ to interact with a certain set of proteins, but for future experiments, we need a new method that will allow us to probe those interactions directly in *L. monocytogenes* at different growth stages or conditions.

Enzyme-catalyzed proximity labeling is an exciting method to address the issues presented above. In particular, labeling via a biotin ligase fusion. The protein of interest is expressed as a fusion with a promiscuous biotin ligase, and exogenous biotin is added to live cells. The enzyme will biotinylate proteins that are proximal to the protein of interest, and all biotinylated proteins can subsequently be isolated from the culture for analysis. Recently, the effective but slow (~18 hours to label) BioID enzyme that had been in use for these experiments was modified, resulting in the enzymes TurboID and miniTurbo that can biotinylate nearby proteins in approximately 10 minutes[111]. MiniTurbo is slightly less active than TurboID, but exhibits less labeling prior to the addition of exogenous biotin and is therefore the more precise enzyme[111]. Both are excellent options for our study of YjbH$_{Lm}$, as they will allow us to examine proteins that are proximal to YjbH$_{Lm}$ in different growth conditions.

Future studies on YjbH$_{Lm}$ will take advantage of these biotin ligase fusions to learn which interacting partners are biologically important in *L. monocytogenes*. This method can be applied during different growth stages and treatment with SNP or other nitrosative or oxidative stressors. Given the important role of cysteine residues to YjbH$_{Lm}$ function, it would also be interesting to use proximity labeling to find out which cysteine-dependent interactions are biologically significant. Understanding the various interacting partners of YjbH$_{Lm}$, and how they may change between conditions, might help us to explain some of the phenotypes that remain a mystery at this point. If YjbH$_{Lm}$ is a protease adaptor for proteins other than SpxA1; whether YjbH$_{Lm}$ could be regulating proteins by aggregation or sequestration; and, potentially, how YjbH$_{Lm}$ acts to increase the protein abundance of some proteins like LLO and ActA.

## Future whole-cell proteomics studies

In an effort to identify the proteins that are changed in abundance in the Δ*yjbH*$_{Lm}$ strain, we performed whole-cell proteomics comparing the mutant to wild type *L. monocytogenes*. We expected to identify proteins that were more abundant in Δ*yjbH*$_{Lm}$ compared to wild type, like SpxA1, because YjbH is a known protease adaptor in *B. subtilis* and *S. aureus*[79,86]. Studies on YjbH have focused on its relation to Spx, with no indication of how YjbH might act to increase

the abundance of a protein. While we did observe many proteins that increased in abundance in the absence of YjbH$_{Lm}$, like SpxA1, there were even more whose abundance decreased in the mutant (Table 4). Importantly, this change in abundance of proteins in Table 4 cannot solely be explained by the SpxA1 regulon[112]. One of the proteins with increased abundance in Δ*yjbH*$_{Lm}$ was the predicted transcriptional regulator Lmo0597. As this protein has not been studied, it is possible that its regulon could be responsible for some of the changes in protein abundance observed in Δ*yjbH*$_{Lm}$.

Identifying the proteins that are up- or down-regulated in Δ*yjbH*$_{Lm}$ is critical in helping us to understand the complex role of YjbH$_{Lm}$, and whole-cell proteomics is a powerful tool to do that. However, there are several limitations to consider with these whole-cell proteomics data, especially if these experiments will used in future studies of YjbH$_{Lm}$. Perhaps most importantly, only the soluble fraction from Δ*yjbH*$_{Lm}$ and wild type cultures were analyzed. YjbH$_{Lm}$ aggregation has not yet been studied, but it is possible that aggregation is different in *L. monocytogenes* compared to *B. subtilis* and could even be used as a method of protein regulation by sequestration into inclusion bodies. This speculation has not been tested, but it is interesting to note that YjbH$_{Lm}$ appears to be able to bind a larger subset of proteins than its *B. subtilis* homologue[89], indicating that a method of regulation in which YjbH$_{Lm}$ binds several proteins in an insoluble cluster could be possible in *L. monocytogenes*. Therefore, we cannot fully understand protein regulation by YjbH$_{Lm}$ without knowing more about the composition of the insoluble fraction as well as the soluble fraction.

A second limitation is that peptides mapping to a total of 659 proteins were detected during LC/MS-MS analysis, out of approximately 2900 protein-coding genes in the *L. monocytogenes* genome. Thus, while this study is a very informative first step into understanding the possible changes YjbH$_{Lm}$ enacts on the proteome, it is very likely that our dataset is incomplete. Future proteomics studies with broader coverage will demonstrate a more holistic picture of the proteins that are changed in abundance in a Δ*yjbH*$_{Lm}$ mutant.

The final limitation of this whole-cell proteomics study is that it tests only a single condition: mid-log phase growth in rich media. Given what we know about the role of YjbH homologues in stress conditions, these proteomics data represent only a fraction of the potential changes YjbH$_{Lm}$ may be enacting on the proteome. It will be important to examine other conditions by proteomics: for example, SNP treatment, disulfide stress, or even with the YjbH$_{Lm}$ cysteine mutants replacing the wild type protein.

# Chapter 6: Materials and methods

## Bacterial strains and culture conditions

All *L. monocytogenes* strains are a derivative of 10403S[113,114]. *L. monocytogenes* strains were cultivated in Brain Heart Infusion broth (BHI, Difco) or Tryptic Soy Broth (TSB, Difco) shaking at 37 °C, and *E. coli* strains were cultivated in LB broth (Miller) shaking at 37 °C. Antibiotics were used at the following concentrations for Gram-negative strains: carbenicillin (100 µg/mL), kanamycin (50 µg/mL). Antibiotics were used at the following concentrations for Gram-positive strains: streptomycin (200 µg/mL), chloramphenicol (5 µg/mL), tetracycline (2 µg/mL).

## Cloning and plasmid construction

The integrating plasmid pPL2 was used to generate *L. monocytogenes* mutants, as previously described[115]. Briefly, genes of interest were amplified from *L. monocytogenes* 10403S and digested with the same restriction endonucleases (New England Biolabs) used to digest the pPL2 vector, followed by a ligation reaction to join the insert with the vector. Ligation products were transformed into SM10 *E. coli* and sequenced before proceeding.

Constructed plasmids in SM10 *E. coli* were transconjugated into recipient *L. monocytogenes* strains by mixing donor and recipient cells 1:1 and incubating on BHI agar plates for 4-24 hours at 30 °C. Cell mixtures were then streaked on BHI plates containing streptomycin and chloramphenicol to select for cells containing the pPL2 plasmid. Resulting colonies were re-streaked for isolation and sequenced before using.

The strain Δ*yjbH P-spxA1::Tn* was constructed by transducing the *himar1* transposon into the Δ*yjbH* background, as previously described[78,116].

Plasmids for BACTH assays were constructed via Gibson Assembly using the NEBuilder HiFi DNA Assembly Master Mix (New England Biolabs). Briefly, genes of interest were amplified with 5' (ATGGGGTCCAGCGGCGCTGGATCC) and 3' (GCTGCAGGAGGCAGTGGAGCGAGC) linker regions identical to linker regions flanking a *ccdB* toxin cassette in the pUT18x, pUT18Cx, pKT25x, and pKNT25x vectors, which were generously gifted to us by Aaron Whiteley[117]. Vectors were linearized with BamHI and PstI endonucleases that excised the *ccdB* cassette, then combined in the NEB Master Mix with an insert encoding the gene of interest as directed by the manufacturer. The reaction mix was transformed into *E. coli* XL1 Blue cells. XL1 Blue cells containing single BACTH vectors were sequenced, and their plasmid DNA was harvested. Each BTH101 strain used in BACTH assays was co-transformed with one T18 plasmid and one

T25 plasmid. After co-transformations, all BTH101 strains were cultivated in both kanamycin and carbenicillin at all times to retain both plasmids.

## Minimum inhibitory concentration assays

*L. monocytogenes* cultures were grown overnight in TSB media containing streptomycin at 37 °C. The next day, MIC assays were set up in 96-well plates. Overnight cultures were diluted in PBS to $10^4$ CFU/mL. Each well contained 200 µL total of TSB medium supplemented with SNP (solution made fresh daily in TSB with streptomycin), and 2 x $10^4$ CFU of diluted overnight culture (2 µL per well). Each *L. monocytogenes* strain was tested in 120 mM SNP, 100 mM, 80 mM, 60 mM, 40 mM, 20 mM, 10 mM, and 0 mM. Plates were incubated in shaking plate incubator at 37 °C for 24 hours, then the MIC for each strain was determined as the lowest concentration of SNP with no visible bacterial growth.

In Chapter 4, DEA NONOate (Sigma-Aldrich) and KCN (Sigma-Aldrich) were also tested in MIC assays. The set-up for the 96-well plates was identical for DEA NONOate experiments, except each *L. monocytogenes* strain was tested in TSB containing 40 mM DEA NONOate, 35 mM, 30 mM, 25 mM, 20 mM, 15 mM, 10 mM, and 0 mM. The DEA NONOate was dissolved in water. Plates were incubated for 24 hours at 37 °C, and one of the two biological replicates was allowed to continue incubating at room temperature for an additional 24 hours.

The set-up for the 96-well plates was identical for KCN experiments, except each *L. monocytogenes* strain was tested in TSB containing 100 mM KCN, 50 mM, 25 mM, 12.5 mM, 6.25 mM, 3.125 mM, 1.55 mM, and 0 mM. Five replicates were performed because bacterial growth was poor. The KCN was dissolved in water for the first replicate, and TSB + streptomycin in all other replicates. The first two replicates used an inoculum of 2 x $10^4$ CFU of diluted overnight culture per well, and the last three replicates used an inoculum of 1 x $10^5$ CFU per well. Several replicates incubated the plate in a static 37 °C incubator and several used a shaking plate reader, as above. This protocol needs to be further optimized to achieve more robust bacterial growth.

## L2 plaque assays

Plaque assays were performed according to published protocols[103]. Briefly, L2 fibroblasts were seeded at a density of 1.2 x $10^6$ per well in a 6-well dish and overnight cultures of *L. monocytogenes* were incubated at 30 °C in BHI broth. The next day, cultures were diluted 1:10 in sterile PBS and 5 µL was used to infect cells for one hour before washing twice with sterile PBS. Agarose overlays containing DMEM and gentamicin were added to the wells and plates

were incubated for two days before staining the cells with Neutral Red dye. Plaques were imaged 24 hours later and plaque areas were determined using Image J software[118]. All plaque data represent three biological replicates.

## Immunoblotting for LLO protein

Overnight *L. monocytogenes* cultures were subcultured 1:10 into BHI media containing streptomycin and incubated for five hours at 37 °C, shaking. Cultures were pelleted and the supernatant was then TCA-precipitated to collect protein, boiled in loading dye, and separated by gel electrophoresis. Proteins were then transferred to PVDF membrane (Bio-Rad), and the membrane was blocked with Odyssey blocking buffer (LI-COR Biosciences). Proteins of interest were detected using polyclonal rabbit anti-LLO antibody (from the Portnoy Laboratory, University of California at Berkeley) at a dilution of 1:5,000 and monoclonal mouse anti-P60 antibody (Adipogen) at a dilution of 1:2,000. Goat anti-rabbit (Invitrogen) and goat anti-mouse (LI-COR Biosciences) antibodies were used to detect the primary antibodies, each at a dilution of 1:5,000. Immunoblots were imaged on a LI-COR Odyssey Fc and analyzed using Image Studio software.

## Immunoblotting for YjbH protein

Overnight *L. monocytogenes* cultures were subcultured 1:10 into BHI media containing streptomycin and incubated for five hours at 37 °C, shaking. For cultures in Figure 9, the incubation period is as noted on the figure: either 2, 3, or 5 hours of growth. For the stressed cultures in Figure 9, the noted sublethal stressor was added to the culture for the last 30 minutes or one hour of a total of five hours growth at 37 °C before harvesting. These stressors included: stationary incubation at 42 °C heat; 5 mM diamide (Sigma-Aldrich); 5% ethanol (Fisher Scientific); 60 mM sodium nitroprusside (Sigma-Aldrich); and 10 mM hydrogen peroxide (Invitrogen). At the end of the stress period, $OD_{600}$ measurements were taken with a spectrophotometer. Cultures were pelleted, washed, and resuspended in a volume of 0.1% NP-40 + 0.1 mM PMSF equal to 10X the $OD_{600}$. Zirconium beads (0.1 mm diameter, Benchmark Scientific) were added to each sample before bead-beating twice for 30 seconds each, keeping samples on ice in between. Samples were centrifuged at 4 °C for 15 minutes and then boiled in loading dye. Gel electrophoresis was used to separate each sample. Proteins were then transferred to PVDF membrane (Bio-Rad), and the membrane was blocked with Odyssey blocking buffer (LI-COR Biosciences). Proteins of interest were detected using polyclonal rabbit anti-StrepII antibody (VWR) at a dilution of 1:2,000. Goat anti-rabbit (Invitrogen) antibody was

used to detect the primary antibody, at a dilution of 1:5,000. Immunoblots were imaged on an Azure Biosystems Sapphire Biomolecular Imager.

## Co-immunoprecipitation using YjbH$^{C27S}$ trapping mutant

The *L. monocytogenes* strain used in these co-IP experiments is as follows: Δ*yjbH clpX::Tn* pPL2.P-Hyper.*yjbH*$^{C27S}$*.6X-His.strepII* (#BRR-006). This strain overexpresses a trapping mutant of YjbH$_{Lm}$ that includes both a 6X-His tag and a strepII tag. The following protocol yielded a YjbH$^{C27S}$ band in the co-IP elution fraction on an immunoblot and is the result of optimizing many steps.

Overnight culture of Δ*yjbH clpX::Tn* pPL2.P-Hyper.*yjbH*$^{C27S}$*.6X-His.strepII* in 10 mL of BHI + streptomycin was subcultured into 100 mL BHI + strep in a 1-L flask to an $OD_{600}$ of 0.1. As a control, wild type *L. monocytogenes* was used alongside the co-IP strain. The cultures were grown shaking at 37 °C to an $OD_{600}$ of approximately 2.5 and pelleted by centrifugation. The pellets were resuspended in 10 mL PBS + 0.6 % paraformaldehyde to crosslink, then incubated at 37 °C shaking for 20 minutes. The PFA was quenched with a final concentration of 500 mM glycine and incubated for 5 more minutes at 37 °C shaking. The cultures were pelleted and the supernatants disposed of in hazardous waste. After resuspending the pellets in 1 mL of Wash Buffer (50 mM Tris at pH 8, 150 mM NaCl, 0.1% Triton X100, 1 mM imidazole) + 150 U mutanolysin, the bacteria were incubated for 15 minutes in a 37 °C water bath and mixed by inversion. The bacteria were further diluted in Wash Buffer to 10 mL + 0.1 mM PMSF + 10 mM β-ME and keep on ice. While on ice, the cultures were sonicated 4X at 70% amplitude for 30 seconds per round, pulsing 1 second on/1 second off. The lysed cultures were centrifuged for 30 minutes at 4 °C at max speed. A small amount of both the supernatants (“lysate”) and pellets were sampled and boiled in loading dye for analysis later.

To equilibrate the HisPur Ni-NTA resin (Thermo Fisher), 2 mL of 50% resin slurry were applied to a 5-mL volume column and washed twice with 5 mL of Wash Buffer, always allowing the full volume to exit the column before adding more. The equilibrated resin was added to a 50-mL conical tube that contained the lysate and incubated at 4 °C rocking overnight. The next morning, the resin-lysate mixture was gently applied to the column, taking care to remove as much resin as possible from the conical. The flowthrough was collected and sampled for analysis, as were all washes and elutions. Wash 1 = 5 mL Wash Buffer + 500 mM NaCl. Wash 2 = 5 mL Wash Buffer + 10 mM imidazole. Elutions 1-4 = 4 mL Wash Buffer + 250 mM imidazole, adjusted to pH 8. To analyze the IP fractions, all fractions were mixed with loading buffer and boiled before separation by SDS-PAGE and immunoblotting and/or silver staining.

For immunoblotting, YjbH$^{C27S}$ was detected with anti-StrepII (VWR) and goat anti-rabbit (Invitrogen) antibodies, both used at a dilution of 1:5000.

## Recombinant protein expression of MBP-YjbH$_{Lm}$ and MBP

Overnight culture of *E. coli* BL21(DE3) pET16.*His.mbp.yjbH$_{Lm}$.strepII* (which encodes both a 6X-His tag and a StrepII tag; #BRR-035) was subcultured 1:100 into 200 mL BHI + carbenicillin. Culture was grown shaking at 37 °C to $OD_{600}$ = 1. IPTG was added to a final concentration of 1 mM before shaking for 5 hours at room temperature. Bacteria were collected by centrifugation and washed once in PBS before centrifuging again. The pellet was aspirated and frozen at -80 °C overnight.

After thawing on ice, the pellet was resuspended in 20 mL Lysis Buffer (650 mM NaCl, 50 mM Tris pH 8, 0.1% Triton X100, 10% glycerol, 10 mM β-mercaptoethanol). Bacteria were sonicated in 3 rounds of 70% amplitude, pulsing 1 sec on/1 sec off, 30 seconds per round. Sample was kept on ice in between rounds and then centrifuged for 30 minutes at 20,000 x g, 4 °C. After centrifuging, a small sample of the lysate and pellet was reserved for SDS-PAGE.

1.5 mL packed HisPur Ni-NTA resin (Thermo Fisher) was equilibrated with 2X column volumes (CVs; 5-mL columns were used in this protocol) PBS followed by 1 CV Lysis Buffer + 1 mM imidazole. The column was stoppered before adding lysate, which incubated together 1 hour at 4 °C while rotating. The column was opened and flowthrough was collected. Wash 1: 1 CV Lysis Buffer + 1 mM imidazole. Wash 2: 1 CV Wash Buffer (50 mM Tris at pH 8, 150 mM NaCl, 10% glycerol) + 50 mM imidazole. Wash 3: Wash Buffer + 200 mM imidazole. Collect all washes. Protein was eluted by three rounds of 2 mL Elution Buffer (Wash Buffer + 500 mM imidazole).

All samples were combined with loading dye and boiled, then separated by SDS-PAGE on a 4-20% pre-cast gel (BioRad). The gel was stained with Coomassie to ensure there was a correctly sized band present in the elution fraction. All desired elutions were combined, then dialyzed in regenerated cellulose dialysis tubing (Fisher). Two rounds of dialysis in 800 mL PBS + 10% glycerol for 3 hours each were performed while gently shaking at 4 °C. The dialyzed, eluted protein was then filtered using a 50-kD cutoff column (Amicon). Aliquots of the purified protein were frozen in PBS + 10% glycerol for future use.

## *L. monocytogenes* lysate preparation and co-immunoprecipitations

Lysate preparation: In biological triplicate, Δ*yjbH$_{Lm}$* overnight cultures were subcultured 1:100 into 15 mL BHI + streptomycin and grown to approximately $OD_{600}$ = 1.7. Cultures were

centrifuged, the pellets were washed once in PBS, and centrifuged again. Pellets were resuspended in 2 mL Wash Buffer (50 mM Tris pH 8.0, 150 mM NaCl, 0.1% Triton X100) and transferred to Eppendorf tubes. 37.5 units of mutanolysin (Sigma-Aldrich) were added before incubating in 37 °C water bath for 15 minutes. PMSF was added to 0.1 mM and β-mercaptoethanol was added to 10 mM. Bacteria were lysed by sonication (70% amplitude for 30 seconds, 3X on ice) and centrifuged 30 minutes at 12k rpm at 4 °C. A small aliquot was reserved for analysis by SDS-PAGE, and lysate was separated from pellet for use in co-immunoprecipitations.

Co-immunoprecipitations: Fresh lysate was prepared as described above. Equilibrate 40 µL of magnetic HisPur Ni-NTA resin (Thermo Fisher Scientific) per sample in Eppendorf tubes, as instructed by manufacturer. For each species of bait (MBP-YjbH$_{Lm}$ and MBP), 10 µg purified protein in 25 µL was combined with 200 µL lysate and 200 µL Equilibration Buffer (20 mM sodium phosphate, 300 mM sodium chloride, 10 mM imidazole, pH 7.4). Protein mixes were applied to equilibrated resin aliquots and incubated 30 minutes rotating at room temperature. Tubes were placed in a magnetic rack and the flowthrough collected. Two 100-µL washes were performed using PBS supplemented with 50 mM and 100 mM imidazole, sequentially. Each wash incubated for 15 minutes rotating at room temperature. Two 25-µL elutions were performed using PBS supplemented with 1 M imidazole. Elutions incubated for 15 minutes rotating at room temperature before collection. Small aliquots were taken at each step for analysis by SDS-PAGE and silver staining. Elutions were subsequently prepared for mass spectrometry. Co-immunoprecipitations were performed in biological triplicate for each bait species. Co-IPs to detect an interaction between MBP-YjbH$_{Lm}$ and Lmo2638 used amylose resin (New England Biolabs) and the corresponding buffers recommended by the manufacturer.

## Co-immunoprecipitation sample preparation for LC-MS/MS

Acetone/TCA precipitation protocol: Eight times the sample volume of cold acetone was added to the elution sample. Acetone was added in increments and vortexed between additions before adding one sample volume of cold TCA, gently vortexing, and spinning briefly. Incubate overnight at -20 °C. Next morning, solution was centrifuged for 15 minutes at 13,000 x g at 4 °C. The supernatant was removed. Samples were kept on ice during this preparation. 200 µL cold acetone was added to the pellets, and the samples were centrifuged as before. Supernatant was again removed. Two more cold acetone washes were performed. The acetone was allowed to completely evaporate in a chemical hood for one hour.

In-solution digestion protocol: Dry protein pellets were resuspended in 50 µL of 8 M urea and 0.4 M ammonium bicarbonate. It was verified using litmus paper that the pH was greater than 7.0. 2 µL of 100 mM dithiothreitol (Promega) in water was added and samples were incubated at 50 °C for 30 minutes and then cooled to room temperature. 3 µL of 300 mM iodoacetamide (Fisher) in water was added and samples were incubated at room temperature in the dark for 30 minutes. It was again verified that the pH of samples was above 7. Water was added to the sample solution to dilute the 8 M urea by (145 µL water added). To digest protein samples, 1 µg Trypsin Gold (Promega) was added to each sample and incubated overnight shaking at 37 °C.

Desalting with C18 spin columns: Solvent A = 5 % acetonitrile (Fisher) + 0.1% formic acid (Fisher). Activation solution = 50 % MeOH. Trypsin-digested samples were dried in a speedvac and resuspended in 100 µL Solvent A. It was verified that the sample pH was between 2 and 3. C18 Spin Columns (Pierce) were activated by adding 200 µL Activation Solution and centrifuging 1 minute at 1300 x g, discarding the flowthrough, and repeating. Columns were then placed on new receiver tubes. To equilibrate columns, 200 µL Solvent A was added and spun as before. Flowthrough was discard and two more washes with Solvent A were performed. Columns were placed on new receiver tubes. Samples were loaded onto columns and centrifuged at 1300 x g for 1 minute. Flowthrough was reapplied to columns and centrifuged again. This was repeated again for a total of 3 sample applications. The columns were placed on new low protein-binding tubes. Proteins were eluted by adding 40 µL of 80 % acetonitrile + 0.1 % formic acid to the resin bed and centrifuging at 1300 x g for 1 minute. Elution was repeated twice more to collect a total of 120 µL in the tube. Samples were then dried in a speedvac until dry and resuspended in 30 µL Solvent A. Samples were then sent to Northwestern University Proteomics Core for analysis by mass spectrometry. This sample preparation protocol is from the Northwestern University Proteomics Core.

## Bacterial two-hybrid broth quantification

*E. coli* BTH101 strains, each containing one pUT18x vector (carbenicillin resistance) and one pKT25x vector (kanamycin resistance), were grown overnight at 37 °C in LB broth containing kanamycin and carbenicillin. Cultures were permeabilized by combining 800 µL Z-Buffer, 20 µL 0.1% SDS, 40 µL chloroform, and 200 µL overnight culture. The assay was performed in a 96-well plate, and each strain was assayed in technical triplicate. Each well contained 150 µL Z-Buffer, 50 µL permeabilized culture solution, and 40 µL 0.4% ONPG (Fisher Scientific) to start the reaction. A420 and A550 values were collected every two minutes for 30 minutes at 28 °C.

A420 data were graphed to determine the linear portion of the reaction, from which the calculations were performed. Miller Units were calculated with the following equation: [(A420-(1.75*A550))/(*t**v**A600)]*1000 where *t* equals time in minutes and *v* equals culture volume used in the assay in milliliters[119]. All BACTH data represent three biological replicates.

## Whole-cell proteomics sample preparation

Wild type and *L. monocytogenes* Δ*yjbH* were grown overnight, then subcultured for 5 hours shaking at 37 °C in BHI broth containing streptomycin. Cultures were then centrifuged for 20 minutes at 4 °C. Pellets were sonicated in lysis buffer [0.1 M ammonium bicarbonate, 8 M urea, 0.1% w/v Rapigest detergent (Waters)] and centrifuged at maximum speed. Tris(2-carboxyethyl)phosphine hydrochloride (TCEP, Sigma-Aldrich) was added to supernatant fractions to a final concentration of 5 mM. Samples were incubated at room temperature for one hour before adding iodoacetamide to 10 mM. Samples were then incubated in the dark at room temperature for 30 minutes before adding N-acetylcysteine to 15 mM. Samples were then digested with Trypsin Gold (Promega) overnight at 37 °C by combining 200 µg of each sample (determined by BCA assay) with trypsin in a 1:20 w/w (trypsin:protein) ratio. Following trypsinization, 2 M HCl was added drop-wise to each sample until samples became acidic (pH 1-2), as monitored with pH paper. Detergent was removed by centrifugation at 10,000 x g for 5 minutes, and the supernatant transferred into new tubes. Acetonitrile (ACN) and trifluoroacetic acid (TFA) were added to 5% and 0.1% v/v, respectively. Samples were processed through MacroSpin C18 Columns (30-300 µg capacity, The Nest Group) as directed, and washed with 5% ACN, 0.1% TFA. Samples were eluted with 80% ACN, 25 mM formic acid. Samples were then sent to Northwestern University Proteomics Core for analysis by mass spectrometry. Sample preparation protocol is adapted from the Mougous Laboratory[120].

## LC-MS/MS analysis

Peptides were analyzed by LC-MS/MS using a Dionex UltiMate 3000 Rapid Separation nanoLC and an Orbitrap Elite Mass Spectrometer (Thermo Fisher Scientific Inc, San Jose, CA). Samples were loaded onto the trap column, which was 150 µm x 3 cm in-house packed with 3 µm ReproSil-Pur® beads. The analytical column was a 75 µm x 10.5 cm PicoChip column packed with 3 µm ReproSil-Pur® beads (New Objective, Inc. Woburn, MA). The flow rate was kept at 300nL/min. Solvent A was 0.1% FA in water and Solvent B was 0.1% FA in ACN. The peptide was separated on a 120-min analytical gradient from 5% ACN/0.1% FA to 40% ACN/0.1% FA. $MS^1$ scans were acquired from 400-2000m/z at 60,000 resolving power and

automatic gain control (AGC) set to $1x10^6$. The 15 most abundant precursor ions in each $MS^1$ scan were selected for fragmentation by collision-induced dissociation (CID) at 35% normalized collision energy in the ion trap. Previously selected ions were dynamically excluded from re-selection for 60 seconds. This protocol was performed by the Northwestern Proteomics Core.

## Data analysis

Proteins were identified from the MS raw files using Mascot search engine (Matrix Science, London, UK; version 2.5.1). MS/MS spectra were searched against the UniProt *Listeria monocytogenes* database. All searches included carbamidomethyl cysteine as a fixed modification and oxidized Met, deamidated Asn and Gln, acetylated N-term as variable modifications. Three missed tryptic cleavages were allowed. The $MS^1$ precursor mass tolerance was set to 10 ppm and the $MS^2$ tolerance was set to 0.6 Da. The search result was visualized by Scaffold (version 4.8.3. Proteome Software, Inc., Portland, OR). A 1% false discovery rate cutoff was applied at the peptide level. Only proteins with a minimum of two unique peptides above the cutoff were considered for further study. This protocol was performed by the Northwestern Proteomics Core.

## Quantitative RT-PCR of bacterial transcripts

Overnight cultures of wild type and Δ*yjbH L. monocytogenes* were diluted 1:100 into 25 mL of BHI in a 250-mL flask and grown in BHI broth at 37 °C shaking until cultures reached an $OD_{600}$ of 1.0. At this point 5 mL of each culture was pipetted into 5 mL ice-cold MeOH, inverted to mix, and centrifuged at 4 °C to pellet. All supernatant was removed and pellets were frozen in liquid nitrogen before storing at -80 °C overnight.

Frozen pellets were resuspended in 400 µL AE Buffer (50 mM NaOAc at pH 5.2, 10 mM EDTA, DEPC-treated and autoclaved) and vortexed vigorously. Samples were kept on ice as much as possible during entire protocol. 400 µL of resuspended pellet mixture was transferred to an RNase-free 1.5-mL tube on ice containing 50 µL 10% SDS and 500 µL 1:1 acidified phenol:chloroform (made fresh, with aqueous layer removed before addition of pellet mixture). Samples were then lysed by bead-beating and returned to ice. Lysed samples were applied to pre-spun 5PRIME Phase Lock Gel Heavy tubes (Quantabio) and centrifuged at maximum speed for 5 minutes. The aqueous layer was pipetted into a new 1.5-mL tube containing 50 µL 3 M NaOAc at pH 5.2 and 1 mL 100% EtOH and vortexed to mix. Samples were centrifuged at 4 °C for 30 minutes at maximum speed, at which point the EtOH was removed by aspiration. 500 µL 70% EtOH was added to each sample and vortexed to mix. After centrifuging at room

temperature for 10 minutes at maximum speed, the EtOH was removed by aspiration and then by running samples in a speed-vac. Samples were resuspended in 50 µL water and reverse-transcribed using an iScript cDNA Synthesis Kit (Bio-Rad). Quantitative RT-PCR was performed on cDNA with iTaq Universal SYBR Green Supermix (Bio-Rad).

## Statistical analysis

Data collected from plaque assays, minimum inhibitory concentration assays, immunoblot quantifications, and quantitative RT-PCR were analyzed using Student's unpaired *t*-test in GraphPad Prism. *p* values greater than 0.05 were deemed statistically insignificant. Asterisks were used to denote the following *p* values: **, p* < 0.05*; **, p* < 0.01*, ***, p* < 0.001.

**Table 5**. *Listeria monocytogenes* strains used in this work.

| Strain | Description | Reference or Source |
|---|---|---|
| 10403S | Wild type | [114] |
| MLR-L081 | Δ*yjbH* | [40] |
| MLR-L273 | *P-spxA1::Tn* | [40] |
| MLR-L354 | Δ*yjbH P-spxA1::Tn* | This study |
| MLR-L905 | Δ*yjbH* pPL2.P-native.*yjbH* | This study |
| MLR-L906 | Δ*yjbH* pPL2.P-native.$yjbH^{C27A}$ | This study |
| MLR-L907 | Δ*yjbH* pPL2.P-native.$yjbH^{C30A}$ | This study |
| MLR-L908 | Δ*yjbH* pPL2.P-native.$yjbH^{C63A}$ | This study |
| MLR-L909 | Δ*yjbH* pPL2.P-native.$yjbH^{C89A}$ | This study |
| MLR-L910 | Δ*yjbH* pPL2.P-native.$yjbH^{C27/30A}$ | This study |
| MLR-L911 | Δ*yjbH* pPL2.P-native.$yjbH^{C63/89A}$ | This study |
| MLR-L912 | Δ*yjbH* pPL2.P-native.$yjbH^{\Delta cys}$ | This study |
| MLR-L913 | Δ*yjbH* pPL2.P-native.$yjbH_{Bs}$ | This study |
| MLR-L526 | Δ*yjbH* pPL2.P-Hyper.*yjbH* | This study |
| MLR-L914 | Δ*yjbH* pPL2.P-Hyper.$yjbH^{C27/30A}$ | This study |

| | | |
|---|---|---|
| MLR-L915 | Δ*yjbH* pPL2.P-Hyper.*yjbH*$^{C63/89A}$ | This study |
| MLR-L916 | Δ*yjbH* pPL2.P-Hyper.*yjbH*$^{\Delta cys}$ | This study |
| BRR-006 | *clpX::Tn* Δ*yjbH* pPL2.P-Hyper.*yjbH*$^{C27S}$*.6X-His.strepII* | This study |
| BRR-068 | Δ*yjbH* pPL2.P-Hyper.*lmo2638.FLAG* | This study |
| BRR-075 | Δ*yjbH* pPL2.P-Hyper.*mntA.6X-His* | This study |

**Table 6**. *Escherichia coli* strains used in this work.

| Strain | Description | Reference or Source |
|---|---|---|
| XL1 Blue | For vector construction | Stratagene |
| SM10 | For transconjugation | [121] |
| BTH101 | For BACTH system | [105] |
| DB3.1 | For vector construction | Invitrogen |
| MLR-E006 | pPL2 | [115] |
| MLR-E234 | pPL2t | [122] |
| MLR-E531 | DB3.1/pUT18x | This study |
| MLR-E532 | DB3.1/pUT18Cx | This study |
| MLR-E533 | DB3.1/pKNT25x | This study |
| MLR-E534 | DB3.1/pKT25x | This study |
| MLR-E080 | SM10/pPL2.P-native.*yjbH* | This study |
| BRR-092 | SM10/pPL2.P-native.*yjbH*$^{C27A}$ | This study |
| MLR-E150 | SM10/pPL2.P-native.*yjbH*$^{C30A}$ | This study |
| BRR-106 | SM10/pPL2.P-native.*yjbH*$^{C63A}$ | This study |
| BRR-107 | SM10/pPL2.P-native.*yjbH*$^{C89A}$ | This study |
| BRR-120 | SM10/pPL2.P-native.*yjbH*$^{C27/30A}$ | This study |
| BRR-238 | SM10/pPL2.P-native.*yjbH*$^{C63/89A}$ | This study |
| BRR-113 | SM10/pPL2.P-native.*yjbH*$^{\Delta cys}$ | This study |
| MLR-E522 | SM10/pPL2t.P-hyper.*yjbH* | This study |

| | | |
|---|---|---|
| BRR-143 | BTH101/pUT18Cx.*zip*; pKT25x.*zip* | This study |
| BRR-291 | BTH101/pUT18x.*yjbH*; pKNT25x | This study |
| BRR-144 | BTH101/pUT18x.*yjbH*; pKNT25x.*spxA1* | This study |
| BRR-169 | BTH101/pUT18x.*yjbH*; pKNT25x.$spx_{Bs}$ | This study |
| BRR-204 | BTH101/pUT18x.$yjbH^{C27/30A}$; pKNT25x.*spxA1* | This study |
| BRR-227 | BTH101/pUT18x.$yjbH^{C63/89A}$; pKNT25x.*spxA1* | This study |
| BRR-191 | BTH101/pUT18x.*yjbH*; pKNT25x.*lmo0218* | This study |
| BRR-247 | BTH101/pUT18x.*yjbH*; pKT25x.*lmo0256* | This study |
| BRR-248 | BTH101/pUT18x.*yjbH*; pKT25x.*lmo1258* | This study |
| BRR-249 | BTH101/pUT18x.*yjbH*; pKT25x.*lmo1387* | This study |
| BRR-250 | BTH101/pUT18x.*yjbH*; pKT25x.*lmo1636* | This study |
| BRR-251 | BTH101/yjpUT18x.*yjbH*; pKT25x.*lmo1647* | This study |
| BRR-206 | BTH101/pUT18x.*yjbH*; pKNT25x.*lmo1782* | This study |
| BRR-252 | BTH101/pUT18x.*yjbH*; pKT25x.*lmo2390* | This study |
| BRR-228 | BTH101/pUT18x.$yjbH^{C27/30A}$; pKNT25x.*lmo0218* | This study |
| BRR-253 | BTH101/pUT18x.$yjbH^{C27/30A}$; pKT25x.*lmo0256* | This study |
| BRR-254 | BTH101/pUT18x.$yjbH^{C27/30A}$; pKT25x.*lmo1258* | This study |
| BRR-255 | BTH101/pUT18x.$yjbH^{C27/30A}$; pKT25x.*lmo1387* | This study |
| BRR-256 | BTH101/pUT18x.$yjbH^{C27/30A}$; pKT25x.*lmo1636* | This study |
| BRR-257 | BTH101/pUT18x.$yjbH^{C27/30A}$; pKT25x.*lmo1647* | This study |
| BRR-208 | BTH101/pUT18x.$yjbH^{C27/30A}$; pKNT25x.*lmo1782* | This study |
| BRR-258 | BTH101/pUT18x.$yjbH^{C27/30A}$; pKT25x.*lmo2390* | This study |
| BRR-259 | BTH101/pUT18x.$yjbH^{C63/89A}$; pKNT25x.*lmo0218* | This study |
| BRR-260 | BTH101/pUT18x.$yjbH^{C63/89A}$; pKT25x.*lmo0256* | This study |
| BRR-261 | BTH101/pUT18x.$yjbH^{C63/89A}$; pKT25x.*lmo1258* | This study |
| BRR-262 | BTH101/pUT18x.$yjbH^{C63/89A}$; pKT25x.*lmo1387* | This study |
| BRR-263 | BTH101/pUT18x.$yjbH^{C63/89A}$; pKT25x.*lmo1636* | This study |
| BRR-264 | BTH101/pUT18x.$yjbH^{C63/89A}$; pKT25x.*lmo1647* | This study |
| BRR-265 | BTH101/pUT18x.$yjbH^{C63/89A}$; pKNT25x.*lmo1782* | This study |

| | | |
|---|---|---|
| BRR-266 | BTH101/pUT18x.*yjbH*$^{C63/89A}$; pKT25x.*lmo2390* | This study |
| BRR-153 | BTH101/pUT18x.*yjbH;* pKNT25x.*clpX* | This study |
| BRR-270 | BTH101/pUT18x.*yjbH;* pKT25x.*clpC* | This study |
| MRC-089 | BTH101/pUT18x; pKT25x.*spxA1* | This study |
| BRR-035 | BL21(DE3)/pET16.*6X-His.mbp.yjbH.strepII* | This study |

# Chapter 7: Referenced literature


1. McLauchlin, J., Mitchell, R., Smerdon, W. & Jewell, K. *Listeria monocytogenes* and listeriosis: A review of hazard characterization for use in microbiological risk assessment of foods. *International Journal of Food Microbiology* **92**, 15–33 (2004).
2. Schlech, W. F., Lavigne, P. M., Bortolussi, R. A., Allen, A. C. & Haldane, E. V. Epidemic listeriosis - evidence for transmission by food. *New England Journal of Medicine* **308**, 203–206 (1983).
3. Dewey-Mattia, D., Manikonda, K., Hall, A. J., Wise, M. E. & Crowe, S. J. Surveillance for foodborne disease outbreaks - United States, 2009-2015. *MMWR Surveillance Summaries* **67**, 1–11 (2018).
4. Doganay, M. Listeriosis: Clinical presentation. *FEMS Immunology & Medical Microbiology* **35**, 173–175 (2003).
5. Disson, O. & Lecuit, M. Targeting of the central nervous system by *Listeria monocytogenes*. *Virulence* **3**, 213–221 (2012).
6. Becroft, D. M. O., Farmer, K., Seddon, R. J., Sowden, R., Stewart, J. H., Vines, A., Wattie, D. A. Epidemic listeriosis in the newborn. *British Medical Journal* **3**, 747–751 (1971).
7. Johnston, W. H., Morton, S. A., H Wong, D. M. & Roy, T. E. Septicaemia of the newborn due to *Listeria monocytogenes*. *Canadian Medical Association Journal* **73**, 962 (1955).
8. Vazquez-Boland, J., Kuhn, M., Berche, P., Chakraborty, T. & Dominguez-Bernal, G. *Listeria* pathogenesis and molecular virulence determinants. *Clinical Microbiology Reviews* **14**, 584–640 (2001).
9. Reniere, M. L. Reduce, induce, thrive: Bacterial redox sensing during pathogenesis. *Journal of Bacteriology* **200**, (2018).
10. Freitag, N. E., Port, G. C. & Miner, M. D. *Listeria monocytogenes* - From saprophyte to intracellular pathogen. *Nature Reviews Microbiology* **7**, 623–628 (2009).
11. Myers, J. T., Tsang, A. W. & Swanson, J. A. Localized reactive oxygen and nitrogen intermediates inhibit escape of *Listeria monocytogenes* from vacuoles in activated macrophages. *Journal of Immunology* **171**, 5447–5453 (2003).
12. Schnupf, P. & Portnoy, D. A. Listeriolysin O: A phagosome-specific lysin. *Microbes and Infection* **9**, 1176–1187 (2007).
13. Kocks, C., Gouin, E., Tabouret, M., Berche, P. & Ohayon, H. *L. monocytogenes*-induced actin assembly requires the *actA* gene product, a surface protein. *Cell* **68**, 521–531 (1992).
14. Tilney, L. G. & Portnoy, D. A. Actin filaments and the growth, movement, and spread of the intracellular bacterial parasite, *Listeria monocytogenes*.
15. Milohanic, E., Glaser, P., Coppée, J.-Y., Frangeul, L. & Vega, Y. Transcriptome analysis of Listeria monocytogenes identifies three groups of genes differently regulated by PrfA: Analysis of the PrfA regulon of *L. monocytogenes*. *Molecular Microbiology* **47**, 1613–1625 (2003).
16. de las Heras, A., Cain, R. J., Bielecka, M. K. & Vazquez-Boland, J. A. Regulation of *Listeria* virulence: PrfA master and commander. *Current Opinion in Microbiology* **14**, 118–127 (2011).

17. Reniere, M. L., Whiteley, A., Hamilton, K., John, S., Lauer, P., Brennan, R., & Portnoy, D. Glutathione activates virulence gene expression of an intracellular pathogen. *Nature* **517**, 170–173 (2015).
18. Vasanthakrishnan, R. B., de las Heras, A., Scortti, M., Deshayes, C., Colegrave, N., & Vázquez-Boland, J. PrfA regulation offsets the cost of *Listeria* virulence outside the host. *Environmental Microbiology* **17**, 4566–4579 (2015).
19. Freitag, N. & Portnoy, D. Dual promoters of the *Listeria monocytogenes prfA* transcriptional activator appear essential *in vitro* but are redundant *in vivo*. *Molecular Microbiology* **12**, 845–853 (1994).
20. Mengaud, J., Dramsi, S., Gouin, E., Vázquez-Boland, J. & Milon, G. Pleiotropic control of *Listeria monocytogenes* virulence factors by a gene that is autoregulated. *Molecular Microbiology* **5**, 2273–2283 (1991).
21. Johansson, J., Mandin, P., Renzoni, A., Chiaruttini, C. & Springer, M. An RNA thermosensor controls expression of virulence genes in *Listeria monocytogenes*. *Cell* **110**, 551–561 (2002).
22. Wong, K., Bouwer, H. & Freitag, N. Evidence implicating the 5' untranslated region of *Listeria monocytogenes actA* in the regulation of bacterial actin-based motility. *Cellular Microbiology* **6**, 155–166 (2004).
23. Xayarath, B. & Freitag, N. E. Optimizing the balance between host and environmental survival skills: Lessons learned from *Listeria monocytogenes*. *Future Microbiology* vol. 7 839–852 (2012).
24. Hall, M., Grundström, C., Begum, A., Lindberg, M. & Sauer, U. Structural basis for glutathione-mediated activation of the virulence regulatory protein PrfA in *Listeria*. *Proceedings of the National Academy of Sciences* **113**, 14733–14738 (2016).
25. Wang, Y., Feng, H., Zhu, Y. & Gao, P. Structural insights into glutathione-mediated activation of the master regulator PrfA in *Listeria monocytogenes*. *Protein & Cell* **8**, 308–312 (2017).
26. Chico-Calero, I., Suárez, M., González-Zorn, B., Scortti, M., Slaghuis, J., Goebel, W., The European *Listeria* Genome Consortium, & Vázquez-Boland, J. Hpt, a bacterial homolog of the microsomal glucose-6-phosphate translocase, mediates rapid intracellular proliferation in *Listeria*. *Proceedings for the National Academy of Sciences* (2002).
27. Sheehan, B., Klarsfeld, A., Msadek, T. & Cossart, P. Differential activation of virulence gene expression by PrfA, the *Listeria monocytogenes* virulence regulator. *Journal of Bacteriology* **177**, 6469–6476 (1995).
28. Bischofberger, M., Iacovache, I. & van der Goot, F. Pathogenic pore-forming proteins: Function and host response. *Cell Host & Microbe* **12**, 266–275 (2012).
29. Dunstone, M. A. & Tweten, R. K. Packing a punch: The mechanism of pore formation by cholesterol dependent cytolysins and membrane attack complex/perforin-like proteins. *Current Opinion in Structural Biology* vol. 22 342–349 (2012).
30. Nguyen, B. N., Peterson, B. N. & Portnoy, D. A. Listeriolysin O: A phagosome-specific cytolysin revisited. *Cellular Microbiology* vol. 21 (2019).
31. Shen, A. & Higgens, D. E. The 5' untranslated region-mediated enhancement of intracellular listeriolysin O production is required for *Listeria monocytogenes* pathogenicity. *Molecular Microbiology* **57**, 1460–1473 (2005).

32. Schnupf, P., Hofmann, J., Norseen, J., Glomski, I. J. & Schwartzstein, H. Regulated translation of listeriolysin O controls virulence of *Listeria monocytogenes*. *Molecular Microbiology* **61**, 999–1012 (2006).
33. Glomski, I. J., Gedde, M. M., Tsang, A. W., Swanson, J. A. & Portnoy, D. A. The *Listeria monocytogenes* hemolysin has an acidic pH optimum to compartmentalize activity and prevent damage to infected host cells. *Journal of Cell Biology* **156**, 1029–1038 (2002).
34. Decatur, A. L. & Portnoy, D. A. A PEST-like sequence in listeriolysin O essential for *Listeria monocytogenes* pathogenicity. *Science* **290**, 992–995 (2000).
35. Schnupf, P., Portnoy, D. A. & Decatur, A. L. Phosphorylation, ubiquitination and degradation of listeriolysin O in mammalian cells: Role of the PEST-like sequence. *Cellular Microbiology* **8**, 353–364 (2006).
36. Schnupf, P., Zhou, J., Varshavsky, A. & Portnoy, D. A. Listeriolysin O secreted by *Listeria monocytogenes* into the host cell cytosol is degraded by the N-end rule pathway. *Infection and Immunity* **75**, 5135–5147 (2007).
37. Moors, M. A., Levitt, B., Youngman, P. & Portnoy, D. A. Expression of listeriolysin O and ActA by intracellular and extracellular *Listeria monocytogenes*. *Infection and Immunity* **67**, 131–139 (1999).
38. Brundage, R., Smith, G., Camilli, A., Theriot, J. & Portnoy, D. Expression and phosphorylation of the *Listeria monocytogenes* ActA protein in mammalian cells. *Proceedings of the National Academy of Sciences* **90**, 11890–11894 (1993).
39. Shetron-Rama, L. M., Marquis, H., Bouwer, H. G. A. & Freitag, N. E. Intracellular induction of *Listeria monocytogenes actA* expression. *Infection and Immunity* **70**, 1087–1096 (2002).
40. Reniere, M. L., Whiteley, A. T. & Portnoy, D. A. An *in vivo* selection identifies *Listeria monocytogenes* genes required to sense the intracellular environment and activate virulence factor expression. *PLoS Pathogens* (2016) doi:10.1371/journal.ppat.1005741.
41. Imlay, J. A. Cellular defenses against superoxide and hydrogen peroxide. *Annual Review of Biochemistry* **77**, 755–776 (2008).
42. Mishra, S. & Imlay, J. Why do bacteria use so many enzymes to scavenge hydrogen peroxide? *Archives of Biochemistry and Biophysics* **525**, 145–160 (2012).
43. Ruhland, B. & Reniere, M. Sense and sensor ability: redox-responsive regulators in *Listeria monocytogenes*. *Current Opinion in Microbiology* **47**, 20–25 (2019).
44. Cain, J., Solis, N. & Cordwell, S. Beyond gene expression: The impact of protein post-translational modifications in bacteria. *Journal of Proteomics* **97**, 265–286 (2014).
45. Bednarska, N. G., Schymkowitz, J., Rousseau, F. & van Eldere, J. Protein aggregation in bacteria: The thin boundary between functionality and toxicity. *Microbiology* **159**, 1795–1806 (2013).
46. Kuhlmann, N. & Chien, P. Selective adaptor dependent protein degradation in bacteria. *Current Opinion in Microbiology* **36**, 118–127 (2017).
47. Fuangthong, M., Atichartpongkul, S., Mongkolsuk, S. & Helmann, J. D. OhrR is a repressor of *ohrA*, a key organic hydroperoxide resistance determinant in *Bacillus subtilis*. *Journal of Bacteriology* **183**, 4134–4141 (2001).

48. Lee, J.-W., Soonsanga, S., Helmann, J. D. & Gottesman, S. A complex thiolate switch regulates the *Bacillus subtilis* organic peroxide sensor OhrR. *Proceedings of the National Academy of Sciences* (2007).
49. Garnica, O., Das, K. & Dhanayuthapani, S. OhrR of Mycobacterium smegmatis sense and responds to intracellular organic hydroperoxide stress. *Scientific Reports* **7**, 3922 (2017).
50. Imlay, J. A. Transcription factors that defend bacteria against reactive oxygen species. *Annual Review of Microbiology* **69**, 93–108 (2015).
51. Lee, J. & Helmann, J. The PerR transcription factor senses $H_2O_2$ by metal-catalyzed histidine oxidation. *Nature* **440**, 363–367 (2006).
52. Ahn, B. E. & Baker, T. A. Oxidization without substrate unfolding triggers proteolysis of the peroxide-sensor, PerR. *Proceedings of the National Academy of Sciences* **113**, E23–E31 (2016).
53. Rea, R., Hill, C. & Gahan, C. G. M. *Listeria monocytogenes* PerR mutants display a small-colony phenotype, increased sensitivity to hydrogen peroxide, and significantly reduced murine virulence. *Applied and Environmental Microbiology* **71**, 8314–8322 (2005).
54. Lee, J. & Helmann, J. Biochemical characterization of the structural Zn 2+ site in the *Bacillus subtilis* peroxide sensor PerR. *Journal of Biological Chemistry* **281**, 23567–23578 (2006).
55. Fuangthong, M., Herbig, A. F., Bsat, N. & Helmann, J. D. Regulation of the *Bacillus subtilis fur* and *perR* genes by PerR: Not all members of the PerR regulon are peroxide inducible. *Journal of Bacteriology* **184**, 3276–3286 (2002).
56. Faulkner, M. J., Ma, Z., Fuangthong, M. & Helmann, J. D. Derepression of the *Bacillus subtilis* PerR peroxide stress response leads to iron deficiency. *Journal of Bacteriology* **194**, 1226–1235 (2012).
57. Ravcheev, D. A. *et al.* Transcriptional regulation of central carbon and energy metabolism in bacteria by redox-responsive repressor rex. *Journal of Bacteriology* **194**, 1145–1157 (2012).
58. Gyan, S., Shiohira, Y., Sato, I., Takeuchi, M. & Sato, T. Regulatory loop between redox sensing of the NADH/NAD+ ratio by Rex (YdiH) and oxidation of NADH by NADH dehydrogenase Ndh in *Bacillus subtilis*. *Journal of Bacteriology* **188**, 7062–7071 (2006).
59. Richardson, A. R., Somerville, G. A. & Sonenshein, A. L. Regulating the intersection of metabolism and pathogenesis in Gram-positive bacteria. *Microbiology Spectrum* **3**, (2015).
60. Zuber, P. Spx-RNA polymerase interaction and global transcriptional control during oxidative stress. *Journal of Bacteriology* **186**, 1911–1918 (2004).
61. Newberry, K. J., Nakano, S., Zuber, P. & Brennan, R. G. Crystal structure of the *Bacillus subtilis* anti-alpha, global transcriptional regulator, Spx, in complex with the C-terminal domain of RNA polymerase. *Proceedings of the National Academy of Sciences* **102**, 15839–15844 (2005).
62. Nakano, S., Küster-Schöck, E., Grossman, A. D. & Zuber, P. Spx-dependent global transcriptional control is induced by thiol-specific oxidative stress in *Bacillus subtilis*. *Proceedings of the National Academy of Sciences* **100**, 13603–13608 (2003).

63. Nakano, S., Nakano, M. M., Zhang, Y., Leelakriangsak, M. & Zuber, P. A regulatory protein that interferes with activator- stimulated transcription in bacteria. *Proceedings of the National Academy of Sciences* **100**, 4233–4238 (2003).
64. Landeta, C., Boyd, D. & Beckwith, J. Disulfide bond formation in prokaryotes. *Nature Microbiology* **3**, 270–280 (2018).
65. Rochat, T., Nicolas, P., Delumeau, O., Rabatinová, A., Korelusová, J., Leduc, A., Bessières, P., Dervyn, E., Krásny, L., & Noirot, P. Genome-wide identification of genes directly regulated by the pleiotropic transcription factor Spx in *Bacillus subtilis*. *Nucleic Acids Research* **40**, 9571–9583 (2012).
66. Gaballa, A., Antelmann, H., Hamilton, C. & Helmann, J. Regulation of *Bacillus subtilis* bacillithiol biosynthesis operons by Spx. *Microbiology* **159**, 2035–2035 (2013).
67. Choi, S. Y., Reyes, D., Leelakriangsak, M. & Zuber, P. The global regulator Spx functions in the control of organosulfur metabolism in *Bacillus subtilis*. *Journal of Bacteriology* **188**, 5741–5751 (2006).
68. Jousselin, A., Kelley, W. L., Barras, C., Lew, D. P. & Renzoni, A. The *Staphylococcus aureus* thiol/oxidative stress global regulator Spx controls trfA, a gene implicated in cell wall antibiotic resistance. *Antimicrobial Agents and Chemotherapy* **57**, 3283–3292 (2013).
69. Veiga, P., Bulbarela-Sampieri, C., Furlan, S., Maisons, A., Chapot-Chartier, M., Erkelenz, M., Mervelet, P., Noirot, P., Frees, D., Kuipers, O., Kok, J., Gruss, A., Buist, G., & Kulakauskas, S. SpxB regulates O-acetylation-dependent resistance of *Lactococcus lactis* peptidoglycan to hydrolysis. *Journal of Biological Chemistry* **282**, 19342–19354 (2007).
70. Turlan, C., Prudhomme, M., Fichant, G., Martin, B. & Gutierrez, C. SpxA1, a novel transcriptional regulator involved in X-state (competence) development in *Staphylococcus aureus*. *Molecular Microbiology* **73**, 492–506 (2009).
71. Pamp, S. J., Frees, D., Engelmann, S., Hecker, M. & Ingmer, H. Spx is a global effector impacting stress tolerance and biofilm formation in *Staphylococcus aureus*. *Journal of Bacteriology* **188**, 4861–4870 (2006).
72. Kajfasz, J. K., Mendoza, J., Gaca, A., Miller, J., Koselny, K., Giambiagi-deMarvel, M., Wellington, M., Abranches, J., & Lemos, J. The Spx regulator modulates stress responses and virulence in *Enterococcus faecalis*. *Infection and Immunity* **80**, 2265–2275 (2012).
73. Kajfasz, J. K., Rivera-Ramos, I., Abranches, J., Martinez, A., Rosalen, P., Derr, A., Quivey, R., & Lemos, J. Two Spx proteins modulate stress tolerance, survival, and virulence in *Streptococcus mutans*. *Journal of Bacteriology* **192**, 2546–2556 (2010).
74. Galvão, L., Rosalen, P., Rivera-Ramos, I., Franco, G., Kajfasz, J., Abranches, J., Bueno-Silva, B., Koo, H., & Lemos, J. Inactivation of the *spxA1* or *spxA2* gene of *Streptococcus mutans* decreases virulence in the rat caries model. *Molecular Oral Microbiology* **32**, 142–153 (2016).
75. Chen, L., Ge, X., Wang, X., Patel, J. R. & Xu, P. SpxA1 involved in hydrogen peroxide production, stress tolerance and endocarditis virulence in *Streptococcus sanguinis*. *PLoS ONE* **7**, (2012).

76. Whiteley, A., Ruhland, B., Edrozo, M. & Reniere, M. A redox-responsive transcription factor is critical for pathogenesis and aerobic growth of *Listeria monocytogenes*. *Infection and Immunity* **85**, (2017).
77. Hillion, M. & Antelmann, H. Thiol-based redox switches in prokaryotes. *Biological Chemistry* vol. 396 415–444 (2015).
78. Zemansky, J., Kline, B., Woodward, J., Leber, J., Marquis, H., & Portnoy, D. Development of a mariner-based transposon and identification of *Listeria monocytogenes* determinants, including the peptidyl-prolyl isomerase PrsA2, that contribute to its hemolytic phenotype. *Journal of Bacteriology* **191**, 3950–3964 (2009).
79. Göhring, N., Fedtke, I., Xia, G., Jorge, A., Pinho, M., Bertsche, U., & Peschel, A. New role of the disulfide stress effector YjbH in B-lactam susceptibility of *Staphylococcus aureus*. *Antimicrobial Agents and Chemotherapy* **55**, 5452–5458 (2011).
80. Rogstam, A., Larsson, J. T., Kjelgaard, P. & von Wachenfeldt, C. Mechanisms of adaptation to nitrosative stress in *Bacillus subtilis*. *Journal of Bacteriology* **189**, 3063–3071 (2007).
81. Ferrières, L., Aslam, S. N., Cooper, R. M. & Clarke, D. J. The *yjbEFGH* locus in *Escherichia coli* K-12 is an operon encoding proteins involved in exopolysaccharide production. *Microbiology* (2007) doi:10.1099/mic.0.2006/002907-0.
82. Wurtzel, O., Sesto, N., Mellin, J., Karunker, I., Edelheit, S., Bécavin, C., Archambaud, C., Cossart, P., & Sorek, R. Comparative transcriptomics of pathogenic and non-pathogenic *Listeria* species. *Molecular Systems Biology* **8**, (2012).
83. Michna, R., Zhu, B., Mäder, U. & Stülke, J. SubtiWiki 2.0 - an integrated database for the model organism *Bacillus subtilis*. *Nucleic Acids Research* **44**, 654–662 (2016).
84. Mäder, U., Nicolas, P., Depke, M., Pané-Farré, J., Debarbouille, M., van der Kooi-Pol, M., Guérin, C., Dérozier, S., Hiron, A., Jarmer, H., Leduc, A., Michalik, S., Reilman, E., Schaffer, M., Schmidt, F., Bessières, P., Noirot, P., Hecker, M., Msadek, T., Völker, U., & van Dijl, J. *Staphylococcus aureus* transcriptome architecture: From laboratory to infection-mimicking conditions. *PLOS Genetics* **12**, (2016).
85. Larsson, J. T., Rogstam, A. & von Wachenfeldt, C. YjbH is a novel negative effector of the disulphide stress regulator, Spx, in *Bacillus subtilis. Molecular Microbiology* (2007) doi:10.1111/j.1365-2958.2007.05949.x.
86. Garg, S. K., Kommineni, S., Henslee, L., Zhang, Y. & Zuber, P. The YjbH protein of *Bacillus subtilis* enhances ClpXP-catalyzed proteolysis of Spx. *Journal of Bacteriology* **191**, 1268–1277 (2009).
87. Chan, C. M., Garg, S., Lin, A. A., Correspondence, P. Z. & Zuber, P. *Geobacillus thermodenitrificans* YjbH recognizes the C-terminal end of *Bacillus subtilis* Spx to accelerate Spx proteolysis by ClpXP. *Microbiology* (2012) doi:10.1099/mic.0.057661-0.
88. Engman, J. & von Wachenfeldt, C. Regulated protein aggregation: A mechanism to control the activity of the ClpXP adaptor protein YjbH. *Molecular Microbiology* (2015) doi:10.1111/mmi.12842.
89. Kommineni, S., Garg, S. K., Chan, C. M. & Zuber, P. YjbH-enhanced proteolysis of Spx by ClpXP in *Bacillus subtilis* is inhibited by the small protein YirB (YuzO). *Journal of Bacteriology* **193**, 2133–2140 (2011).

90. Engman, J., Rogstam, A., Frees, D., Ingmer, H. & von Wachenfeldt, C. The YjbH adaptor protein enhances proteolysis of the transcriptional regulator Spx in *Staphylococcus aureus*. *Journal of Bacteriology* (2012) doi:10.1128/JB.06414-11.
91. Renzoni, A., Andrey, D., Jousselin, A., Barras, C., Monod, A., Vaudaux, P., Lew, D., & Kelley, W. Whole genome sequencing and complete genetic analysis reveals novel pathways to glycopeptide resistance in *Staphylococcus aureus*. *PLoS ONE* **6**, (2011).
92. Austin, C. M., Garabaglu, S., Krute, C., Ridder, M., Seawell, N., Markiewicz, M., Boyd, J., & Bose, J. Contribution of YjbIH to virulence factor expression and host colonization in *Staphylococcus aureus*. *Infection and Immunity* **87**, (2019).
93. Donegan, N. P., Manna, A. C., Tseng, C. W., Liu, G. Y. & Cheung, A. L. CspA regulation of *Staphylococcus aureus* carotenoid levels and σB activity is controlled by YjbH and Spx. *Molecular Microbiology* **112**, 532–551 (2019).
94. Angeles Argudín, M., Roisin, S., Nienhaus, L., Dodémont, M., de Mendonça, R., Nonhoff, C., Deplano, A., & Denisa, O. Genetic diversity among *Staphylococcus aureus* isolates showing oxacillin and/or cefoxitin resistance not linked to the presence of *mec* genes. *Antimicrobial Agents and Chemotherapy* **62**, (2018).
95. Arnér, E. & Holmgren, A. Physiological functions of thioredoxin and thioredoxin reductase. *European Journal of Biochemistry* **267**, 6102–6109 (2000).
96. Lu, J. & Holmgren, A. The thioredoxin antioxidant system. *Free Radical Biology and Medicine* **66**, 75–87 (2014).
97. Nakao, L., Everley, R., Marino, S., Lo, S., de Souza, L., Gygi, S., & Gladyshev, V. Mechanism-based proteomic screening identifies targets of thioredoxin-like proteins. *Journal of Biological Chemistry* **290**, 5685–5695 (2015).
98. Awad, W., Al-Eryani, Y., Ekström, S., Logan, D. & von Wachenfeldt, C. Structural basis for YjbH adaptor-mediated recognition of transcription factor Spx. *Structure* **27**, 923–936 (2019).
99. Kirstein, J., Schlothauer, T., Dougan, D., Lilie, H., Tischendorf, G., Mogk, A., Bukau, B., & Turgay, K. Adaptor protein controlled oligomerization activates the AAA+ protein ClpC. *The EMBO Journal* **25**, 1481–1491 (2006).
100. Trentini, D., Suskiewicz, M., Heuck, A., Kurzbauer, R., Deszcz, L., Mechtler, K., & Clausen, T. Arginine phosphorylation marks proteins for degradation by a Clp protease. *Nature* **539**, 48–53 (2016).
101. Chan, C. M., Hahn, E. & Zuber, P. Adaptor bypass mutations of *Bacillus subtilis spx* suggest a mechanism for YjbH-enhanced proteolysis of the regulator Spx by ClpXP. *Molecular Microbiology* (2014) doi:10.1111/mmi.12671.
102. Al-Eryani, Y., Rasmussen, M., Kjellström, S., Højrup, P. & Emanuelsson, C. Exploring structure and interactions of the bacterial adaptor protein YjbH by crosslinking mass spectrometry. *Proteins: Structure, Function, and Bioinformatics* **84**, 1234–1245 (2016).
103. Sun, A., Camilli, A. & Portnoy, D. Isolation of *Listeria monocytogenes* small-plaque mutants defective for intracellular growth and cell-to-cell spread. *Infection and Immunity* **58**, 3770–3778 (1990).
104. Ruhland, B. & Reniere, M. YjbH requires its thioredoxin active motif for the nitrosative stress response, cell-to-cell spread, and protein-protein interactions in *Listeria monocytogenes*. *Journal of Bacteriology* **202**, (2020).

105. Karimova, G., Pidoux, J., Ullmann, A. & Ladant, D. A bacterial two-hybrid system based on a reconstituted signal transduction pathway. *Proceedings of the National Academy of Sciences* **95**, 5752–5756 (1998).
106. Battesti, A. & Bouveret, E. The bacterial two-hybrid system based on adenylate cyclase reconstitution in *Escherichia coli. Methods* **58**, 325–334 (2012).
107. Nakano, M. M., Nakano, S. & Zuber, P. Spx (YjbD), a negative effector of competence in *Bacillus subtilis*, enhances ClpC-MecA-ComK interaction. *Molecular Microbiology* **44**, 1341–1349 (2002).
108. Nakano, S., Zheng, G., Nakano, M. M. & Zuber, P. Multiple pathways of Spx (YjbD) proteolysis in *Bacillus subtilis*. *Journal of Bacteriology* **184**, 3664–3670 (2002).
109. Portman, J. L., Huang, Q., Reniere, M. L., Iavarone, A. T. & Portnoy, D. A. Activity of the pore-forming virulence factor listeriolysin O is reversibly inhibited by naturally occurring S-glutathionylation. *Infection and Immunity* **85**, (2017).
110. Zhu, L., Yang, Z., Yao, R., Xu, L., Chen, H., Gu, X., Wu, T., & Yang, X. Potential mechanism of detoxification of cyanide compounds by gut microbiomes of bamboo-eating pandas. *mSphere* **3**, (2018).
111. Branon, T., Bosch, J., Sanchez, A., Udeshi, N., Svinkina, T., Carr, S., Feldman, J., Perrimon, N., & Ting, A. Efficient proximity labeling in living cells and organisms with TurboID. *Nature Biotechnology* **36**, 880–887 (2018).
112. Cesinger, M., Thomason, M., Edrozo, M., Halsey, C. & Reniere, M. *Listeria monocytogenes* SpxA1 is a global regulator required to activate genes encoding catalase and heme biosynthesis enzymes for aerobic growth. *Molecular Microbiology* (2020) doi:doi: 10.1111/mmi.14508.
113. Bishop, D. & Hinrichs, D. Adoptive transfer of immunity to *Listeria monocytogenes*. The influence of in vitro stimulation on lymphocyte subset requirements. *Journal of Immunology* **139**, 2005–2009 (1987).
114. Bécavin, C., Bouchier, C., Lechat, P., Archambaud, C., Creno, S., Gouin, E., Wu, Z., Kühbacher, A., Brisse, S., Graciela Pucciarelli, M., García-del Portillo, F., Hain, T., Portnoy, D., Chakraborty, T., Lecuit, M., Pizarro-Cerdá, J., Moszer, I., Bierne, H., & Cossart, P. Comparison of widely used *Listeria monocytogenes* strains EGD, 10403S, and EGD-e highlights genomic differences underlying variations in pathogenicity. *mBio* **5**, (2014).
115. Lauer, P., Chow, M. Y. N., Loessner, M. J., Portnoy, D. A. & Calendar, R. Construction, characterization, and use of two *Listeria monocytogenes* site-specific phage integration vectors. *Journal of Bacteriology* **184**, 4177–4186 (2002).
116. Hodgson, D. A. Generalized transduction of serotype 1/2 and serotype 4b strains of *Listeria monocytogenes*. *Molecular Microbiology* **35**, 312–323 (2000).
117. Whiteley, A. T., Garelis, N., Peterson, B., Choi, P., Tong, L., Woodward, J., & Portnoy, D. c-di-AMP modulates *Listeria monocytogenes* central metabolism to regulate growth, antibiotic resistance and osmoregulation. *Molecular Microbiology* **104**, 212–233 (2017).
118. Schneider, C. A., Rasband, W. S. & Eliceiri, K. W. NIH Image to ImageJ: 25 years of image analysis. *Nature Methods* vol. 9 671–675 (2012).
119. Miller, J. *Experiments in molecular genetics*. (Cold Spring Harbor Laboratory, 1972).

120. Ting, S. Y., Bosch, D., Mangiameli, S., Radey, M., Huang, S., Park, Y., Kelly, K., Filip, S., Goo, Y., Eng, J., Allaire, M., Veesler, D., Wiggins, P., Peterson, S., & Mougous, J. Bifunctional immunity proteins protect bacteria against FtsZ-targeting ADP-ribosylating toxins. *Cell* **175**, 1380-1392.e14 (2018).
121. Simon, R., Priefer, U. & Puhler, A. A broad host range mobilization system for in vivo genetic engineering: transposon mutagenesis in Gram negative bacteria. *Bio/Technology* (1983).
122. Whiteley, A. T., Pollock, A. J. & Portnoy, D. A. The PAMP c-di-AMP is essential for *Listeria monocytogenes* growth in rich but not minimal media due to a toxic increase in (p)ppGpp. *Cell Host and Microbe* **17**, 788–798 (2015).